EXPERIMENTAL INVESTIGATION OF CEREAL CROP DRYING IN AN INCLINED BUBBLING FLUIDIZED BED

A THESIS SUBMITTED IN PARTIAL FULFILLMENT OF THE REQUIREMENTS FOR THE DEGREE OF

DOCTOR OF PHILOSOPHY

BY

PHYU PHYU THANT
(Roll No: 126103037)

DEPARTMENT OF MECHANICAL ENGINEERING
INDIAN INSTITUTE OF TECHNOLOGY GUWAHATI
MAY 2016

ACKNOWLEDGEMENTS

First of all, I'd like to express my deep appreciation to my supervisors Prof. P. S. Robi and Prof. Pinakeswar Mahanta for their valuable guidance for the whole of my Ph.D programme. I treat it as an excellent opportunity to work on this Ph.D programme under their care and control.

I would like to thank to Doctoral Committee: Prof. Anoop K. Dass, Head of Mechanical Engineering Department, Dr Sukhomay Pal and Dr G. Pugazhenthi for their suggestions.

Also, I desire to extend my gratitude to Prof. Uday. S. Dixit, Dr S. N. Joshi and Dr Ganesh R. Narayanan, Dr. Karuna Kalita and Dr. Deepak Sharma for their support.

I am specially grateful to my parents for their patience and continued encouragement which contribute greatly towards the completion of this work.

Finally, I appreciate the help of my colleagues, technicians from IIT Guwahati central workshop who incorporated the fabrication of this setup and all those who supported me in this research successfully.

Phyu Phyu Thant

Roll No: 126103037

TH-1488_126103037

CERTIFICATE

This is to certify that **Phyu Phyu Thant (Roll no: 126103037)** has been working under my supervision since July 2012. I hereby forward her thesis entitled **"Experimental investigation of cereal crop drying in an inclined bubbling fluidized bed"** to be submitted for the award of the degree of Doctor of Philosophy to IIT Guwahati. I certify that she has fulfilled all the requirements according to the rules of this institute and the investigations embodied in her thesis have not been submitted elsewhere.

Dr. P. S. Robi
Professor
Department of Mechanical Engineering
Indian Institute of Technology Guwahati
Guwahati – 781039, Assam, India

Dr. Pinakeswar Mahanta
Professor and Dean of Faculty Affairs
Department of Mechanical Engineering
Indian Institute of Technology Guwahati
Guwahati – 781039, Assam, India

TH-1488_126103037

ABSTRACT

Rice is the primary source of staple food for more than half of the world's population. Drying of cereal crop is important in terms of maintenance of nutritional value of food, loss due to pest and fungi attack as well as to maintain long storage life. Paddy drying process consumes high energy due to the removal of internal moisture. The main objective for a sustainable dryer is to reduce required energy input by means of designing an efficient drying system which can provide the dried products with acceptable quality level. Paddy drying was carried out in four different inclined positions, viz., vertical bed (0˚ inclined), 15˚, 30˚ and 45˚ in a bubbling fluidized bed. Experiments were conducted for 0.5 to 2.5 kg batch size with superficial velocities of 1.1ms^{-1} to 2.6 ms^{-1} and drying air temperatures of 55˚C to 65˚C to evaluate the hydrodynamic behaviour, drying characteristics and energy consumption during the drying process. Better results in terms of energy consumption and moisture removal rate were observed with bed inclination of 15˚ due to the secondary motion created because of the pressure difference between the vertical faces of the dryer.

Considering the particle mixing behaviour observed during the experiments with the inclined bed dryer, the distributor plate was modified for better drying efficiency and reduction in drying energy consumption and experiments were conducted with the modified distributor plate. The heat transfer rate and drying efficiency increased due to the proper motion of air flow while using the modified distributor plate in the bubbling fluidized bed dryer. Spirals were inserted inside the drying chamber and all the experiments were repeated with and without the use of spirals inserts. Use of spirals inside the drying chamber enhanced better mixing of paddy, reduces drying time as well as reduces energy consumption significantly.

Best performance with a combination of minimum energy consumption and faster moisture removal rate was obtained with a bed inclination of 15˚, an inventory of 2.5 kg, air velocity of 2.1 ms^{-1}, air temperature of 65˚C using modified distributor plate with the use of spirals inserts. Energy consumptions decreased by12.2% when modified distributor plate is used. Energy consumptions decreased by 48.8% when spiral inserts are used. Energy consumptions decreased by 67.7% when the inventory

TH-1488_126103037

is increased from 0.5 kg to 2.5kg, 48.8% when the temperature is increased from 55˚C to 65˚C, 43.2% when the inclination is increased from 0˚ to 15˚ and 32.3% when the velocity is increased from 1.1 m/s to 2.1 m/s at the optimum condition. In addition, energy consumption reduced 10% by the effect of scale up.

TH-1488_126103037

CONTENTS

TH-1488_126103037

TH-1488_126103037

TH-1488_126103037

LIST OF TABLES

TH-1488_126103037

LIST OF FIGURES

TH-1488_126103037

TH-1488_126103037

TH-1488_126103037

NOMENCLATURE

Notation

A_b	Cross sectional area of dryer, m^2
$P.F$	Power factor
T	Drying time (minute)
I	Current, Ampere
V	Input voltage, volts
Q	Heat input, MJ s^{-1}
D_B	Bubble diameter
D_{bed}	Diameter of the bed
N_0	Number of holes in the distributor plate
$U_{mf,}$	Minimum fluidization velocity
U	Superficial fluid velocity
I	Inventory, kg
V_{bed}	Volume occupied by the fluidized bed
d_p	Diameter of paddy
C_D	Draft coefficient
U_t	Terminal velocity
$\dot{m}_a$	Mass flow rate of air, kg s^{-1}
ρ_{sus}	Suspension density of the bed, kg m^{-3}
ρ_w	Density of water, kg m^{-3}
ρ_s	Density of paddy, kg m^{-3}
ΔP_b	Pressure drop in manometric fluid
Δh_l	Different of height in manometric fluid, cm of water
G	Acceleration due to gravity
T_{da}	Drying air temperature, ˚C
C_{pa}	Specific heat capacity of air
MC	Moisture content, %
L	Length of the fluidized bed dryer column
H	Height of the bubble in the fluidized bed

TH-1488_126103037

Greek symbols

$\mathcal{E}$	Bed voidage
ε_{mf}	Void fraction at minimum fluidization
Φ_s	Sphericity factor
μ	Viscosity of air, Pa-sec
Θ	Bed inclination angle

Subscript

Wb	Wet basis
Db	Dry basis

TH-1488_126103037

ABBREVIATIONS

BFB	Bubbling Fluidized Bed
MC	Moisture Content
STD	Standard Distributor
MD	Modified Distributor
XSP	Without the use of Spirals
SP	With the use of Spirals
LS	Lower Side of riser column
TS	Top/Upper Side of riser column

TH-1488_126103037

CHAPTER 1

INTRODUCTION

1.1 MOTIVATION

Paddy is the major cereal crop cultivated in South East Asia contributing to 90% of production in the world [Kiple and Ornelas 2003]. Rice, obtained after processing of paddy, is the primary source of staple food for more than half of the world's population. Fig. 1.1 presents the country-wise production of paddy.

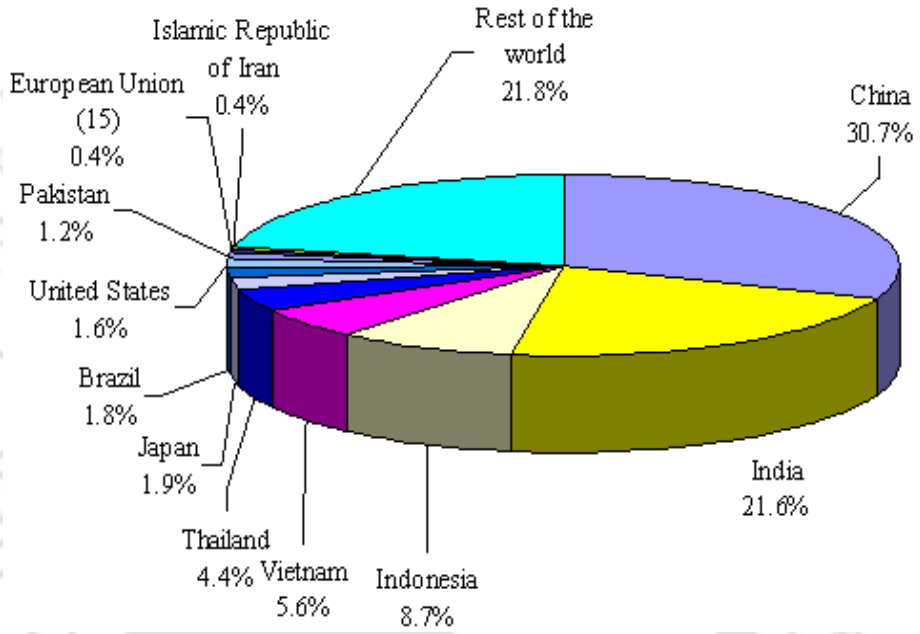

Fig. 1.1 Average distribution of paddy production during 1999-2003.
[http://www.unctad.info/en/Infocomm/Agricultural_Products/Riz/Market]

Geographically, the paddy production is concentrated in western and eastern Asia with more than 90% of world's output. China and India account for more than one-third of global population (52.3% over the period 1999–2003) and supply over half of the world's rice. India is in second position in terms of production of white rice.

Consumption pattern of rice in terms of calorie is presented in Table 1.1. It is clear from this table that the average per capita consumption of rice per year is 58 kg.

TH-1488_126103037

Table 1.1 Rice consumption, calories intake and percentage of calories from rice. (http://www.knowledgebank.irri.org/ericeproduction/Importance_of_Rice.htm)

Country	Milled rice consumption (kg/capita/year)	Total calories/capita/ day	Rice calories/capita /day	% calories from rice
Myanmar	211	2803	2050	73
Lao	171	2152	1516	70
Vietnam	170	2564	1676	65
Bangladesh	168	2201	1676	76
Cambodia	165	2000	1527	76
Indonesia	154	2931	1525	52
Thailand	101	2411	1004	42
Philippines	100	2357	974	41
Madagascar	91	1994	926	46
China	91	3045	911	30
India	74	2417	736	30
Japan	60	2782	642	23
Egypt	41	3323	426	13
Brazil	40	3012	409	14
Nigeria	23	2833	237	8
Pakistan	15	2462	150	6
South Africa	12	2805	119	4
UAS	9	3754	94	3
Turkey	7	3469	65	2
Mexico	6	3168	61	2
USSR (former area)	5	2778	47	2
world	58	2808	577	21

Processing of paddy involves drying after harvesting for maintenance of quality of rice grain in terms of nutritional value. During the process, moisture content of paddy grain is reduced to 14% w.b (approx) for preventing attack by fungus, pests and germs. In addition, the quality of the rice will also have to be maintained above certain levels for acceptance by the consumers. A variety of techniques exist for drying rice grains. Sun drying is traditional and weather dependant leading to long drying time. Moreover, uneven drying of grain is frequently encountered in sun drying. Formation of mould, attack by rodents and pests are also common in traditional sun drying [Hien (1998), Somchart (1996)]. Mechanical drying with heated air is also popular for community services in which running cost are significant. Solar dryers are evolved in recent time but the same are not time tested in the field. Considering the viability of various drying techniques, newer techniques with high energy efficiency and throughput are being developed. The fluidized bed dryer

TH-1488_126103037

appears to be a very efficient and fast. Several fluidized bed crop drying techniques have been developed. A proper control of process parameters is required for quality drying of rice grains at a cheaper rate with minimum environmental impact. Present work is an attempt towards the development of a bubbling fluidized bed dryer in terms of reduction of energy consumption and reduction in drying time maintaining the quality drying of paddy grain.

1.2 STRUCTURE AND CONSTITUENTS OF CEREAL CROPS

The rice grain has both physical and chemical characteristics. The structure of a typical paddy is shown in Fig. 1.2.

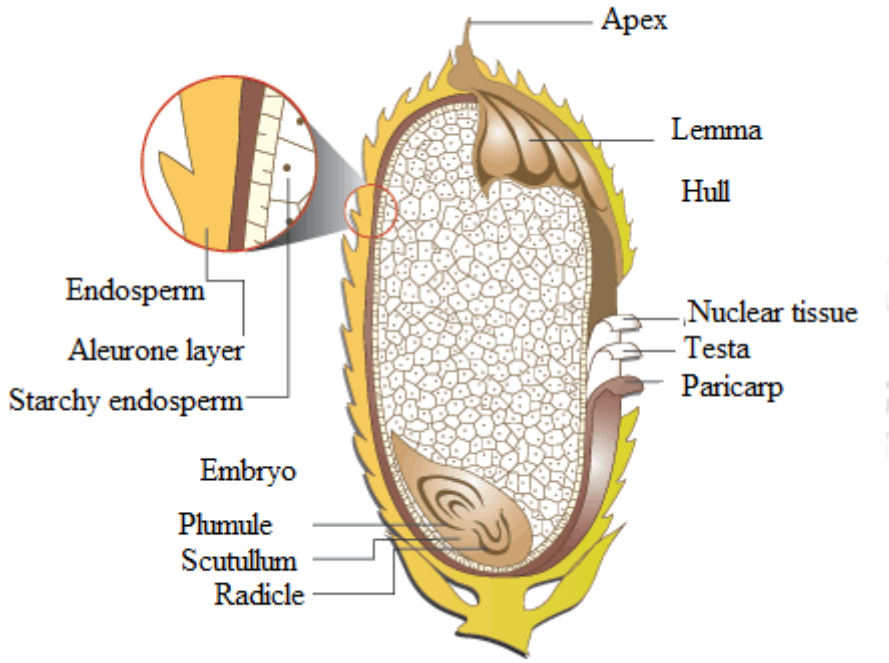

Fig. 1.2 Structure of Paddy [www.capasas.com.my]

Physically a rice grain is made up of an outside husk layer, a bran layer, and the endosperm. The husk layer (lemma and palea) accounts for 20% of the weight of paddy and helps in protecting the grain kernel from insect and fungal attack. When the husk is removed, the rice is called brown rice. Brown rice contains the bran layer and the endosperm. The bran layer is made up of the pericarp and testa, the aluerone layer and the embryo. The degree to which this bran layer is removed is known as the milling degree. The desired amount of bran removed depends on the country. In Japan, the aluerone layer is often not removed however in many other countries all bran layers are removed to give very highly polished rice. The storage life of milled

TH-1488_126103037

rice is improved when all of the bran layers are removed. Chemically, rice at 12% moisture contains approximately 80% starch and 7% protein (Teter, 1987). Starch occurs in the endosperm as small many-sided granules while protein is present as particles that lie between the starch granules. Rice grain also contains sugar, fat, dietary fiber and minerals. Starch is the primary carbohydrate source for growing seeds and leaf tissue development and is found in leaves, tubers, fruits and seeds. Two general types of starch exist – amylose and amylopectin. Both are polymers of glucopyranose molecules, but differ in structure and functional properties.

1.3 MECHANISM OF DRYING

Drying of cereal crop is important in terms of maintenance of nutritional value of food, loss due to pest and fungi attack as well as to maintain long storage life. In paddy grain, moisture is present at two places: (a) at the surface of the grain i.e. the surface moisture and (b) in the kernel i.e. the internal moisture. Surface moisture will readily evaporate when grain is exposed to hot air. Internal moisture evaporates much slower because it first has to move from the kernel to the outside surface. As a result, surface moisture and internal moisture evaporate at a different rate. This difference results in a different drying rate, i.e. the rate at which grain moisture content declines during the drying process. A typical drying curve illustrated in Fig. 1.3 indicates the grain moisture content and the grain surface temperature versus time during the drying process. It is observed from the Fig. that drying rate changes over time.

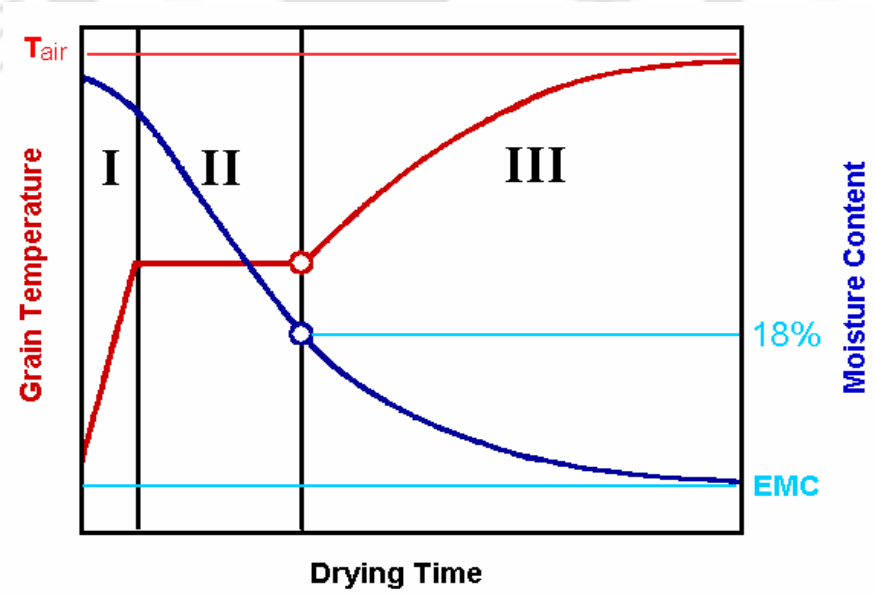

Fig. 1.3 Typical drying curve

TH-1488_126103037

1.4 STAGES OF DRYING

In case of cereal crop drying following 3(Three) stages of drying period are reported in literature [IRRI, Mujumdar, 2006].

1. Preheating Period (Stage I)
2. Constant Rate Period (Stage II)
3. Falling Rate Period (Stage III)

1.4.1 Preheating period: In this stage (stage I) the drying rate as well as the decrease in moisture content (MC) is high. Decrease in MC at the surface of the grain is due to the sharp temperature gradient at the surface.

1.4.2Constant-rate period: In this stage, the drying rate remains constant. Once the grain is at the drying temperature, water starts to evaporate from the surface of the grain. During this period, all the heat from the drying air is used to evaporate surface moisture and the rate of moisture removal from the grain remains constant. It is therefore called the constant-rate period. During this period, grain temperature also remains constant.

1.4.3 Falling-rate period: Here the drying rate decreases with time. As drying process continues, it takes more time for transport of the internal moisture to reach the grain surface, and evaporation of water is no longer constant with time resulting in fall in drying rate. For paddy grains, the falling-rate period typically starts at grain MC of 18% w.b to the end of the drying process. For safe storage level, grain should attain equilibrium moisture content (EMC) state. Usually it reported in the literature that EMC for safe storage of paddy grain to be14% w.b.

1.5 DRYING METHODS

Several drying methods are used for the drying of agricultural products in practice. Some of the methods are as follows:

1. Traditional sun drying
2. Solar drying
3. Low temperature drying
4. Heated air drying (Mechanical as well as chemical), etc.

TH-1488_126103037

1.5.1. Traditional sun drying

Traditional sun drying is drying the paddy grains under the direct sunlight. Traditional sun drying are: field drying, sun drying, panicle drying, mat drying and pavement drying.

Sun Drying: In this the heat source for drying is the sun. The limitations of sun drying are:

- It cannot be adopted during night times or when there is rain.
- Fungal growth and or excess respiration resulting in losses and yellowing may occur during due to any delay in sun drying.
- It has limited capacity and is labour intensive and hence can be adopted only for small scale or medium scale drying.
- Since the source of heat is the sunlight, the temperature control is difficult. Overheating or re-wetting of grains can result in low milling quality.

Field Drying: Field drying (Fig. 1.4(a)) is normally due to unavailability of thresher. There is not enough air circulation to dry properly, massive heat build up inside the stacks, moulds grow quickly, discoloration developed, dry grains often absorb water from the wet straw leading to fissuring of the dry grains thereby reducing the potential rice recovery. Field drying should be avoided as far as possible since it is almost impossible to produce good quality grains by field drying.

Panicle drying: At small levels the paddy, along with the panicles are harvested with a knife and bound together as shown in Fig. 1.4(b). They are then transferred to the drying locations, which generally is the farmer's house or they are stored in the farmer's house by hanging then under the roof for protection. In this drying process, the panicles dry slower than the grains which are directly exposed to the sun and drying is non-uniform.

TH-1488_126103037

(a)

(b)

(c)

(d)

Figs. 1.4 Traditional sun drying (a) Field drying (b) Panicle drying (c) Mat drying (d) Pavement drying (www.georgianewsday.com)

Mat Drying: This is practiced extensively in rural areas. In this process, paddy grains are placed on mats or plastic sheets and dried in the sun as shown in Fig. 1.4(c). This drying process is only for small scale.

Pavement Drying: This is used for higher capacity drying and needs pavements where the grains are dried. Usually manual tools are used for mixing and grain collections. Large capacity mills may use even tractors for mixing and drying. In this drying process, labour intensive, capital cost for payments is expensive, large space requirement, dried paddy will have dust and stone and long drying time. Above all traditional sun drying methods are shown in Fig. 1.4(d) [Somchart (1996)].

TH-1488_126103037

1.5.2. Solar Drying

In solar drying there are three types of solar dryers as shown in Fig. 1.5(a)-(c).

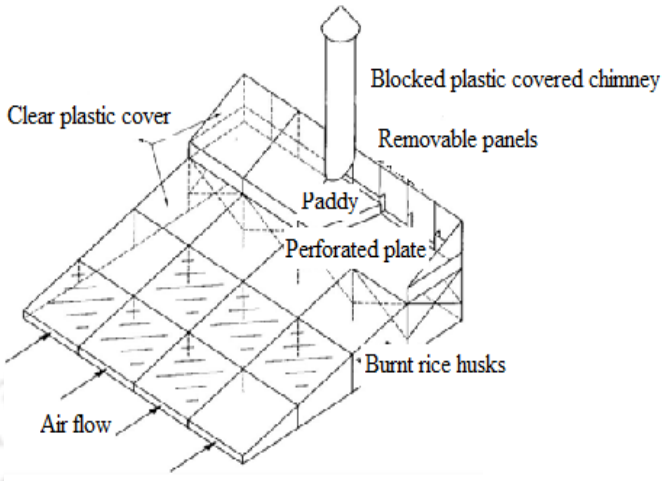

(a)

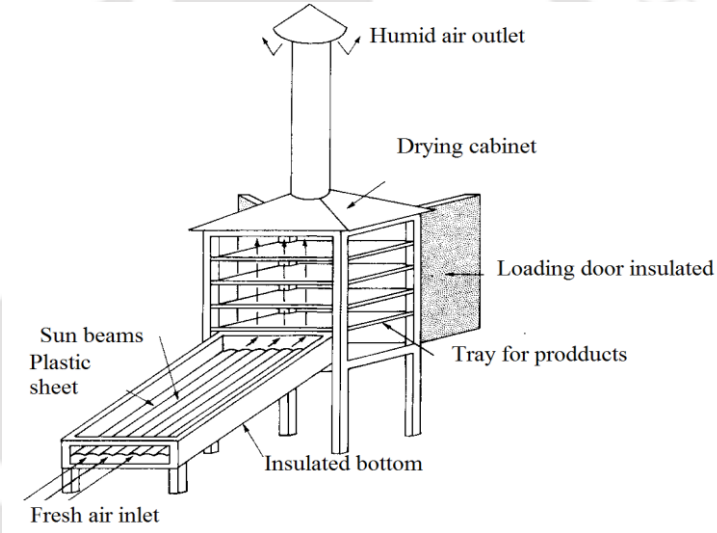

(c)

Figs. 1.5 Types of Solar dryer (a) Direct (b) Indirect (c) Forced circulation (en.wikipidea.org, www.indiamart.com)

TH-1488_126103037

- **Natural Convection or Direct type Solar Dryer**: In this type of dryers, the agricultural product is placed in shallow layers in a blackened enclosure with a transparent cover as shown in Fig. 1.5(a). The solar radiations are directly absorbed by the product and are heated up. The moisture from the product evaporates which is let out by the natural convection or circulation.

- **Indirect type dryers**: In these dryers the food product is placed in a drying chamber and air heated by solar energy is blown in to the drying chamber (Fig. 1.5(b)), where the moisture in the grains gets evaporated and is blown out along with the heated air. In some of the designs, in addition to the air heated from solar heaters, the grains also receive direct solar radiations for drying.

- **Active or forced circulation types dryers** (Fig. 1.5(c)): In these dryers, hot air is continuously blown over the food product which is loaded or unloaded continuously or periodically [Ekechukwu and Norton 1999].

The disadvantages of solar drying system are: limited time i.e. drying can only be done during day-time, large space requirement and weather dependent.

1.5.3 Mechanical Driers

Mechanical dryers are classified based on the capacity and methods of drying: heated air drying and low temperature drying.

1.5.3.1 Low-Temperature Drying

In-Store Drying: This type of dryer is slow equilibrium moisture content drying with ambient air or slightly pre-heated air and drying time is 4 days to 2 weeks for moisture removal. Air temperature is generally 3˚C - 6˚C above ambient and air velocity is around 0.1 m/s. It produces very high quality grain, low energy requirement and drying in storage bin. However the quality would deteriorate in if the moisture content is above 18% when exposed for a long drying time. Low-temperature drying system is shown in Fig. 1.6.

TH-1488_126103037

Fig. 1.6: In-store drying [Gummert et.al., (1993)]

1.5.3.2 Heated Air Drying

Heated air drying or mechanical drying can be carried out any time of the day or night and can reduce the labour costs. It can be used for mass production with very less time. Better quality rice can be obtained by mechanical dryers compared to sun dried grains. This will lead to more uniform drying of grain and higher milling yield and head rice recovery. Grain re-circulation allows for uniformly dried grain. Automatic drying by proper air temperature control will maximize the drying rate and at the same time reduce over-heating or over-drying. Three types of air heated dryer are (a) fixed bed batch dryers, (b) re-circulation batch dryers and (c) continuous flow dryers.

Fixed-Bed Batch Dryers: Fixed-bed batch dryer (flat) has 1-10 tons per batch and drying time 6-8 hrs are required for moisture removal. Kerosene or rice hull can be used as fuel. They are normally flat bed, inclined bed, and circular bind dryers. Fixed bed batch dryers are shown in Figs. 1.7 (a) and (b), respectively. Flat bed dryers are cheap and labour intensive. Inclined bed dryers are having the advantage of easy loading but more expensive. Circular bin dryers are compact and cheap where as there is uneven air flow inside and outside the drying chamber.

TH-1488_126103037

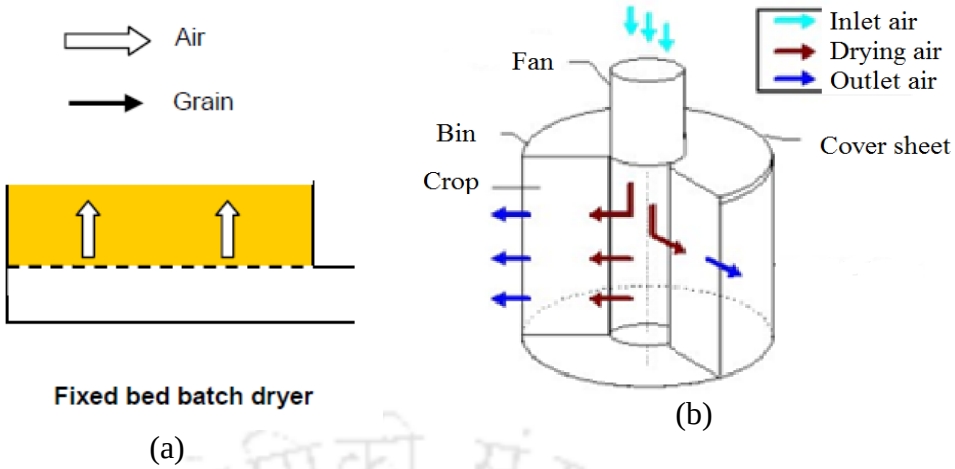

(a) (b)

Figs. 1.7 Fixed-bed batch dryers (a) Flat bed and (b) Low cost (Hien, 2009, Mcneal, 1957)

Re-Circulating Batch Dryers: This dryer has 4-12 tons per batch capacity and 8 hours is required for moisture removal. Kerosene is used as the fuel. The recirculation batch dryers have has automatic operation, requires less floor space, and produces grains with excellent quality. Re-circulating batch dryer is shown in Fig. 1.8.

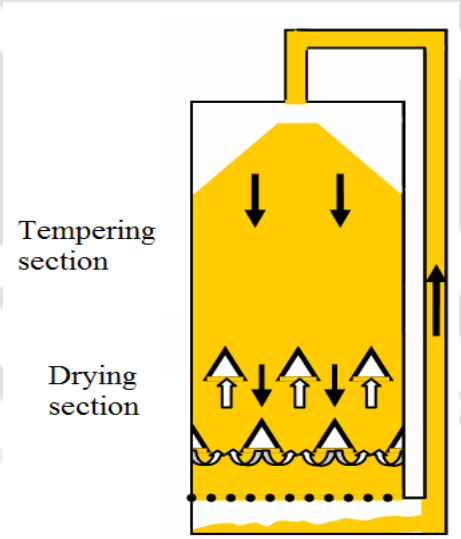

Fig. 1.8: Re-circulating batch dryer [knowledegbank.irri.org]

Continuous flow drier: Continuous flow dryer and factory are shown in Figs. 1.9 (a) and (b). This requires costly capital investment. In this a larger system consisting of the dryer, blower, several tempering bins and conveying equipment needs to be integrated. The operation needs to be carefully planned and requires good management in order to fully utilize the expensive equipment in addition to the

TH-1488_126103037

continuous input of wet grains at a steady rate. It is difficult to dry paddy in a continuous flow dryer from typical moisture content down to levels for safe storage in one single pass (Hall, 1957).

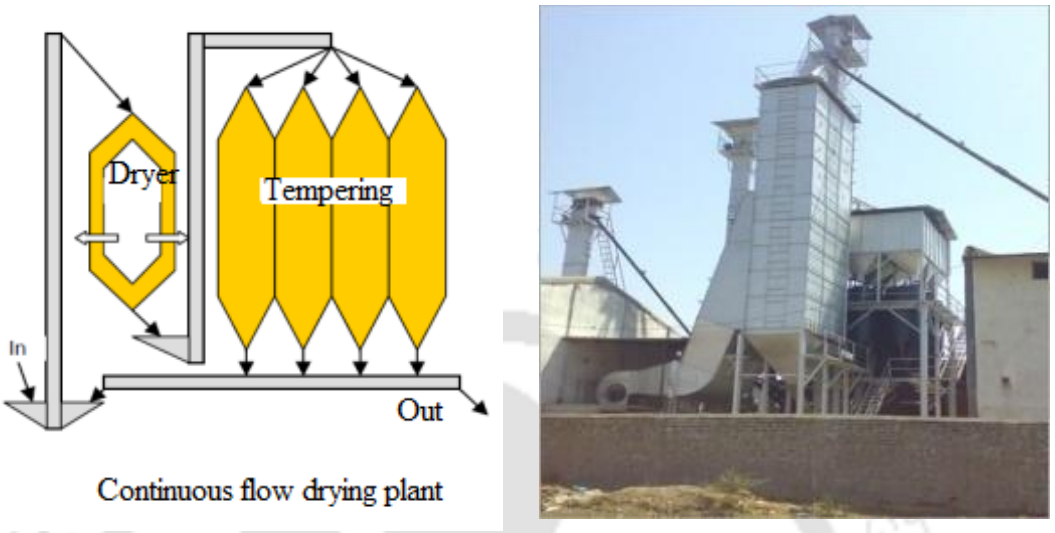

(a) (b)

Figs. 1.9 Continuous flow dryer (a) basic principle (b) factory [www.lineupdb.com]

1.6 FLASH DRIER

These are special continuous type dryers where is carried out in two stages. The two variants are the rotary drum dryers developed in Philippines and the fluidized bed dryers which were successfully commercialized in Thailand in the nineties. Both types use extremely high temperatures (up to 110-120˚C) for rapid removal of the surface moisture and can only dry down to 18% MC without damaging the grains. The fluidized bed dryers include either large scale in-store drying facilities with several hundred tons capacity or mixed flow heated air dryers for second stage drying to storage moisture content (Amos, 1998).

1.6.1 Fluidized bed drier

The fluidized bed dryer consists of a drying chamber with an air speed of around 2.3 m/s, a bed thickness of 10 cm in which the grain is exposed to the drying air for 10-15 minutes. Capacities of commercial units range from 1-10 tons per hour. A diesel burner or a rice hull furnace is used as heat source and a system for re-cycling 50-70% of the drying air is provided to improve energy efficiency [Jeon et al. 1990]. Fluidized bed dryer is shown in Fig. 1.10.

TH-1488_126103037

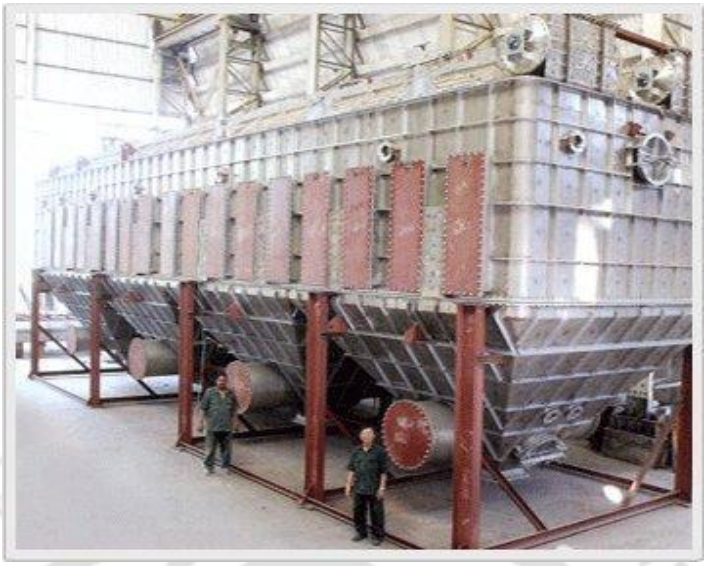

Fig. 1.10: Fluidized bed dryer [tradeindia.com]

1.7 AIM AND SCOPE

The aim of the work is an attempt towards the development of a bubbling fluidized bed dryer in terms of reduction of energy consumption and reduction in drying time maintaining the quality drying of paddy grain.

Following are the scope of the work:

1. To develop an efficient and economic forced convection inclined bubbling fluidized bed cereal crop drier.
2. To investigate the hydrodynamic behaviour of the above system
3. To study the effect of various process parameters on the drying characteristics of cereal crop like:
    - Effect of bed inclination, inventory, air temperature and air velocity
    - Effect of modification of distributor plate
    - Effect of use of spirals inside the drying chamber
    - Blower as well as thermal energy consumptions of the system

1.8 LAYOUT OF THE THESIS

This thesis consists of seven chapters which are summarized as follows:

- Chapter 1 introduces the importance of paddy drying and highlights the importance of the thesis work.

TH-1488_126103037

- Chapter-2 presents the survey of literature available regarding paddy drying, various paddy dryers in the relative advantages and disadvantages. Finally the technical gaps which are to be addressed in this area are highlighted.
- Chapter-3 describes the methodology adopted for achieving the objectives of the thesis work. These includes the design, development, calibration of the paddy dryer and the detailed experimental procedures carried out for meeting the objectives of the work.
- The results and discussions regarding the paddy drying with the standard distributor plate in the fluidized bed dryer are presented in chapter-4.
- Chapter 5 presents the results of paddy drying using the modified distributor plate and the enhancement of drying process due to the use of spirals in the fluidized bed dryer.
- Chapter 6 presents the results and discussions regarding the energy consumptions of the drying system.
- Chapter-7 presents the conclusions and future scope of work and is followed by references and appendices.

TH-1488_126103037

CHAPTER 2

LITERATURE REVIEW

2.1 INTRODUCTION

Drying is an important process for the processing of paddy to obtain quality grains with minimum damage and resistance to pests. Various paddy drying techniques are used throughout the world. Traditional sun drying is commonly used by farmers for small scale drying whereas various types of paddy dryers are used in case of commercial drying. Each of the drying techniques has its own merit and demerits. The performance characteristics of various dryers have been studied by researchers. An extensive literature review on various drying techniques and influence of various parameters on drying rate are elaborately discussed in this chapter.

2.2 TRADITIONAL CROP DRYING

Open sun drying is extensively used in developing countries [Martinello et. al.(2013)]. Traditional sun drying has many disadvantageous like being a slow and labour intensive drying process. In addition, products may be contaminated with dust, insects, animals or microbial infections during drying. Moreover, drying process is unprotected from environmental conditions like rain or storm. Kouchakzadeh and Ghobadi (2012) had suggested the use of ultrasound-assisted sun drying In order to improve the traditional sun drying process. They had reported drying of unshelled pistachios in mono layer and observed better quality of product compared to traditional sun drying with reduction in drying time by 4 hours.

2.3 PARAMETRIC STUDY ON QUALITY OF CEREAL CROP DRYING

Post-harvest drying is to maintain the desired qualities of the grain. Desirable characteristics of the dried grain include: low and uniform final moisture content, low mould count of the dried kernels, low percentage of broken and damaged kernels, high viability and high head-yield, etc. Drying air temperature, grain moisture content, relative humidity of air, air velocity and air flow rate and depth of the grain bed are recognised to be main factors for drying of cereal crop [Brooker et al. (1974)]. Muyanja et al. (2012) investigated the dynamics of maize grains stored in both shelled and unshelled form in traditional structures. They had reported decrease in MC of

TH-1488_126103037

maize grains within two months of storage. Grain is dried to safe storage MC using different drying systems. Drying can be completed within the allowable safe storage time [Jayas and Ghosh (2006)].

2.3.1 Effect of drying air temperature on moisture removal rate

Extensive studies on drying of various products like silk cocoons, water chestnut, quinoa, etc were reported by Singh et al. (2011), Saxena et al. (2008) and Galvez et al. (2010), respectively. Singh et al. (2011) carried out experiments with forced convective type solar dryer for drying of silk cocoons. The air temperature in the drying chamber was maintained in the range of 50–80 ˚C and it was observed that the drying time for a batch of raw cocoons was 16–19 h depending upon intensity of sun and ambient temperature. Drying characteristics of water chestnut were evaluated by Saxena et al. (2008) in a commercially available cabinet oven at different air temperatures (50-90˚C). They observed that the water-chestnut had better dehydration characteristics with drying air temperature of 70˚C. They had reported the decrease in drying efficiency with increase in drying air temperature.

Meeso et al. (2012) developed the mathematical model for investigating the evolution of moisture content and qualities during air convection drying of pineapple rings. They had mentioned that the moisture diffusion coefficient values increase with increasing air temperature. The combination of high power ultrasound and convective air for drying of pistachios was performed in a laboratory scale ultrasonic dryer by Kouchakzadeh et al. (2012). They presented that the drying rate curves showed first rapid decrease in moisture ratio with time. Subsequently very little reduction in moisture ratio was observed with the increase in drying time. Marcos et al. (2013) studied the shrinkage, moisture loss and drying rate of pasta during the constant drying rate period. They predicted the drying time with an uncertainty of ±3.5 hour at a 90% confidence level and found strong influence of moisture diffusion coefficient on drying. Galvez et al. (2010) performed the dehydration of quinoa seeds with air temperature between 40˚C and 80˚C. It was observed that drying operation led to reductions of 10% in proteins, 12% in fat and 27% in both fibres and ashes. Similar studies were reported by Mabrouk et al. (2012) with special emphasis on drying kinetics. Sologubik et al. (2013) determined the physical properties of barley seeds as a function of moisture content. Effect of temperature and moisture content on

TH-1488_126103037

allowable storage time of wheat, oats, and barley are reported by Friesen and Huminicki (1987) shown in Fig. 2.1.

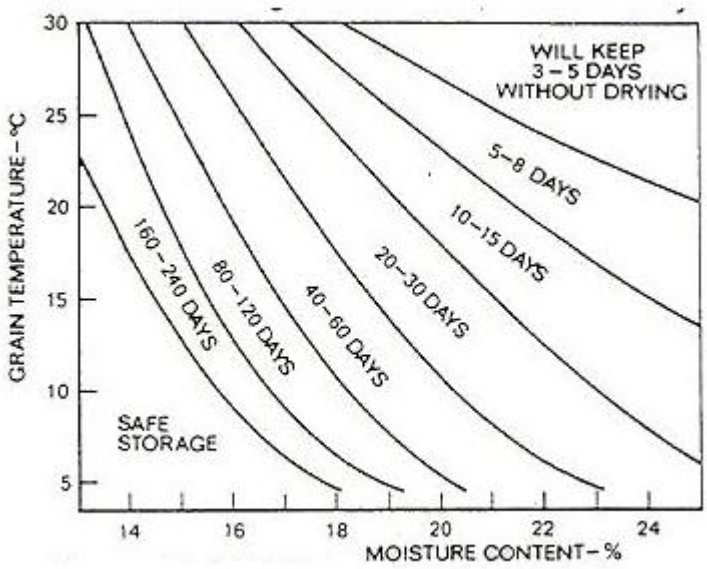

Fig. 2.1. Effect of temperature and moisture content on allowable storage time of wheat, oats, and barley. [Friesen and Huminicki (1987)]

Thin-layer drying tests were conducted by Khatchatourian et al. (2012) for soya bean in the temperature range 45 to 120˚C, velocity range 0 to 3 m/s, initial grain moisture content 0.13 to 0.32 dry basis with variations in relative humidity (RH) of air from 5 to 50%. They observed that the influence of velocity on drying dynamics depends on initial grain MC. They had mentioned that increase in air velocity led to acceleration in the drying process initially.Keum et al. (2011) reported drying of rapeseed at air temperature of 40, 50, and 60 ˚C and relative humidity levels of 30, 45, and 60%, respectively assuming thin layer drying. It was observed that the effective drying occurred in the falling rate period.

Malumba et al. (2012) assessed the effect of heat treatments on the extractability of salt-soluble protein (SSP) for corn kernels heated between 60˚C and 120˚C. They had reported that the temperature, moisture content and time of processing influenced the kinetic of SSP of corn kernels. Lightness and colour-intensity was found to decrease with increased in drying time. Wheat samples with initial moisture levels of 15 to 25% wet basis were dried by Hemis et al. (2012) under Microwave power for 3 min. The rate of drying increased with increase in the initial moisture content of wheat seeds. Thin layer drying characteristics of rice was studied by Hasan et al. (2014) at

TH-1488_126103037

the temperature levels of 40 ˚C, 50 ˚C and 60 ˚C, RH ranging 10 to 15% and air velocity ranging 0.55 to 0.65 m/s and they reported drying rate increases with the increase in drying air temperature. Thin-layer drying experiments of rough, brown and crushed rice for animal feed were conducted by Tanaka et al. (2014) to determine drying characteristics. Rice samples were dried at 40–80 ˚C with 10% RH and reported the optimum drying temperature of crushed rice was 80 ˚C.Summary of the literature on the effect of drying air temperature on the drying of various agricultural products are presented in Table 2.1.

Table 2.1 Effect of drying air temperature on various agricultural products drying

No	Researchers	Studies	Observations
1	Saxena et al. (2008)	commercial cabinet oven T= (50-90)˚C (water chestnut)	The drying efficiency value decreased while increasing the air temperature with the values varied from 91.17 to 89.66. The water chestnut dried at 70 ºC had better rehydration characteristics.
2	Meeso et al. (2012)	Combined far infrared radiation and air convection drying (40-60)˚C (pineapple rings)	The moisture diffusion coefficient values were found to increase with increasing air temperature.
3	Singh et al. (2011).	Forced convection type solar dryer	The air temperature in the drying chamber was 50–80 ºC and drying time for a batch of raw cocoons was 16–19 h depending upon intensity of sun and ambient temperature.
4	Galvez et al. (2010)	a convective dryer 40˚C- 420 min 80˚C-150 min (quinoa seeds)	High drying air temperature reduced nutritional values (10% in proteins, 12% in fat and 27% in both fibres and ashes).
5	Malumba et al. (2012)	Laboratory scale fluidized bed dryer (corn kernels) (60˚C and 120˚C)	Temperature, MC and time of processing influenced the kinetic of salt-soluble protein of corn kernels. Color decreased with increase in drying time
6	Hasan et al. (2014)	Thin layer drying, (40, 50, 60 ˚C), RH = 10 - 15% V = 0.55 - 0.65 m/s Rice	Drying rate increases with the increase in drying air temperature.
7	Tanaka et al. (2014)	Thin layer drying, 40–80 ˚C, 10% RH rough, brown and crushed rice	Optimum drying temperature of crushed rice was 80 ˚C.

TH-1488_126103037

2.3.2 Effect of relative humidity (RH) of air on drying

The quality of aromatic Pandanus leaves dried at low temperature (35˚C) and low RH (27%) in a heat pump dryer was evaluated by Rayaguru et al. (2010) and compared with those obtained from hot air drying at 45˚C. It was observed that the effect of low RH was prominent during the initial drying when the product was moist. The effect of temperature was prominent and hence the total drying time was reduced. The effect of drying air temperature and humidity on the drying kinetics of seaweed was studied by Fudholi et al. (2011) at air temperature of 40, 50 and 60˚C and relative humidity of 10, 25 and 40% in the Solar Energy Laboratory and they reported higher drying temperatures and low relative humidity reduced the moisture content rapidly. Drying of celery leaves was carried out by Roman and Hensel (2010) under different conditions of air temperature (20-50˚ C) and RH (10-60%) in a through-flow laboratory dryer. They reported that (1) both parameters influenced the drying time, although the effect of air temperature was more pronounced, (2)the effect of air RH was practically negligible at 50˚C. The higher the temperature, the lower the RH and hence the faster the drying rate. [Ajadi and Sanusi (2013)]

2.3.3 Effect of air velocity on drying

Keppler et al. (2012) carried out corn drying in a mixed flow dryer. They reported that large differences in velocity in this type of dryer are causing differences in the residence time. Uneven drying occurred causing under-drying or over-drying of grain portions. Akpinar (2005) conducted the drying of potato, apple and pumpkin slices at the drying air temperatures of 60, 70 and 80 ˚C and velocities of 1 and 1.5 m/s in a convective cyclone type dryer. They reported that the convective heat transfer coefficient increased in large amounts with the increase of the drying air velocity but increased in small amounts with the rise of the drying air temperature.

Drying of the garlic cloves was carried out by Sharma et al. (2009) in a laboratory scale microwave dryer applying microwave power in the range of 10–40 W, air temperature in the range of 40–70 ˚C and air velocity in the range of 1.0–2.0 m/s. They presented that the effective moisture diffusivity, which ranged between 1.29–31.68 × 10^{-10} m^2/s increased with the increase in microwave power but decreased with increase in air velocity.Thermal analysis in fluidized bed drying of moist particles was investigated by Syahrul et al. (2002) and reported that the moisture

TH-1488_126103037

transfer from the corn depends strongly on the air temperature, air velocity and the moisture content of material. Mellmann et al. (2011**)** studied the mixed-flow dryer at a semi-technical dryer test station with a transparent acrylic glass front wall using wheat as bed material. They presented that decrease in the particle–wall friction ratio results in even velocity distribution.

2.4DRYING WITH NATURAL CONVECTION

Drying of agricultural products in natural convection dryer is reported in literature extensively.Ginger slices were dried in a natural convection dryer by Pati et al. (2015) from initial MC 88-90% (w.b) to final MC 11-12% (w.b) with hot air maintained at temperature 60°C. They reported drying time is 5.5 h for 2 mm thick ginger slices. Drying of tapioca in a direct natural convection solar dryer was studied by Ogheneruona and Yusuf (2011). They presented 20 hours (two days drying period) is required for a batch of 100 kg tapioca from the initial MC 79 % to the final MC 10 % (w.b) at 32 ºC and 74 % RH with daily global solar radiation incident on horizontal surface of 13 MJ/m^2/day. Natural/forced convection solar vegetable dryer with heat storage was studied by Babagana et al. (2012) at the temperatures of 36-53˚C. They reported the drying time and the drying rate of tomato, onion, pepper, okra and spinach were 24, 27, 25, 21 and 2 hrs and 0.12, 0.08, 0.09, 0.11 and 0.39kg/h, respectively for the natural mode system whereas, revealed drying time and the drying rate were 14, 15, 12, 11 and 1 hr (s) and 0.20, 0.020, 0.21, 0.22 and 0.77 kg/h, respectively when using the forced mode system. Lerman et al. (2011) carried out the drying of wooden biomass in a small batch drier and indicated that the drying zone velocity increases with increasing drying temperature and air velocity.

Allaf et al. (2013) experimented different drying processes for drying of strawberry and reported that drying time of swell drying is shorter than that of classical hot air drying. Drying behaviour of paris was investigated in microwave, convective and microwave assisted convective drier by Pillai et al. (2013) and reported the values of specific energy consumption and the drying efficiency involved in the microwave process were 0.4557 MJ kg^{-1} and 82.56%, respectively. The effects of drying temperature and drying velocity on colour change of shrimp were investigated by Hosseinpour et al. (2013) at drying air temperatures of 50–90 ºC, superheated steam drying temperatures of 110–120 ºC, velocities of 1–2 m/s. They reported increasing

TH-1488_126103037

drying temperature increased color parameters. Zlatanovi et al. (2013) carried out experimental investigation of convective drying of apple in full recirculation laboratory scale dryer. It was observed that drying time decreased with increase in drying air temperature and velocity. In addition, drying time decreased with decrease in relative humidity and material sample size.

The drying behaviour of sweet potato was investigated in a cabinet convective air drying system by Pandey et al. (2012). They observed that the effect of temperature on effective diffusivity was correlated with an activation energy value of 11.38 kJ/mol. Mixed-mode solar dryer was studied by Bukola and Ayoola (2008) for drying of yam chips and reported that this dryer was able to remove 85.4% of moisture, dry basis, from 6.2 kg of yam chips in one day of 10 h drying time, which is about 0.62 kg/h drying rate.An intermittent hot air dehumidified air dryer, a heat pump dryer and a convective vacuum microwave dryer were studied by Chung et al. (2010) to dry fruits: apple, pear, papaya and mango. They reported the effective diffusivity value obtained by convective vacuum microwave dryer was between 7.08 x 10^{-8} to 4.30 x 10^{6} m/min and total drying time needed was between 310 to 490 minutes for drying of selected fruits.Martinello et al. (2013) reported low temperature/natural drying of grains depends strongly on the climate. Natural convection drier has been tested by Mohapotra et al. (2013) and reported that required drying time is 3hrs 30 min for 10 kg of paddy from initial MC of 30.1% to final MC of 14.6%. Summary of the literature of above researchers for drying with natural convection dryers are tabulated in Table 2.2.

Table 2.2 Drying with natural convection dryer

No	Researchers	Studies	Observations
1	Pati et al. (2015)	Natural convection dryer, IMC = 90%, FMC = 12% 60˚C, ginger	Required drying time is 5.5 hr for 2mm ginger slices.
2	Allaf et al. (2013)	swell drying and classical hot air drying (strawberry)	Drying time is shorter in case of swell dried compared to the classical hot air dried products
3	Hosseinpour et al. (2013).	hot air drying (50–90)ºC, superheated steam drying (110–120)ºC, (1–2) m/s.	Increasing drying temperature increased colour parameters.
4	Zlatanovi et al. (2013)	Laboratory scale convective air dryer (apple)	Drying time decreased with increase in drying air temperature and velocity.

TH-1488_126103037

5	Babagana et al. (2012)	Natural convection dryer, 36-53˚C, tomato, onion, pepper, okra and spinach	The drying time and the drying rate of tomato, onion, pepper, okra and spinach were 24, 27, 25, 21 and 2 hrs and 0.12, 0.08, 0.09, 0.11 and 0.39kg/h, respectively
6	Ogheneruona and Yusuf (2011).	Direct natural convection solar dryer, 32˚C and 74 % RH Tapioca	20 hours (two days drying period) is required for a batch of 100 kg tapioca from the initial MC 79 % to the final MC 10 % wet basis
7	Chung et al. (2010)	Convective vacuum microwave dryer (apple, pear, papaya and mango)	The effective diffusivity value was between 7.08 x 10^{-8} to 4.30 x 10^{6} m/min and total drying time needed was between 310 to 490 minutes for drying of selected fruits.
8	Bukola and Ayoola (2008)	Mixed-mode solar dryer, yam chips	This dryer was able to remove 85.4% of moisture, dry basis, from 6.2 kg of yam chips in one day of 10 h drying time, which is about 0.62 kg/h drying rate.
9	Martinello et al. (2013)	low temperature or natural drying (grains)	Low temperature/natural drying of grains depends strongly on the climate.
10	Mohapotra et al. (2013)	Natural convection drier using biomass with phase change material IMC = 30.1% FMC =14.6% , Paddy	Required drying time is 3hrs 30 min for 10 kg of paddy to attain the final MC of 14.6%.

2.5 DRYING WITH FORCED CONVECTION

Forced convection drying of different products are reported in literature. Bennamouna et al. (2015) carried out the convective drying of tomato and reported increasing air temperature deceased drying time from 1200 ks at 50˚C to 500 ks at 70˚C for the unpeeled tomato and from 80 ks at 60˚C to 50 ks at 70˚C for the peeled sample. The drying time of the unpeeled sample was 5–10 times higher than that of the peeled sample. The maximum values of the moisture diffusion coefficient for the peeled tomato varied from 3.0 × 10−10m^2/s at 50˚C to 5.0 × 10−10m^2/s at 70˚C.A laboratory scale microwave dryer was carried out by Sharma et al. (2009) to dry the garlic cloves, applying microwave power in the range of 10–40W, air temperature in the range of 40–70˚C and air velocity in the range of 1.0–2.0 m/s. They reported that heat and mass transfer coefficient during the drying process varied in the range of 35.23–79.54W/m^2C and 4.26–6.34×10^{-2} m/s and the effective moisture diffusivity, which ranged between 1.29–31.68×10^{-10} m^2/s increased with the increase in microwave

TH-1488_126103037

power but decreased with increase in air velocity. Solar greenhouse dryer was carried out by Elkhadraoui, et al. (2015) for drying of red pepper and grape and reported that 17 h and 50 h is required to get the final MC of 16% (w.b) for drying of red pepper and 18% (w.b) for grape. 76 h and 50 h is required drying of pepper and grape, respectively in open sun drying. The effect of open sun and indoor forced convection on heat transfer coefficients for the drying of papad was carried out by Kumar et al. (2011) and reported that the values of convective heat transfer coefficients under open sun drying and forced convection modes were 3.54W/m^2 ˚C and 1.56 W/m^2 ˚C and revealed experimental errors were 23.92% and 35.23%, respectively.

A solar assisted heat pump system with flat plate collectors and a water source heat pump has been proposed by Aktas et al. (2013) for drying mushroom. They reported the products could be dried with less energy input and more controlled conditions. The coefficients of performance of system were in a range from 2.1 to 3.1 and the energy utilization ratios were between 0.42 and 0.66. Specific moisture extraction rate values were between 0.26 and 0.92 kg/kW h. Sebaiia and Shalaby (2013) fabricated an indirect-mode forced convection solar dryer. Drying experiments were performed for thymus and mint at an initial temperature of 29 ˚C revealed that the drying times of thymus and mint depend on the mass of the drying product and temperature of the drying air. Sevik et al. (2013) reported solar dryer using a double pass solar air collector, heat pump and photovoltaic unit. Carrot slices were dried at 50˚C drying air temperature and variable air volume flow rate. The results showed the thermal efficiency of the double-pass collector was increased from 60% to 78% by the incorporation of the photovoltaic unit. Lamnatou et al. (2012) studied a thermodynamic performance analysis of a solar dryer with an evacuated tube collector for drying apples, carrots and apricots. It was observed that the warm outlet air of the collector attained temperature levels suitable for drying of agricultural products without the need of preheating.

Kumar et al. (2013) investigated drying kinetics of potato samples for various drying process variables viz., absorbed thermal energy, air mass flow rate, food sample thickness and loading density. The results indicated that dryer performance index can be used as a test parameter for performance comparison between different dryer designs. Hossain et al. (2013) reported the performance of heat pump dryer using

TH-1488_126103037

fixed bed drying for drying valerian root at an average drying temperature of 37˚C. They reported about 89 hours were required to reduce MC of valerian roots from 89 to 9% w.b. The average COP (coefficient of performance), MER (moisture evaporating rate) and SMER (specific moisture evaporating rate) and drying efficiency were 5.45, 140.03 kg/h, 0.038 kg/kWh, and 78.23%, respectively. Celma et al. (2012) experimented the thin layer drying behaviour of sludge from water treatment plants in tomato processing industries, using a convective dryer. The drying experiments were conducted at inlet drying air temperatures of 30-50 ˚C and at an airflow rate of 0.9 m/s and 1.3 m/s. They mentioned the drying rate increased with temperature and velocity, hence reducing the total drying time. Heat pump drying kinetics and quality characteristics of yacon at different drying temperatures and air velocities were investigated by Shi et al. (2013). Drying took place in the falling rate period. Drying time decreased with increasing drying temperature and air velocity. Drying temperature and air velocity had little effects on the color difference, shrinkage rate and rehydration rate of dried yacon slices.

The effect of multi-stage heat pump (HP) fluidized bed (FB) atmospheric freeze drying (AFD) and microwave vacuum drying (MVD) on the drying kinetics, moisture diffusivities, micro-structure and physical parameters of green peas was evaluated by Zielinska et al. (2013). They reported high product quality was achieved by HP FB AFD and MVD and increased the drying rates in the final stage due to application of microwave heating. Sahin et al. (2012) studied the effects of solar-assisted spouted bed and open sun drying on the drying rate and quality parameters of pea. They observed that drying rate for solar-assisted spouted bed was about 3.5 times of drying rate for open sun drying. Shrinkage was more for open sun dried samples. Dehydration capacity for solar-assisted spouted bed dried sample was higher than that for open sun dried samples.

A comparative simulation study on different intermittent heat pump dryings with respect to moisture diffusion, energy consumption and drying time on Chinese cabbage seeds was carried out by Yang et al. (2013). The resulted indicated that in intermittent drying, the percentage energy saving was 48.1% over continuous drying. The effect of spouted bed and microwave-assisted spouted bed drying on drying rates of parboiled wheat was investigated by Sahin et al. (2012). The results indicated

TH-1488_126103037

microwave-assisted spouted bed drying at microwave power of 3.5 W/g and 7.5 W/g reduced drying time by at least 60% and 85%, respectively compared to spouted bed drying. Doungporn et al. (2012) experimented the thin layer drying kinetics of dried Thai Hom Mali paddy using different drying gases (hot air, CO_2 and N_2), initial MC of 32% d.b was dried in a heat pump dryer at 0.4 m/s velocity, drying temperatures of 40, 50, 60 and 70 ˚C, respectively. It was observed that drying rate was not affected by drying gases but increased with drying temperatures. Summary of the literature of above researchers for the forced convection type dryers for cereal crop drying are tabulated in Table 2.3.

Table 2.3 Drying with forced convection dryer

No	Researchers	Studies	Observations
1	Aktas et al. (2013)	solar assisted heat pump, water source heat pump (mushroom)	Products could be dried with less energy input and more controlled conditions. EUR (0.42-0.66), COP (2.1-3.1)
2	Sebaiia and Shalaby (2013)	indirect-mode forced convection solar dryer (29 ºC), (mint)	Drying time depend on the mass of the drying product and temperature of the drying air.
3	Sevik et al. (2013)	solar dryer with heat pump and photovoltaic unit. (50˚C), (Carrot)	The thermal efficiency of sloar dryer was increased from 60% to 78% by the incorporation of the photovoltaic unit.
4	Lamnatou et al. (2012)	solar dryer with an evacuated tube collector (apple)	The warm outlet air of the collector attains temperature levels suitable for drying of agricultural products without the need of preheating.
5	Chandrakumar et al. (2013)	mixed-mode solar dryer	Larger values of absorbed energy and load density resulted in increased specific energy consumption.
6	Celma et al. (2012)	convective dryer (tomato),(30-50)°C (0.9 -1.3) m/s	The drying rate increased with temperature and velocity, hence reducing the total drying time.
7	Shi et al. (2013)	Heat pump (yacon)	Drying took place in the falling rate period. Drying time decreased with increasing drying temperature and air velocity.
8	Bennamouna et al. (2015)	convective drying, tomatoe	Increasing air temperature deceased drying time from 1200 ks at 50˚C to 500 ks at 70˚C for the unpeeled tomatoe and from 80 ks at 60˚C to 50 ks at 70˚C for the peeled sample.

TH-1488_126103037

9	Shrama et al. (2009)	laboratory scale microwave dryer, 10-40W, 40-70˚C, 1-2 m/s, garlic	Heat and mass transfer coefficient during the drying process varied in the range of 35.23–79.54W/m^2C and 4.26–6.34×10^{-2} m/s and the effective moisture diffusivity, which ranged between1.29–31.68×10^{-10} m^2/s increased with increase in microwave power but decreased with increase in air velocity.
10	Elkhadraoui, et al. (2015)	Solar greenhouse dryer, pepper and grape	17 h and 50 h is required to get the final MC of 16% (w.b) for drying of red pepper and 18% (w.b) for grape using solar green house dryer whereas it took 76 h and 50 h, respectively in open sun drying
11	Kumar et al. (2011)	open sun drying and indoor forced convection drying papad	The values of convective heat transfer coefficients under open sun drying and forced convection modes were 3.54W/m^2 ˚C and 1.56 W/m^2 ˚C and revealed experimental errors were 23.92% and 35.23% respectively.
12	Zielinska et al. (2013).	heat pump fluidized bed atmospheric freeze drying (HP FB AFD) and microwave vacuum drying (MVD) (green peas)	High product quality was achieved by HP FB AFD and MVD and increased the drying rates in the final stage due to application of microwave heating.
13	Sahin et al. (2012)	solar-assisted spouted bed and open sun drying (pea)	Drying rate for solar-assisted spouted bed was about 3.5 times of drying rate for open sun drying. Rehydration capacity for solar-assisted spouted bed dried sample was higher than that for open sun dried samples.
14	Yang et al. (2013)	intermittent heat pump drying (cabbage seeds)	In Intermittent drying, the percentage energy saving was 48.1% over continuous drying.
15	Sahin et al. (2012).	spouted bed and microwave-assisted spouted bed (wheat)	Microwave-assisted spouted bed drying at microwave power of 3.5 W/g and 7.5 W/g reduced drying time by at least 60% and 85%, respectively compared to spouted bed drying.
16	Doungporn et al. (2012)	Thin layer drying in Heat pump dryer (hot air, CO_2, N_2) (40-70)˚C, (Paddy)	Drying rate was not affected by drying gases but increased with drying temperatures.

TH-1488_126103037

2.6 FLUIDIZED BED DRYING

Fluidized bed drying is extensively employed for drying wet particulate and granular materials. Fluidized bed drying has many advantages like uniform moisture content and fineness of the products, effective control of final moisture content, automatically operate, good mixing of solids, high rate of heat and mass transfer, easy material transport, very fast pre-drying, high capacity, requires less space and able to increase milling yield. However, this drying system drops the MC to 18% only for pre-drying and high blower power costs in addition to the heat requirement for drying [Isvilanonda and Wattanutchariya, (1999)]. The process parameters for fluidized bed dryer are mainly drying medium temperature, capacity of dryer, distributor structure and vessel geometry, type of heater, mode of feeding (continuous or batch), etc [Kunii and levenspiel (1991)].

2.6.1 Hydrodynamic effect

Bizmark et al. (2010) studied the sequential modelling of fluidized bed paddy dryer and observed that the drying kinetics and fluidized bed hydrodynamics affect the behaviour of the dryer. Wilde (2014) reviewed the gas–solid fluidized beds in vortex chambers. Lim et al. (2014) investigated the hydrodynamic characteristics of gas–solid fluidized beds with shroud nozzle distributors and it was found that the bed pressure drop fluctuation is proportional to the superficial gas velocity. Bizhaem and Tabrizi (2013) investigated hydrodynamic characteristics of gas–solid pulsed fluidized bed experimentally and observed that the pulsating airflow decreases the minimum fluidization velocity and enhances fluidization of fine cohesive particles. The hydrodynamic and heat transfer characteristics at four different % (2.5%, 7.5%, 12.5% and 20%) mixing of biomass in sand in a pressurized circulating fluidized bed have been investigated by Kalita et al. (2013) at superficial velocities of 6, 7 and 8 m/s and system pressures of 1, 3 and 5 bar. They reported that higher pressure and higher superficial velocity is found favourable for achieving a higher heat transfer coefficient and biomass blending of 12.5% in sand and a pressure of 5 bar are found to be the optimum to achieve a maximum wall to bed heat transfer coefficient and uniform circulation rate.

TH-1488_126103037

2.6.2 Drying characteristics in fluidized bed

Hematian and Hormozi (2015) investigated the drying behaviour of a batch fluidized bed dryer and observed that the moisture ratio decreased continuously with time. Djomeh et al. (2013) modelled moisture distribution and temperature variation in apple cubes in a microwave-assisted fluidized bed drier. They reported microwave energy enhanced the drying rate and samples were dried faster. Hung et al. (2013) reported individually drying of blueberry and Powder blue in a fluidized bed dryer, an air-impingement dryer and forced air dryer at 85°C and 107 °C. They presented drying times were about 50% longer at 85 °C compared to 107 °C and fluidized bed dryer was fastest followed by air-impingement dryer and forced air dryer to achieve the required moisture content. They reported drying method and drying temperature had significant effect on drying time. Velazquez et al. (2013) studied fluidized bed drying using near infrared spectroscopy to dry and measure moisture content and other granular materials' attributes. They presented airflow and inlet air temperature were controlled based on the physical and chemical behaviour of the process and resulted in a reduction in energy consumption of up to 60% when compared with the current industrial practices. Gornicki et al. (2013) reported the drying behaviour of apple dried in a fluidized bed dryer. It was observed that increase in drying air temperature caused a decrease in the drying time and an increase in drying rate. They reported the values of the drying rate constant and moisture diffusion coefficient increased with the increase in drying air temperature. Drying temperature did not influence the shrinkage of apple cubes.

Villegas et al. (2009) studied that a distributed parameter approach was used to model and control a batch fluidised bed dryer. The experimental results showed that it can be successfully used to control a batch fluidized bed dryer even though using only inlet air velocity as manipulated variable imposes some restrictions on the shapes that can be achieved. Geng et al. (2009) reported three-dimensional Euler–Euler model simulations carried out to examine the gas–particle flow behaviour of tobacco material in a fluidized bed dryer. The simulation results indicated that tobacco particles usually concentrate in the near-wall region, and there exists a maximum particle concentration in the feed pipe. They reported the particle clusters can directly influence the dryer efficiency and quality of the product. The numerical experiments indicated that the better uniformity in particle distribution can be obtained by

TH-1488_126103037

improvement in the process variables. Okoronkwo et al. (2013) carried out fluidized bed dryer performance in drying of cassava and reported that drying at temperature below the optimal temperature results in lower rate of moisture removal and longer drying time. Drying above the optimum temperature leads to products having physical defects such as decoration, cracking, shrinking and non-uniform drying.

Oluwaleye and Adeyemi (2013) reported uniform drying of products were achieved using a batch hot air fluidized bed dryer. Law et al. (2004) experimentally investigated the effect of vertical baffles in batch fluidized bed dryer. The study involving installation of inner vertical baffles revealed improvement in the performance of the fluidized bed dryer and it is useful for a large scale fluidized bed system processing group D particles. They reported drying rate increased 10% to 25%. Thao et al. (2011) carried out experiments for establishing the drying behaviour of sweet potato starches under tray, infrared and fluidized bed drying at temperatures in the range 45, 55 and 65 °C. The results indicated that to reach a final moisture content of 10 %, the respective drying time at these temperatures were 15, 8.5 and 5.5 h for tray drying, 12, 6.5 and 4.5 h for infrared drying and for 0.42, 0.28 and 0.2 h fluidized bed drying. They reported the activation energies in tray and infrared drying were nearly double that for fluidized bed drying.

Srinivasakannan et al. (2012) studied that spirals as internals are utilized to reduce the axial mixing of solids in fluidized beds by localizing the solids mixing. The results indicated that the kinetic parameter increased with temperature. They reported the drying rate in the continuous bed increased with increase in temperature and height of the down comer. The drying rate in a continuous fluidized bed is lower than the rate of drying in batch fluidized bed, while the drying rate in a continuous fluidized bed with internals approximates drying rate in batch fluidized bed. Fluidized bed drying kinetics on the basis of inter-phase mass transfer coefficient and the conception of general kinetic curve has been experimented by Ciesielczyk and Iwanowski (2006) and observed this method of presentation of drying kinetics can be fully recommended for substances from B group of Geldert classification. The drying kinetics of castor oil seeds during fluidized bed drying at a constant air velocity of 7 m/s and high air temperatures (80, 90, 100, 110 ◦C) were studied by Pereza et al. (2012). From the findings, simulation of fluidized bed drying of Communis seeds

TH-1488_126103037

between 80 and 110 °C could be established successfully. Meeso et al. (2011) observed that combined near infrared radiation and fluidized-bed drying reduced cracking and breakage of soybean grains.

Janas et al. (2010), by means of a finite element method, accurately modelled the evolutions of moisture and salt-soluble protein content in maize during fluidized-bed drying with constant drying air temperature between 50˚C and 100˚C. They presented the initial protein content heterogeneity and the evolution of moisture content spatial heterogeneity during the process significantly influenced the salt-soluble protein.Khanali et al. (2012) carried out fluidized bed drying experiments for rough rice for drying at air temperatures of 50 - 70 °C and velocities of 2.3 - 2.8 m/s. It was observed that increase in drying air temperature increased the drying rate. They presented the drying rate increased marginally with increase in air velocity. Bed-to-wall heat transfer coefficient was studied by Kalita et al. (2014) at the upper splash region of a pressurized circulating fluidized bed riser of internal diameter 54 mm and height of 2000 mm and reported the overall uncertainty in calculating the heat transfer coefficient was ±12.3%. Demir et al. (2014) studied the batch type fluidized bed drying of corn and unshelled pistachio nut and observed that an increase in the drying air velocity reduces the total drying time.Srzednicki et al. (2010) conducted drying experiments in the fluidized bed dryer and spouted bed dryer at temperature 40-80°C using maize, rice and wheat seed. They reported Page's model and two-compartment model models could efficiently predict the drying curves under a wider range of temperatures.

Momenzadeh et al. (2011) researched shrinkage of shelled corn in microwave-assisted fluidized bed drying. It was observed that employing microwave in fluidized bed drying reduces the shrinkage of particles. The effects of heat and mass transfer parameters on the efficiency of fluidized bed drying have been studied by Inaba et al. (2006) to optimize the input and output conditions. It was observed that energy and exergy efficiencies decrease sharply with decreasing moisture content of the wheat and corn. They reported increasing drying air temperature increased the exergy efficiencies of the drying process. The efficiency was slightly higher for the grain material with higher initial moisture content. Pena (2011) reported that bubbling fluidized bed technology offers good performance in terms of efficiency, fuel

TH-1488_126103037

flexibility, and emissions. Mehdizadeh et al. (2008) treated the rough rice, medium and long grain in the fluidized bed drier at 140˚C for 2 minutes and 8-10 hrs by the traditional method. It was found that paddy drying in a fluidized bed dryer at 140˚C would reduce the quality factors. Summary of the literature of above researchers for the drying characteristics of fluidized bed drying are tabulated in Table 2.4.

Table 2.4 Drying characteristics in fluidized bed dryer.

No	Researchers	Studies	Observations
1	Hematian and Hormozi (2015)	conical fluidized bed dryer, (60-80)˚C, (90-120) m^3/hr	Moisture ratio decreased continuously with time.
2	Hung et al. (2013)	fluidized bed dryer, air-impingement dryer and forced air dryer (85, 107)˚C (blueberry)	Drying times were about 50% longer at 85 °C compared to 107 °C. Fluidized bed dryer was fastest followed by air-impingement dryer and forced air dryer to achieve the required moisture content. Drying method and drying temperature had significant effect on drying times.
3	Thao et al. (2011)	tray, infrared and fluidized bed drying (sweet potato) (45, 55, 65) °C	Drying times were 15, 8.5 and 5.5 h for tray drying, 12, 6.5 and 4.5 h for infrared drying and for 0.42, 0.28 and 0.2 h fluidized bed drying. The activation energies in tray and infrared drying were nearly double that for fluidized bed drying.
4	Geng et al. (2009)	Simulation of fluidised bed dryer (tobacco)	The particle clusters directly influence the dryer efficiency and quality of the product
5	Djomeh et al. (2013)	microwave-assisted fluidized bed drier (apple)	Microwave energy enhanced the drying rate and samples were dried faster.
6	Pereza et al. (2012)	Fluidized bed dryer laboratory scale Di = 9.6 cm, H = 43cm (80-110)˚C, 7m/s Castor oil seeds	Effective moisture diffusivity was in the range of 8.21×10^{-10} to 2.61×10^{-9} m^2/s. An activation energy value of 41.41 kJ/mol was obtained.
7	Velazquez et al. (2013)	fluidized bed using near infrared spectroscopy	A reduction in energy consumption of up to 60% when compared with the current industrial practices.
8	Gornicki et al. (2013)	Bubbling fluidized bed (BFB) dryer D = 12 cm, H = 180cm, (40-80)˚C, 6	Increase in drying air temperature caused a decrease in the drying time and an increase in drying rate

TH-1488_126103037

		m/s, MC = 87% w.b, (apple)	
9	Oluwaleye and Adeyemi (2013)	Bubbling fluidized bed dryer, D = 400 mm, H = 2960 mm,(cassava) (60-160)˚C, (0.043, 0.05, 0.056)kg/s	Uniform drying of products were achieved using a batch hot air fluidized bed dryer.
10	Srinivasakannan et al. (2012)	Continuous fluidized bed drying with and without spirals	The drying rate in a continuous fluidized bed is lower than the rate of drying in batch fluidized bed. The drying rate in a continuous fluidized bed with spirals approximates drying rate in batch fluidized bed.
11	Okoronkwo et al. (2013)	Bubbling fluidized bed dryer IMC 75%, FMC 11%, 60˚C, 2.5hrs (Sun drying, 30˚C, 72 hrs) (cassava)	Drying at temperature below the optimal temperature results in lower rate of moisture removal and longer drying time.
12	Meeso et al. (2011)	combined near infrared radiation and fluidized-bed drying (soybean)	This drying system reduced cracking and breakage of soybean grains.
13	Özahi and Demir (2014)	Bubbling batch fluidized bed dryer (corn)	An increase in the drying air velocity reduces the total drying time.
14	Momenzadeh et al. (2011)	microwave-assisted fluidized bed drying (corn)	Employing microwave in fluidized bed drying reduces the shrinkage of shelled corn
15	Janas et al. (2010)	Bubbling fluidized-bed drying (D = 0.12 m, H = 1.6 m), (50, 65, 80, and 100)˚C 5.8 m/s. (maize)	The initial protein content and the evolution of MC during the process significantly influence the salt-soluble protein.
16	Inaba et al. (2006)	fluidized bed drying (wheat and corn)	Energy and exergy efficiencies decrease with decreasing MC of the wheat and corn. Increasing drying air temperature increased the exergy efficiencies of the drying process.
17	Law et al. (2004)	Bubbling batch fluidized bed dryer (Paddy)	Installation of inner vertical baffles improved the performance of fluidized bed dryer and useful for large scale fluidized bed system processing group

TH-1488_126103037

			D particles. A drying rate increased 10% to 25%.
18	Khanali et al. (2012)	fluidized bed drying (rough rice) (50 – 70)°C, (2.3-2.8)m/s	Increase in drying air temperature increased the drying rate. The drying rate increased marginally with increase in the velocity of the drying air.
19	Mehdizadeh et al. (2008)	fluidized bed drying (rough rice)	Paddy drying in a fluidized bed dryer reduced the grain quality at 140˚C for 2 min.
20	Pena (2011)	Bubbling fluidized bed	Bubbling fluidized bed technology offers good performance in terms of efficiency, fuel flexibility, and emissions.

2.6.3 Effect of distributor plate design on fluidization

Samson et al. (2015) investigated a multi-orifice distributor for a gas-fluidized bed and observed that the swirling flow induced by the helix significantly improved the fluidization quality. Chyang et al. (2008) investigated the effect of distributor design on gas dispersion in a bubbling fluidized bed and observed that the effect of superficial gas velocity on the gas mixing depends on the distributor type. The influence of the distributor configuration on inter-phase mass transfer, gas axial dispersion and bubble size was studied by Brink et al. (2011) in fluidized bed reactor. Sobrino et al. (2009) investigated the distributor effects in fluidized beds and observed that the distributor plate has a significant effect on the bed distributor pressure drop decreased at higher temperatures for the same gas velocity. Sobrino et al. (2008) carried out the fluidization of group B particles with a rotating distributor and observed that an increase in the measured pressure drop when the rotational speed was increased. Nakamura et al. (2013) investigated experimentally the improvement of particle mixing and fluidization quality in rotating fluidized bed by inclined injection of fluidizing air and observed that the particle mixing in the rotational axis direction improved when the air distributor with inclined holes was used. Prieto et al. (2014) investigated the effect of temperature on the distributor design in bubbling fluidized beds and observed that the distributor pressure drop decreased at higher temperatures for the same gas velocity. Summary of the literature of above researchers for the effect of distributor plate design of fluidized bed dryers for cereal grains drying are tabulated in Table 2.5.

TH-1488_126103037

Table 2.5 Effect of distributor design on drying

No	Researchers	Studies	Observations
1	Samson et al. (2015)	multi-orifice distributor for a gas-fluidized bed	Swirling flow induced by the helix significantly improved the fluidization quality
2	Chyang et al. (2008)	bubbling fluidized bed	Effect of superficial gas velocity on the gas mixing depends on the distributor type.
3	Sobrino et al. (2009)	distributor effects in fluidized beds	Distributor plate has a significant effect on the bed hydrodynamics.
4	Sobrino et al. (2008)	rotating distributor	An increase in the measured pressure drop when the rotational speed was increased.
5	Nakamura et al. (2013)	rotating fluidized bed	Particle mixing in the rotational axis improved when the air distributor with inclined holes was used.
6	Prieto et al. (2014)	bubbling fluidized beds	Distributor pressure drop decreased at higher temperatures for the same gas velocity.

2.7 ENERGY CONSUMPTION

Energy consumption of various dryers and for drying of different materials are reported in literature.Panwar et al. (2012) studied the solar dryers and reported that exergy efficiency is the actual efficiency of the process. Total energy efficiency is high in spite of low total exergy efficiency. A comprehensive literature review has been carried out on exergy analysis of various solar energy systems by Saidur et al. (2012) and observed exergy efficiency of solar systems is highly dependent on the daily solar radiation and radiation intensity. A gas engine heat pump drying system was analysed by Hepbasli et al. (2013) using both conventional and advanced exergy analyses for drying aromatic plants. They performed drying experiments at an air temperature of 45˚C with an air velocity of 1 m/s and reported the improvement in exergy efficiency for the heat pump from and for the entire drying system to be 6 in the range of 82.51–85.11% and 79.71–81.66%, respectively. A microscopic energy and exergy analysis for an indirect solar cabinet dryer was modelled by Sami et al. (2011). The maximum outlet exergy and energy of collector were reported by them to be 2.5 kW and 1.12 kW, respectively with an outlet air temperature of 69˚C. The minimum total exergy efficiency was found to be 32.3% and 47.2%, respectively. They presented that the total energy efficiency was high in spite of low total exergy efficiency. The energy and exergy analyses of the drying process of olive mill wasted

TH-1488_126103037

water using an indirect type natural convection solar dryer are studied by Celma et al. (2009) using temperature between 34˚C and 52˚C, solar radiation ranged from 227 W/m^2 to 825 W/m^2, and drying air mass flow in the range 0.036–0.042 kg/s. They reported that exergy losses took place, when the available energy was less used. The exergetic efficiencies of the drying chamber decreased as inlet temperature were increased.

Energy efficiency during drying brown algae based on heat circulation with and without steam recirculation was evaluated by Aziz et al. (2013) and reported that this drying process could significantly reduce the energy required for drying compared to the conventional drying process employing based on heat cascade-utilization technology. They presented exergy recovery through exergy elevation and heat pairing applied in heat circulation can recuperate the energy involved in drying effectively. An energy and exergy analysis was carried out on the process of fish oil microencapsulation using spray drying by Aghbashlo et al. (2012) at drying air temperatures of 140, 160, and 180˚C. They report that energy and exergy efficiency values for spray drying process of fish oil microencapsulation at the drying air temperature between 140 and 180˚C were in the ranges of 7.48 to 8.54% and 5.25 to 7.42%, respectively.

The energy and exergy analysis of the thin layer drying process of mulberry via forced solar dryer was studied by Akbulut et al. (2010) and concluded that both energy utilization ratio and exergy loss decreased with increasing drying mass flow rate while the exergetic efficiency increased. Energy and exergy analyses of thin-layer drying of sour pomegranate arils with micro-wave treatment were conducted by Minaei (2013) using the air temperature (50, 60 and 70˚C) and air velocity (0.5, 1 and 1.5m/s). The results indicated energy utilization and energy utilization ratio increased with time, while exergy efficiency decreased with time. Characteristics of thin layer microwave drying of apple were evaluated by Zarein et al. (2015) in a laboratory scale microwave dryer and reported that the highest energy efficiency for the samples dried at 600 W was 54.34% and lowest at 200 W was 17.42%. A solar dryer developed using an evacuated-tube collector by Lamnatou et al. (2012) could dry agricultural products without preheating the outlet air. They reported this dryer has

TH-1488_126103037

the capacity for drying larger quantities of products due to the high efficiency of the collector.

Rattanadecho et al. (2012) reported the energy and exergy analyses in the drying process of non-hygroscopic porous packed bed by combined multi-feed microwave-convective air and continuous belt system. The results indicated energy utilization ratio and exergy efficiency also depend on particle sizes and hot air temperature. Analysis for batch fluidized bed dryer was performed by Assari et al. (2013) for drying wheat. Energy utilization ratio were reported to be as 55.2%, 32.19%, 29.2%, 21.5% and 20.5%, respectively for the five different mass flow rate ranged between 0.014 kg/s and 0.036 kg/s. They observed exergy loss were 10.82 W, 6.41 W, 4.92 W, 4.06 W and 2.65W, respectively. They reported the increase of the inlet gas temperature increased thermodynamic efficiencies and increasing particle size will decrease both efficiencies. Ozahi and Demir (2015) studied the drying performance of a batch type fluidized bed regarding energetic and exergetic efficiencies for drying of corn. They reported that both energetic and exergetic efficiencies are strongly dependent on air mass flow rate, particle mass and MC of particle to be dried.

Determination of optimal conditions for fluidized bed paddy drying and adaptive fuzzy logic control was investigated by Atthajariyakul and Leephakpreeda (2006). They presented the proposed method control the optimal conditions for fluidized bed paddy drying system that maintains paddy moisture content closed to the desire level with efficient energy consumption. Sarker et al. (2015) studied the energy and exergy analysis of industrial fluidized bed drying of paddy and suggested that exergy can be increased through providing sufficient insulation on dryer body and recycling the exhaust air. Jittanit et al. (2010) studied that the energy consumption of paddy drying in a large-scale milling plant. The results indicated that the current drying in the plant consumed specific primary energy of between 3.87- 4.42 MJ/kg of water evaporated. In two-stage drying, fluidised bed dryer was used as first stage at air temperature of between 100 and 110˚C. They concluded lower exergy efficiency leads to higher environmental impact and energy cost. Ozahi and Demir (2013) studied the thermodynamic analysis in a batch type fluidized bed dryer and observed that the effect of air mass flow rate has significant role on exergetic efficiency. Golmohammadi et al. (2015) investigated energy efficiency of intermittent paddy

TH-1488_126103037

dryer experimentally and observed that employing the tempering stages substantially reduced the energy consumption. Sarker et al. (2015) studied the industrial scale fluidized bed paddy dryer and observed that the dryer capacity was limited during drying paddy of higher initial MC. Summary of the literature of above researchers for the energy consumption of various dryers for cereal grains drying are tabulated in Table 2.6.

Table 2.6 Energy consumption on various dryers

No	Researchers	Studies	Observations
1	Hepbasli et al. (2013)	engine heat pump (GEHP) drying system, 45˚C, 1m/s, (aromatic plants)	Exergy efficiency of modified GEHP drying system (85.70–89.26)% was higher than that of conventional one (82.51–85.11)%.
2	Panwar et al. (2012)	Solar dryers	Exergy efficiency is the actual efficiency of the process. Total energy efficiency is high in spite of low total exergy efficiency.
3	Akbulut et al. (2010)	Forced solar dryer (mulberry)	Energy utilization ratio (55.2, 32.19, 29.2, 21.5 and 20.5)% and exergy loss (10.82, 6.41, 4.92, 4.06 and 2.65) W decreased with increasing drying mass flow rate (0.014 - 0.036) kg/s while the exergetic efficiency increased.
4	Sami et al. (2011)	indirect solar cabinet dryer	The total energy efficiency was high in spite of low total exergy efficiency Increasing the air flow rate decreases the exergy efficiency of solar collector.
5	Celma (2009)	indirect type natural convection solar dryer (olive mill)	The exergetic efficiencies of the drying chamber (100-34.4) % decreased as inlet temperature was increased (34-52) ˚C.
6	Minaei et al. (2013)	thin-layer drying with micro-wave treatment (50, 60, 70)˚C (0.5, 1, 1.5) m/s pomegranate arils	Energy utilization and energy utilization ratio increased with time, while exergy efficiency decreased with time.
7	Zarein et al. (2013)	laboratory scale microwave dryer (200, 400, 600)W (apple)	The highest energy efficiency was 54.34% at 600W and lowest energy efficiency was 17.42% at 200W.
8	Aziz et al. (2013)	heat circulation with and without steam recirculation	Exergy recovery through exergy elevation and heat pairing applied in heat circulation can recuperate the energy involved in drying effectively.

TH-1488_126103037

9	Tsutsumi et al. (2012)	advanced drying system (self-heat recuperation technology) Coal	This system reduced the energy consumption 70% compared to conventional heat recovery drying system
10	Saidur et al. (2012)	Solar energy systems	Exergy efficiency of solar systems is highly dependent on the daily solar radiation and radiation intensity.
11	Aghbashlo et al. (2012)	Mini-spray dryer (fish oil)	The energy and exergy efficiency values for spray drying process of fish oil microencapsulation at the drying air temperature between 140 and 180˚C were found to be in the ranges of 7.48 to 8.54% and 5.25 to 7.42%, respectively.
12	Lamnatou et al. (2012)	solar dryer using an evacuated-tube collector (agricultural products)	The proposed dryer has the capacity for drying larger quantities of products due to the high efficiency of the collector.
13	Rattanadecho et al. (2012)	Packed bed with combined microwave-convective air and continuous belt system	Energy utilization ratio and exergy efficiency also depend on particle sizes and hot air temperature.
14	Assari et al. (2013)	batch fluidized bed dryer (wheat)	Lower exergy efficiency leads to higher environmental impact. The increase of the inlet air temperature increased thermodynamic efficiencies. Higher inlet air velocity decreased the thermodynamic efficiencies. Increasing particle size decreased both efficiencies.
15	Ozahi and Demir (2015)	batch type fluidized bed dryer (corn)	Energetic and exergetic efficiencies are strongly depend on air flow rate, particle mass and MC of particle to be dried.
16	Ozahi and Demir (2013)	Batch fluidized bed dryer	Effect of air mass flow rate has significant role on exergetic efficiency.
17	Atthajariyakul and Leephakpreeda (2006)	Fluidized bed dryer (Paddy)	The proposed method control the optimal conditions for fluidized bed paddy drying system that maintains paddy moisture content closed to the desire level with efficient energy consumption.
18	Golmohammai et al. (2015)	intermittent paddy dryer	Employing the tempering stages substantially reduced the energy consumption.
19	Sarker et al. (2015)	industrial scale fluidized bed paddy dryer	Dryer capacity was limited during drying paddy of higher initial MC.

TH-1488_126103037

20	Jittanit et al. (2010)	paddy drying in a large-scale milling plant	The plant consumed specific primary energy of between 3.874 and 4.421 MJ/kg of water evaporated.
21	Sarker et al. (2015)	industrial fluidized bed drying of paddy	Exergy can be increased through providing sufficient insulation on dryer body and recycling the exhaust air.

2.8 INCLINED BEDS

The dynamics and structure of a fluidized bed in inclined columns were investigated experimentally by Yakubov et al., (2007). The results showed the expansion process of the fluidized bed depends strongly on the inclination angle. Consequently the critical velocity for the bed escape varied with the column inclination angle. They reported the column length is a minor effect on the phenomena involved. The performance evaluation of an industrial inclined bed dryer (IBD) was carried out by Sarker et al., (2014). They reported the specific electrical energy consumption was lesser and the specific thermal energy consumption of IBD was higher during drying with air temperature of 41–42°C than drying with 38–39˚C. They presented the bed air flows resulted in higher head rice yield slightly.

2.9 TECHNICAL GAP

An extensive literature review was conducted regarding drying of various agricultural products. It was observed that research towards design and development of various dryers and their performance in terms drying rate, time and thermal energy, etc is popular and widely cited. It is observed that fluidized bed drying is superior to the traditional sun drying and natural convection solar drying [Pena (2011)]. However, fluidized bed drying is reported to be energy intensive with involvement of many complicated parametric relations. [Atthajariyakul and Leephakpreeda (2006), Ozahi and Demir (2015), Rattanadecho et al. (2012), Minaei et al. (2013), Sarker et al. (2015)] A few studies have been reported regarding use of inclined fluidized bed to reduce the energy consumption. However, detail experimental findings in such bed are hardly reported. Present study is an attempt towards design, development and performance analysis of cereal crop drying using an inclined fluidized bed under bubbling regime.

TH-1488_126103037

2.10 SUMMARY

In the present section, extensive literature review is conducted various types of dryers and types of products. In the next chapter, experimental set up and procedure are described.

TH-1488_126103037

CHAPTER 3

EXPERIMENTAL SET UP AND PROCEDURE

3.1 INTRODUCTION

The experimental methodology followed for achieving the objectives of the present work are detailed in the present chapter. This includes design and development of the experimental setup, calibration, and experimental procedure followed for carrying out the work.

3.2EXPERIMENTAL SETUP

The schematic diagram of experimental setup i.e. the inclined bubbling fluidized bed (BFB) dryer is shown in Fig. 3.1

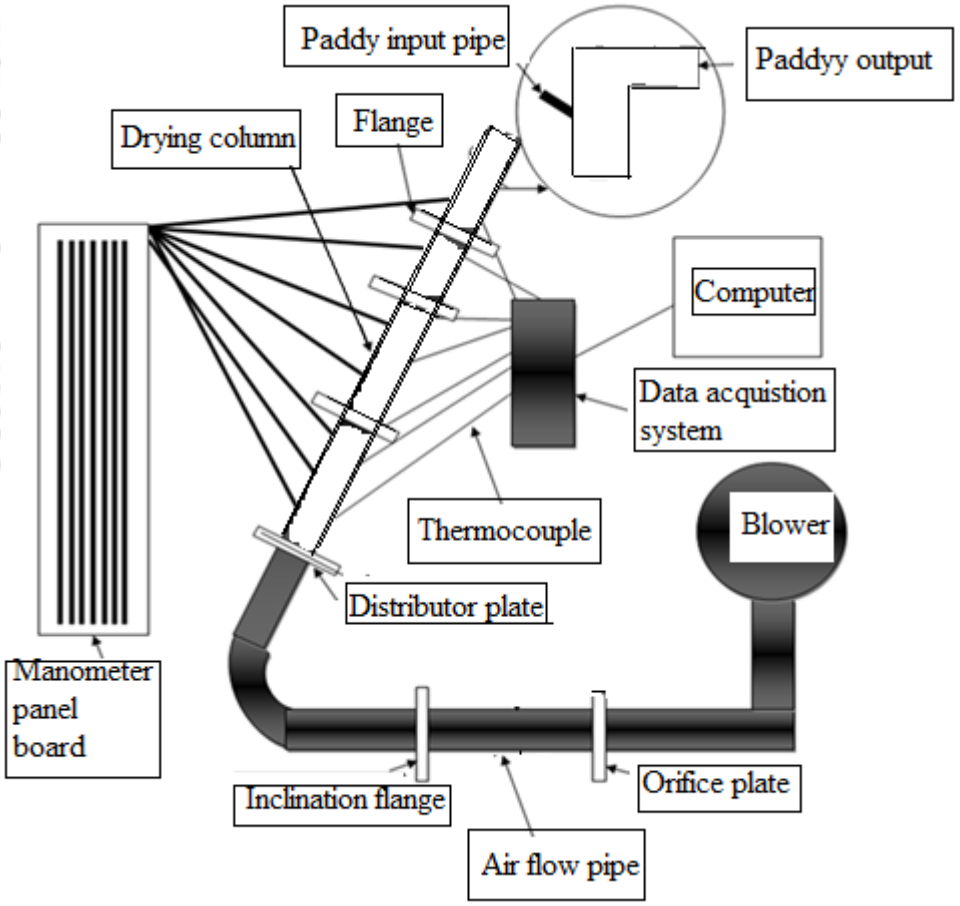

Fig. 3.1 Systematic diagram of Inclined Bubbling Fluidized Bed Dryer

It consists of a centrifugal blower powered by a 15 HP electric motor, three electric heaters each of 1kW capacity fitted inside the air flow pipe, orifice plate, distributor plate, dryer column, manometer, thermocouples and data acquisition system. The

TH-1488_126103037

internal cross sectional area of the dryer (riser column) is 100 mm x 100 mm and the column height is maintained at 1440 mm. 26 (twenty six) pressure taps were used to measure the fluidized bed pressure drops on two parallel sides of the column. The pressure drops were measured with manometers using water as the manometer fluid. The dryer column was fabricated from Perspex for visual observation. The bed is fabricated in such a way that it can be inclined from vertical position at an interval of 15˚ inclination.The photographs of the set up designed and developed for carrying out the experiments are shown in Figs. 3.2 (a) and (b) with θ = 15° and θ = 0˚ (vertical bed), respectively.

Fig. 3.2(a) Photographs of bubbling fluidized bed drier at θ =15°

TH-1488_126103037

Fig. 3.2(b) Photographs of bubbling fluidized bed drier at θ = 0° inclination (vertical bed)

The components of the experimental set up are described below.

3.2.1 Drying column (Riser)

The drying column is made of Perspex to allow visual observation with the ends fixed to flanges. The flange has 8 bolt holes of 12 mm diameter. There are three drying columns and they are connected with bolts and nuts via thickness 6 mm rubber gasket between them for preventing leakage. Each column heights are 590 mm, 600 mm and 250 mm and total column height is 1440 mm. Twenty six pressure tapings, with 13 taps on each of the lateral sides, are provided to record the pressure drops across the column and attached to manometers. These are utilized to study the hydrodynamic behaviour of the fluidized bed during drying. The inside cross-sectional area of the column is 100 mm x 100 mm and the thickness of dryer column is 6 mm.

TH-1488_126103037

3.2.2 Distributor plate

The distributor plate is a square shaped mild steel disc of 190 mm × 190 mm outside dimension and thickness 6 mm. The disc consists of a number of uniformly distributed 3 mm diameter holes drilled at the central square area of 100 mm × 100 mm. The 3 mm diameter holes were drilled uniformly in a square lattice having a pitch of 6.1 mm. A total of 267 holes were provided to have an opening of 18.85% of the area of the disc. The detailed design calculation of distributor plate is shown in appendix A.

3.2.3 Inclination Flange

The inclination flange was provided to adjust the inclination of the fluidized bed column. The flange was designed to facilitate various inclination of the column at 0° (vertical), 15° and 30°.

3.2.4 Air flow pipe

The air flow pipe connects the inclination flange to the distributor plate. This consists of mild steel pipe with an inside diameter of 10.5 cm.

3.2.5 Orifice plate

Orifice plate was used for the measurement of air flow rate. When the fluid flows across the orifice plate, fluid velocity changes with corresponding pressure drop across the orifice plate. By measuring the difference between pressure values immediately before and after the orifice plate, measurement of air flow rate is done. The inside diameter of orifice plate is 4.2 cm and outside diameter is 10.5 cm. A fine wire mesh of 0.1mm grit size was used below the distributor plate to prevent entry of paddy from the fluidized bed into the air chamber. The detail design calculation of orifice plate is shown in appendix B.

3.2.6 Electric Blower

The blower was used to blow air to the fluidized bed. The blower was operated using a 3-phase, 11 kW motor operating at 415 volts A.C supply and rotating at 2880 rpm.

3.2.7 Thermocouple

K - type thermocouples were used for measuring inlet, outlet and bed temperatures of the dryer with the help of data acquisition system and computer. Eleven thermocouples were used.

TH-1488_126103037

3.2.8 Manometer panel Board

The manometer panel board consists of 29 manometer tubes which were used to measure the air velocity and air mass flow rate. Water was used as the manometric liquid. In addition to the fluidized bed set up, a grain moisture meter (Make: PM-410 model) was used to mesure the moisture content of the paddy during the drying (Fig. 3.3).

Fig. 3.3 Grain moisture tester

The moisture meter operates at 1.5 V supply and consists of a sample cup and funnel. The Percentage moisture content was obtained by digital LCD display with an accuracy of ±0.5%. The moisture tester was calibrated initially by drying the paddy in a muffled furnace and determining the change in weight at regular time interval.

3.3 DESIGN CONSIDERATIONS

3.3.1 Fluidization

Fluidization is the process in which solids are caused to behave like a fluid by blowing gas or liquid upwards through the solid filled column. When fluidize the bed of solid particles behaves like a fluid, liquid or gas, the bed tends to occupy the volume of the chamber during the dynamic behaviour. The fluidized bed drying is having the advantage of very good particles mixing, good contact between the particles and the air leading to high heat and mass transfer rates, rapid drying. They can be used for both small and large scale operations.

TH-1488_126103037

3.3.2 Fluidization regimes

When the solid particles are fluidized, the fluidized bed behaves differently as velocity, gas and solid properties are varied. When the flow of a gas passed through a bed of particles is increased continually, a few vibrate and tend to dislocate, but still within the same height as the bed at rest. This is called a fixed bed. With increasing gas velocity, a point is reached where the drag force exerted by the upward moving gas equals the weight of the particles, and the void fraction of the bed increases slightly: this is the onset of fluidization and is called minimum fluidization with a corresponding minimum fluidization velocity, U_{mf}. Increasing the gas flow further, a bubbling fluidized bed occurs. As the velocity is increased further, the bubbles in a bubbling fluidized bed coalesce and grow in size during their ascent across the column. If the ratio of height to the diameter of the bed is high, the size of bubbles may become almost the same as diameter of the bed. This is called slugging bed. If the particles are fluidized at a higher gas flow rates, the velocity exceeds the terminal velocity of the particles. The upper surface of the bed disappears and a turbulent motion of solid clusters and gas voids of various sizes and shapes can be observed. This stage is called the turbulent bed. With further increases in gas velocity, the fluidized bed becomes more turbulent leading to pneumatic transport of solids. As the superficial gas velocity, U, is increased stepwise beyond the minimum fluidization velocity, the different flow regimes depending upon the velocity can be observed. The fixed bed expansion, bubbling fluidization, slug flow, turbulent fluidization, fast fluidization and pneumatic transport during fluidization is shown schematically in Fig. 3.4.

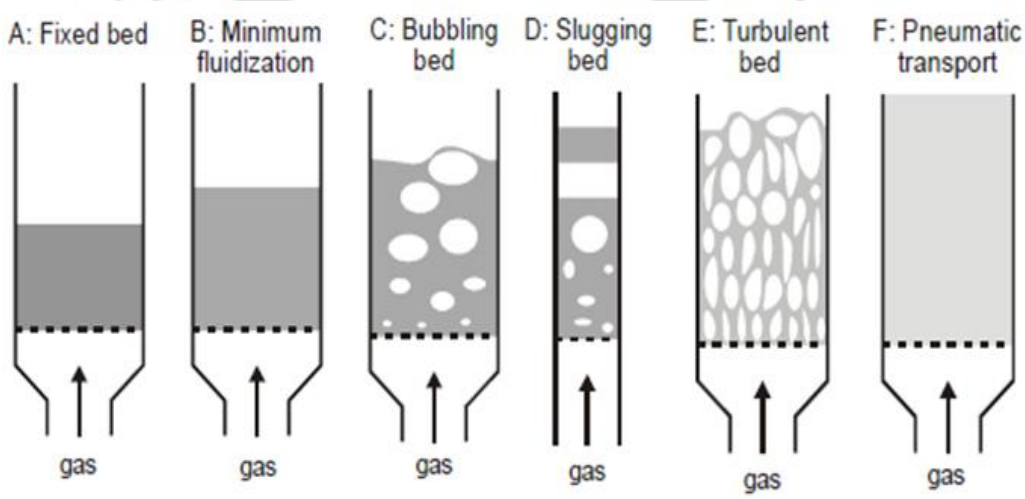

Fig. 3.4 Fluidization regimes (Kunii and Levenspiel 1991)

TH-1488_126103037

3.3.3 Geldart's classification of particle

The behaviour of solid particles in fluidized beds depends on their size and density. The characteristics of the four different powder types were categorized by Geldart (1973). Diagram of the Geldart classification of particles are shown in Fig. 3.5. Group A is designated as 'aeratable' particles. These materials have small mean particle size (d_p< 30 μm) and low particle density (ρ<1.4 g/cm^3). At higher gas velocity when bubbles start to form, the minimum bubbling velocity, U_{mb}, is always greater than U_{mf}. Group B is called 'sandlike' particles. Mostly these are glass beads and coarse sands having particles have size in the range 150 μm to 500 μm and density from 1.4 to 4 g/cm^3. Group C materials are 'cohesive' or very fine powders. Their sizes are usually less than 30 μm, and are difficult to fluidize due to the phenomenon of channelling. Flour and starch are group C materials. Group D is called 'spoutable' and the materials are either very large or very dense. They are difficult to fluidize in deep beds. Coffee beans are group D materials.

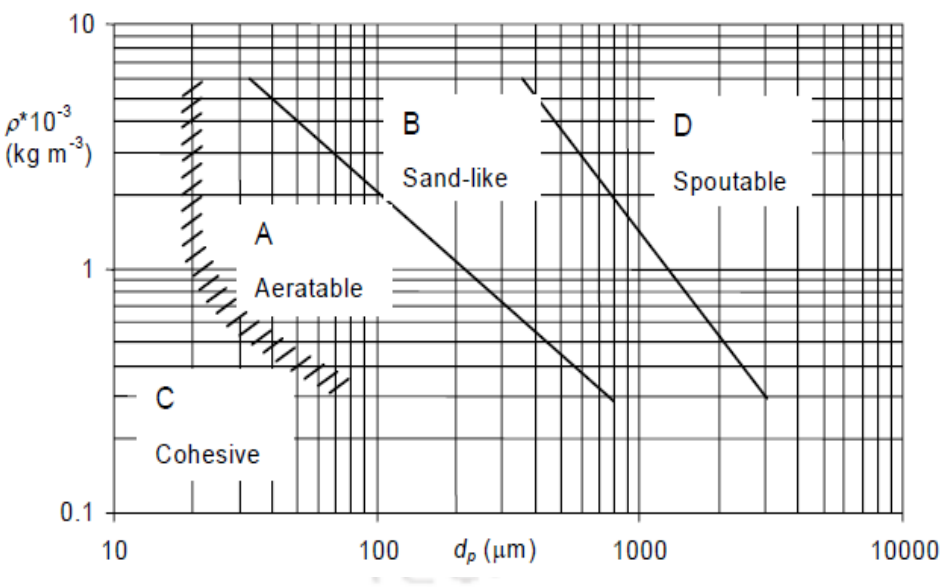

Fig. 3.5 Geldart's classification of particles (Geldart, 1973)

3.3.4 Bubbling Fluidized Beds

Bubbling fluidized bed (BFB) is a very important phase of fluidization. Gas fluidized beds are characterized by the 'bubbles' which are formed at superficial gas velocities only slightly higher than that required to fluidize the particles. This type of fluidization is called 'aggregative fluidization', and the bed can be divided

TH-1488_126103037

into two phases, the bubble phase and the emulsion phase. The bubbles coalesce as they rise through the bed. The movement of particles in fluidized beds depends on bubbles rising through the bed.

3.3.4.1 Bubble Size

The mean size of the bubble population in the bubbling fluidized bed increases with height due to the coalescence of bubbles above the distributor plate. Geldart (1972) used the expression of Kato and Wen (1969) for the mean initial bubble size and subsequent bubble growth with bed height.

$$D_B = \frac{1.43}{g^{0.2}}\left(\frac{(U-U_{mf})\pi {D_{bed}}^2}{4N_o}\right)^{0.4} + 2.05(U-U_{mf})^{0.94}h \qquad (3.1)$$

where D_B is the bubble diameter, D_{bed} is the diameter of the bed and N_0 is the number of holes in the distributor plate.

3.3.4.2 Flow Pattern of Bubbles

As bubbles rise through the bed, they coalesce to form bigger bubbles. These bigger bubbles continuously increase in size as they move upwards and finally break. This phenomenon is illustrated in Fig. 3.6.

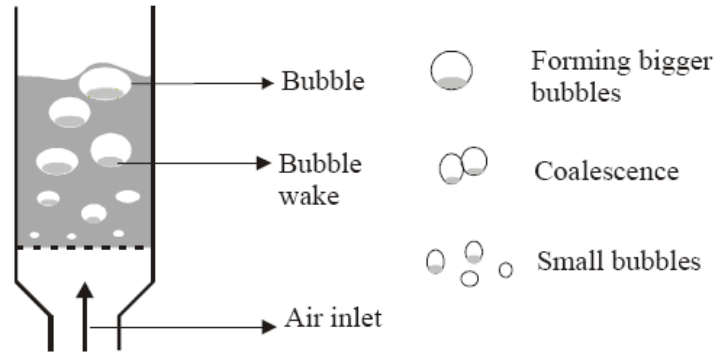

Fig. 3.6 Flow pattern of bubbles (Davies and Taylor, 1950)

Bubbles can coalesce in two ways: by incorporating a bubble in front of it or by moving sideways. At the bed walls, bubbles can only move inwards, while other bubbles can move in vertical direction. As the bubbles move, the solid particles are dragged in to the bubbles, which have a tendency to move downwards in regions with lower bubble densities (Davies and Taylor, 1950). As a consequence of fewer bubbles being close to the wall, the flow of particles near the wall is predominantly

TH-1488_126103037

downward. The overall circulation is upwards away from the walls where as it is downwards near the wall especially at the top regions of the bed. The circulation pattern can be modified by modifications at the distributor plate.

3.3.5 Particle Transportation

The vertical particle transport processes in bubbling fluidized beds were first proposed by Rowe and Partridge (1962). In this the transport of particles is upwards in the wakes of fluidization bubbles and deposition at the bed surface. When the drag force or weight component of the bed particles is considered for inclined fluidized bed an additional factor of gcosθ is multiplied. (where, g is the acceleration due to gravity and θ is angle of inclination).

3.3.6 Minimum fluidization velocity

Onset of fluidization occurs when

$$\begin{bmatrix}\text{Drag force by}\\ \text{upward moving gas}\end{bmatrix} = \begin{bmatrix}\text{weight of}\\ \text{particles}\end{bmatrix}$$

$$\begin{bmatrix}\text{Pressure drop}\\ \text{across the bed}\end{bmatrix} \times \begin{bmatrix}\text{cross sectional}\\ \text{area of the bed}\end{bmatrix}$$
$$= \begin{bmatrix}\text{volume of}\\ \text{bed}\end{bmatrix} \times \begin{bmatrix}\text{specific weight}\\ \text{of solid}\end{bmatrix} \times \begin{bmatrix}\text{fraction consisting}\\ \text{of solids}\end{bmatrix}$$

With ΔP_b always positive, for inclined bed

$$\Delta P_b A_b = A_b L_{mf} (1 - U_{mf})(\rho_s - \rho_g) g cos\theta \tag{3.2}$$

Considering of the minimum fluidization velocity, U_{mf}, basing on the concepts of (Leva and Kunii, 1991) a relation between the inlet velocity or the superficial fluid velocity, U, and height of the fluidized bed can be expressed as

$$\frac{\Delta P}{L} = 150 \frac{(1-\varepsilon_{mf})^2}{{\varepsilon_{mf}}^3} \frac{\mu U_{mf}}{(\emptyset_s d_p)^2} + 1.75 \frac{(1-\varepsilon_{mf})}{{\varepsilon_{mf}}^3} \frac{\rho_g {U_{mf}}^2}{\emptyset_s d_p} \tag{3.3}$$

The LHS of above equation can be expressed as:

TH-1488_126103037

$$\frac{\Delta P}{L} = \frac{\rho_g cos\theta V_{bed}\,(1-\varepsilon_{mf})}{V_{bed}} \tag{3.4}$$

where, V_{bed} is the volume occupied by the fluidized bed. By combining the above two equations become

$$\rho g cos\theta = \frac{150(1-\varepsilon_{mf})\mu U_{mf}}{\varepsilon_{mf}^3 \varphi^2 d_p^2} + \frac{1.75\rho_g U_{mf}^2}{\varepsilon_{mf}^3 \varphi_s d_p} \tag{3.5}$$

The above expression is a quadratic equation for U_{mf}. For drying of paddy, some of the variables can be approximated based on standard values.

Density of paddy (bulk samples) ρ = 600 kg/m^3

Diameter d_p = 2.7mm

Viscosity of air μ = 1.983*10^{-5} Pa-sec (Dynamic viscosity at 27° C)

The Eqn. (3.5) was solved to get the value U_{mf} (m/s). Using this expression the relation between the height of the bed and air velocity for the experiment obtained.

3.3.7 Terminal velocity

When the air velocity in a bubbling fluidized bed is increased, the bubbles will coalesce and grow as they rise. When the particles are fluidized at higher gas flow rate with velocity exceeding the terminal velocity of the particles, the upper surface of the bed disappears and one observes a turbulent motion. The solid particles move in clusters along with the formation of gas voids with various sizes and shapes. The beds under these circumstances are called turbulent beds. With further increases of gas velocity, the fluidized bed becomes a dynamic bed with disperse and turbulent fluidization resulting in pneumatic transport of solids. The terminal velocity for pneumatic transport of solids can be estimated from the drag force equation (Blevins, 2003 and Munson et *al.*, 1998).

$$C_D \times \left(\frac{1}{2}\rho_g {U_t}^2\right) \times \frac{1}{4}\pi \overline{d_p}^2 = \frac{1}{6}\pi \overline{d_p}^3 g(\rho_s - \rho_g) \tag{3.6}$$

i.e, the terminal velocity

$$U_t = \left[\frac{4g cos\theta d_p(\rho_s - \rho_g)}{3\rho_g C_D}\right]^{0.5} \tag{3.7}$$

TH-1488_126103037

3.3.8 Voidage

Glicksman (1988) defined voidage as the volume fraction of the bed occupied by bubbles. The bed voidage (Ɛ) at any cross-section is estimated from the measured pressure drop (ΔP_b) from a differential water filled U-tube manometer connected across it.

From Eq. (3.2),

$$\Delta P_b = L_{mf}(1-\varepsilon_{mf})(\rho_s - \rho_g)gcos\theta$$

we get,

$$\Delta P_b = (1-\mathcal{E}).L.(\rho_s - \rho_g)gcos\theta \tag{3.8}$$

Since, $\rho_s \gg \rho_g$,

$$\Delta P_b = (1-\mathcal{E}).L.\rho_s gcos\theta \tag{3.9}$$

Again,

$$\Delta P_b = \left(\frac{\Delta h_l}{100}\right)\rho_w gcos\theta \tag{3.10}$$

$$\Delta P_b = \left(\frac{\Delta h_l}{100}\right)1000 \times gcos\theta = 10\Delta h_l.gcos\theta \tag{3.11}$$

$$10\Delta h_l.gcos\theta = (1-\mathcal{E}).L.\rho_s gcos\theta \tag{3.12}$$

$$(1-\mathcal{E}) = \frac{10\Delta h_l}{L\rho_s} \tag{3.13}$$

i.e,

$$\mathcal{E} = 1 - \frac{10\Delta h_l}{L\rho_s} \tag{3.14}$$

where, Ɛ = voidage,

1 — Ɛ = fractional volume of the bed occupied by solid particles

Δh_l = different of height in manometric fluid, cm of water

L = length from distributor plate

ρ_s = density of paddy

TH-1488_126103037

ρ_w = density of water = 1000 kg/m^3

3.3.9 Suspension density

The suspension density of the bed has been determined from the relation:

$$\rho_{sus} = \rho_s (1-\varepsilon) + \rho_g \quad (3.15)$$

3.3.10 Superficial velocity

The superficial velocity (U) is defined as the volume flow rate of air per unit cross-section of the bed .i.e.

$$U = \frac{Volume\ flow\ rate\ of\ air\ through\ the\ bed}{cross-sectional\ area\ of\ the\ bed} \quad (3.16)$$

From appendix B

$$U = \frac{\dot{m}_a}{\rho \times A_b} = 1.117\sqrt{\Delta P}\ \text{ms}^{-1} \quad (3.17)$$

From appendix B

$$\dot{m}_a = 46.91 \times \sqrt{\Delta P}\ \text{kgh}^{-1} \quad (3.18)$$

or

$$\dot{m}_a = 0.01303 \times \sqrt{\Delta P}\ \text{kgs}^{-1} \quad (3.19)$$

where U is superfacial velocity (ms^{-1}), A_b is the cross sectional area of the dryer (m^2), ρ is the density of water (kg m^{-3}) and $\dot{m}_a$ is mass flow rate of air (kg s^{-1}).

The heat energy needed in removing the moisture from the wet material was calculated by the following equation;

$$Q = V \times i \times t \times P.F \times 60 \times 10^{-6} \quad (3.20)$$

where Q = heat input(MJs^{-1}) , V = input voltage (volts), i = Current, Ampere, t = time (minutes), $P.F$ = power factor.

3.4 EXPERIMENTAL PROCEDURE

The paddy bed of batch sizes 0.5, 1, 1.5, 2 and 2.5 kg were fluidized at three different dryer positions: vertical bed (0˚ inclined), 15˚, 30˚ and 45˚ inclined beds with drying air temperatures of 55˚C, 60˚C and 65˚C and air velocities of 1.1, 1.6, 2.1 and 2.6 ms^1. At the start of the experiment, the blower was switched on and air mass flow rate and

TH-1488_126103037

velocity were adjusted by means of gate valve installed in the air flow pipe. Air was heated and maintained constant at the required temperature by means of heater coils placed inside the air flow pipe. Drying air temperature was measured by the pre-calibrated K-type thermocouples and continuously recorded using the data acquisition system. Paddy of required inventory was loaded into the bubbling fluidized bed dryer. The pressure at different sections along the column of the dryer was recorded to obtain the pressure drop across the bed for fluidized bed behaviour. The manometer readings from each pressure tapings during the drying processes were recorded at an interval of 10 minutes from which the pressure drops were determined. Few grams of paddy samples were taken out at 10 minutes interval for the determination of the moisture content using a digital grain moisture meter having an accuracy of ±0.5%. The moisture meter was pre-calibrated using the standard oven method. The experiment was terminated when the moisture content in the paddy dropped to 12% wet basis.

3.5 SUMMARY

In this chapter, the detailed design and components of the experimental setup, background theory, experimental methodology, design consideration, calibration and experimental procedures are presented. The results of the experiments viz., the hydrodynamic behaviour of paddy bed and drying characteristics, i.e. the effect of paddy bed inventory, air temperature, air velocity and bed inclination of the bubbling fluidized bed paddy drying without heating system (drying at room temperature) and with heating system using standard distributor plate will be discussed in next chapter.

TH-1488_126103037

CHAPTER 4

RESULTS AND DISCUSSION

4.1INTRODUCTION

Experimental investigation of hydrodynamic behaviour and drying characteristics of paddy grain are conducted in bubbling fluidized bed dryer. Results and discussions of the same are presented in the following subsections.

4.2EXPERIMENTAL CONDITIONS AND INPUT VARIABLES

Experimental conditions and input parameters are given in in Table 4.1. The final moisture content (MC) is controlled at 12% w.b.

Table 4.1 Experimental Matrix

Serial Number	Input	Range
1	Superficial air velocity (U)	1.1-2.6 m/s
2	Temperature of drying air (T_{da})	55˚C, 60˚C, 65˚C
3	Bed Inventory (I)	0.5-2.5 kg
4	Inclination of drying bed from vertical position(θ)	0˚, 15˚, 30˚, 45˚
5	Final moisture content (controlled)	12% w.b
6	Density of paddy grain (ρ)	600 kg/m^3
7	Relative humidity of air in the laboratory (RH)	75 ± 5%

4.3HYDRODYNAMIC BEHAVIOUR OF PADDY DRYING USING STANDARD DISTRIBUTOR PLATE

Hydrodynamic behaviour of paddy drying in bubbling fluidized bed with heating system was studied using standard distributor (STD) plate for vertical (0˚) as well as inclined positions (15˚, 30˚, 45˚). Paddy grains were used as the test material to dry in the fluidized bed dryer. They are classified as D group particles, which contain large particles with the larger dimension greater than 1000 μm. The average density of the grains used for the experimental investigation is 600 kg/m^3. Variation of pressure along the top side (TS) and bottom side (LS) of the riser height were measured for

TH-1488_126103037

different inputs like superficial air velocity, drying air temperature and different amount of bed inventory. Variation of pressure drop along the riser height of the vertical bed ($\theta = 0^0$) using STD plate at different temperatures is presented in Fig. 4.1.

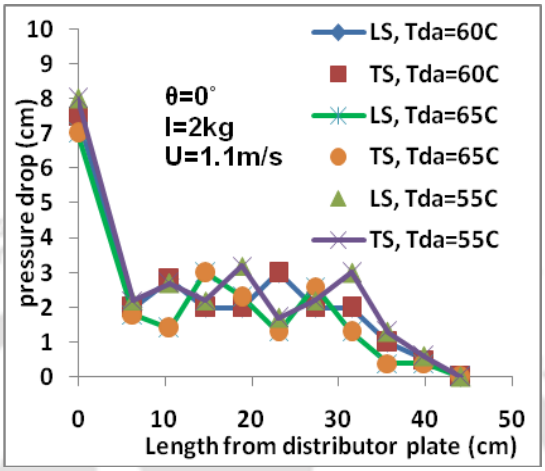

Figs. 4.1 Pressure drop verses fluidization height using STD plate forθ = *0*˚(vertical bed) at different temperature

It is observed that pressure drop is high across the distributor plate and became lower along the riser height and finally it became stable or remains constant. The values of maximum pressure drops are 8 cm at the distributor plate, 3.3cm along the riser height and became constant at the fluidization height of 44.1cm. In the Fig. it is observed that pressure drop at the distributor plate decreased by12.5% when the air temperature was increased from 55 to 65˚C.It was found that variation of pressure drop from both side of the riser column is same for the vertical bed. Hence it will not be expressed as lower side and upper side separately for next investigations.

Figs. 4.2(a) and (b) presents the pressure drop verses fluidization height using STD plate for the vertical bed (θ = *0*˚) at different inventory and different velocity, respectively.

TH-1488_126103037

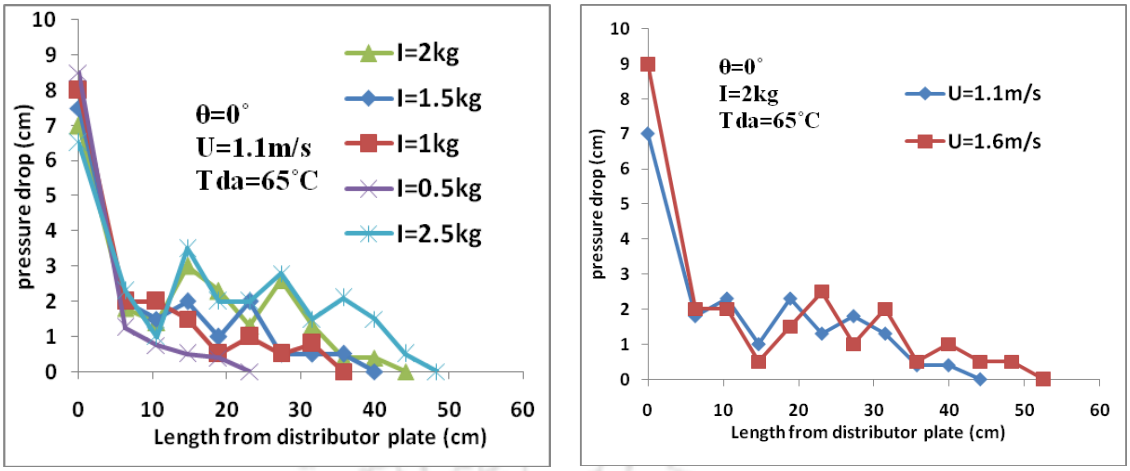

(a) (b)

Figs. 4.2 Pressure drop verses fluidization height using STD plate for $\theta = 0^{\circ}$ at (a) different inventory and (b) different velocity

In the Fig. 4.2(a) it is observed that pressure drop across the distributor plate decreases by 23.5% when the inventory was increased from 0.5 kg to 2.5 kg whereas fluidization height increase by 52.2%. In the Fig. 4.2(b) it is found that pressure drop across the distributor plate increases by 22.2% and fluidization height increases by 16%when the velocity was increased from 1.1 to 1.6 m/s. Figs. 4.3(a) and (b) present the pressure drop along the riser height using STD plate for $\theta = 15^{\circ}$ and 30°.

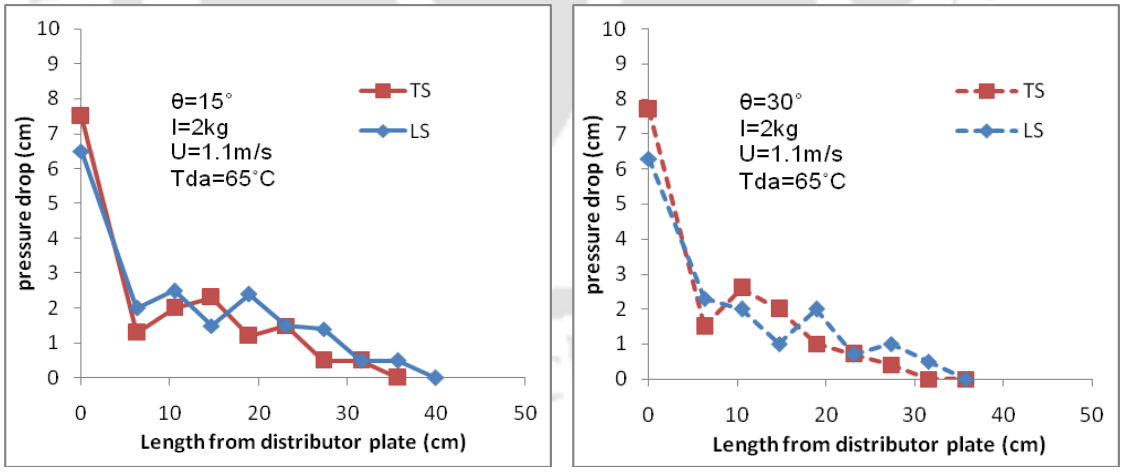

(a) (b)

Figs. 4.3 Pressure drop verses fluidization height using STD plate for lower side and upper side of the riser column for (a) $\theta = 15^{\circ}$ (b) $\theta = 30^{\circ}$

In the Fig. 4.3 (a) it was found that pressure drop variation across the distributor plate of the lower wall of riser column decreased whereas it increased at the top wall of the riser column and swirling action and secondary motion were observed for the inclined

TH-1488_126103037

bed. Moreover, fluidization height at the lower side is more than at the upper side. Similar trend is observed at the θ = 30˚exception pressure drop at the distributor plate slightly decrease for lower side and slightly increase at the upper side resulting in swirling increases slightly as shown in Fig. 4.3(b). However, fluidization heights of θ = 30˚are lower than that of θ = 15˚. Fluidization heights for the lower side and upper side of θ = 15˚are 36cm and 40 cm, respectively whereas it was 27 cm and 36 cm for θ = 30˚. Variations of pressure drop from both side of the riser column are different for the inclined beds. Hence it will be expressed as lower side and upper side separately for next investigations.

Figs. 4.4(a) and (b) present the pressure drop verses fluidization height using STD plate for θ = 15˚.It is observed that pressure drop across the distributor plate decreased 13% for the lower side and 11.7% for the upper side of riser column when the temperature was increased from 55˚C to 65˚C. Moreover, it is found that fluidization heights of upper side decreases by 10.2% in compares with the lower side.

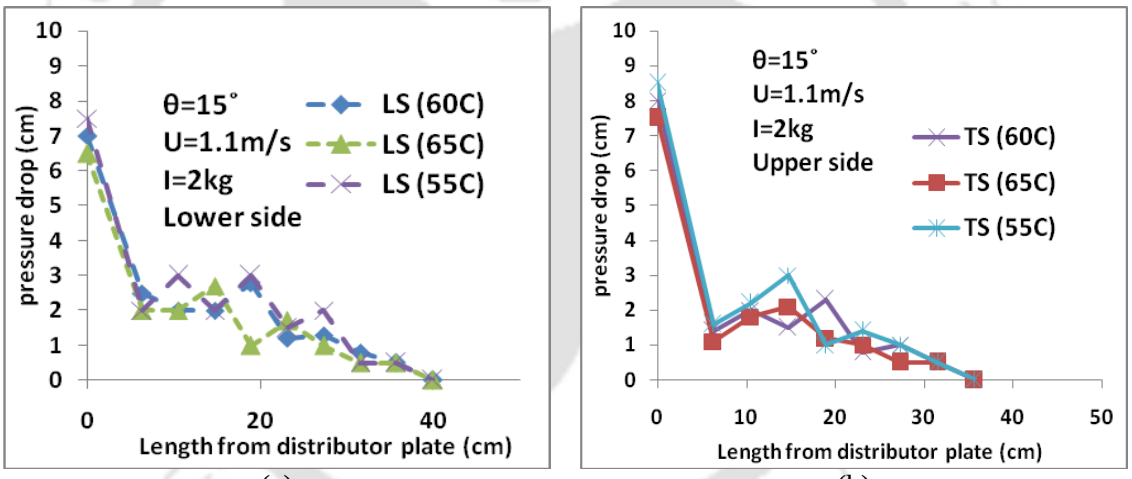

(a) (b)

Figs. 4.4 Pressure drop verses fluidization height using STD plate for θ = 15˚ at different temperature for (a) lower side and (b) upper side of riser column

Figs. 4.5 (a) and (b) present the pressure drop verses fluidization height using STD plate for θ = 15˚ inclined bed at different inventory for lower side and upper side of riser column, respectively. It is observed that pressure drop across the distributor plate decreases by25% for the lower side and 22% for the upper side when the inventory was increased from 0.5 to 2.5kg whereas fluidization height increases by 57% for the lower side and 50% for the upper side.

TH-1488_126103037

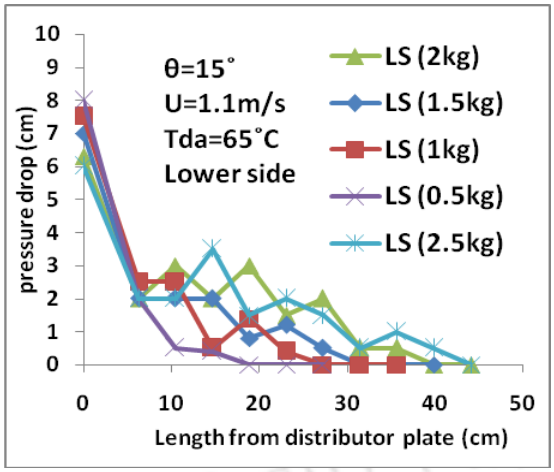

(a)

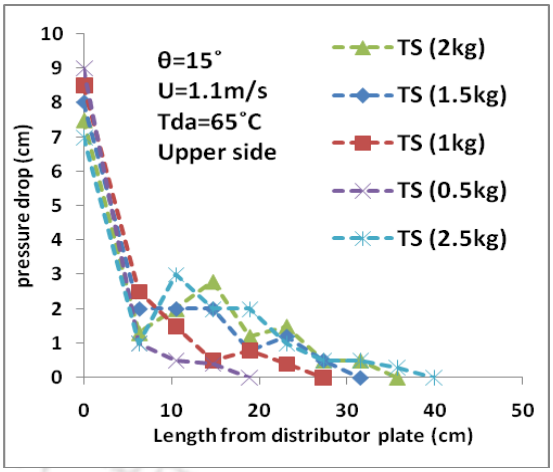

(b)

Figs. 4.5 Pressure drop verses fluidization height using STD plate for θ = 15˚ at different inventory for (a) lower side and (b) upper side of riser column.

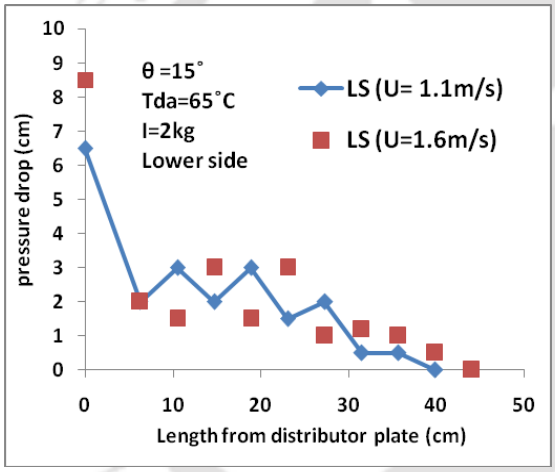

(a)

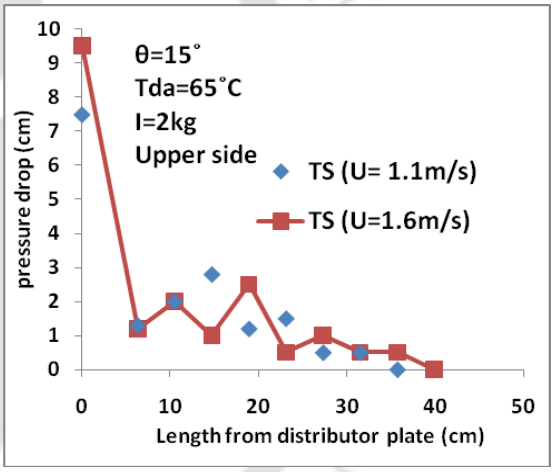

(b)

Figs. 4.6 Pressure drop verses fluidization height using STD plate for θ = 15˚ at different velocity for (a) lower side and (b) upper side.

Figs. 4.6 (a) and (b) present the pressure drop verses fluidization height using STD plate for θ = 15˚ at lower side and upper side of riser column for different velocity. It is found that pressure drop across the distributor plate increases by 23.5% at the lower side in Fig. 4.6 (a) and 27% at the upper side in Fig 4.6 (b) when the velocity was increased from 1.1m/s to 1.6m/s. Moreover, fluidization height increases by 9% at the lower side and 10% at the upper side when the velocity was increased from 1.1m/s to 1.6m/s. It is found that pressure drop across the distributor plate and fluidization height increase with increases in velocity. For θ = 45˚ the bubbling fluidization almost stops and more than 75% of the bed on the top part becomes a single phase with air as

TH-1488_126103037

medium. It was difficult to find bed hydrodynamics under such situation. Figs. 4.7(a) and (b) present the pressure drop along the riser height using STD plate for $\theta = 0^{\circ}$, 15° and 30° at the drying air temperature of 65°C, superficial air velocity of 1.6m/s and the inventory of 2kg.

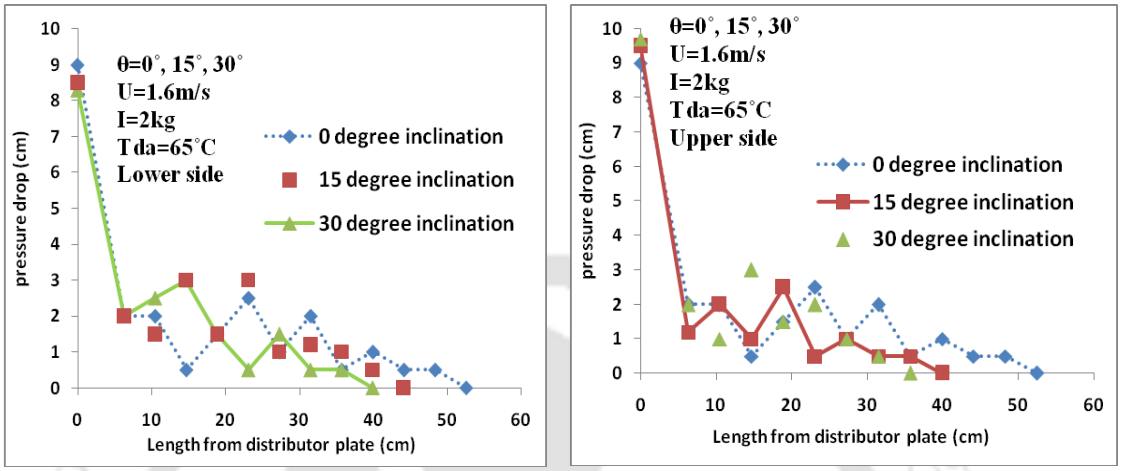

(a) (b)

Figs. 4.7 Pressure drop verses fluidization height using STD plate for different inclination angles of θ = 0°. 15° and 30°(a) lower side and (b) upper side of the riser column

It is observed that pressure drop across the distributor plate decreases by 8% for the lower side whereas it increases by 8% for the upper side when the inclination was increased from 0° to 30°. Moreover, fluidization height decreases by 25% for the lower side and 32% for the upper side. It is observed that pressure drop across the distributor plate and fluidization height decrease with increase in inclination for the lower side of riser column in Fig 4.7(a). For the upper side of riser column in Fig 4.7(b), pressure drop across the distributor plate increases with increases in inclination whereas fluidization height decreases with increases in inclination.

From the Figs. it is clear that a rotation from θ =0° to θ =15° and 30° inclined beds resulting in swirling occured. Drying time and energy consumptions decreased in the inclined bed compared to the vertical bed due to this swirling action. The photographs of air flow patterns inside the $\theta = 0^{\circ}$ dryer and $\theta = 15^{\circ}$ dryer are shown in Figs. 4.8.

TH-1488_126103037

(a) (b)

Figs. 4.8 Photographs of air flow patterns inside the dryer (a) $\theta = 0^{\circ}$ and (b) $\theta = 15^{\circ}$

4.4DRYING CHARACTERISTICS OF FLUIDIZED BED USING STD PLATE

The results of the drying characteristics like different inventory, bed inclination, air velocity and drying air temperature on drying time of bubbling fluidized bed drying using STD plate are presented and discussed in the subsequent sub-sections.

4.4.1 Drying at room temperature using STD plate

Results of the drying experiments carried out at room temperature with the STD plate are shown in Table 4.2.

Table 4.2Time (minutes) required for drying the paddy to attain a moisture level of 12% (w.b) for the experiments carried out at room temperature using STD plate.

Condition	Bed inclination (θ)	**Drying Time (min)**		
		0.5 kg	**1 kg**	**1.5 kg**
U= 1.1m/s using STD plate	**0°**	100	130	160
	15°	95	120	145
	30˚	97	124	150
U= 1.6 m/s using STD plate	**0°**	90	120	150
	15°	85	115	140
	30˚	87	119	145

In the Table 4.2 the drying time is found to vary with load, air velocity and bed inclination. The time required for drying in the bubbling fluidized bed dryer are long when carried out at room temperature. From the Table it is clear that the drying with higher load leads to faster drying per unit weight of paddy in the batch process and

TH-1488_126103037

drying times are slightly lesser at air velocity of 1.6m/s than at1.1m/s. Moreover, the drying times are lesser at θ = 15˚ and 30˚ compared to θ =0˚.

4.4.2 Effect of load, temperature and velocity on drying time using STD plate

Effect of load, temperature and velocity on time dependent moisture content of the grain of fluidized bed drying with heating system using STD plate are shown in Table 4.3.

Table 4.3 Drying time (minutes) for different bed inventories at drying air temperature of 60°C and various operating conditions using STD plate.

Air velocity (U) m.s^{-1}	Bed inclination (Θ)	**Drying Time (min)**				
		0.5 kg	**1 kg**	**1.5 kg**	**2 kg**	**2.5 kg**
1.1	**0°**	41	50	59	68	77
	15°	38	45	52	59	66
	30˚	40	47	54	61	68
	45˚	46	55	64	73	82
1.6	**0°**	40	48	56	64	72
	15°	37	43	49	55	61
	30˚	39	45	51	57	63
	45˚	45	53	61	69	77
2.1	**0°**	39	46	53	60	67
	15°	36	41	46	51	56
	30˚	38	43	48	53	58
2.6	**0°**	38	44	50	56	62

In the Table 4.3 it is observed that the time required for drying 1 kg of paddy for θ = 0˚ at drying air temperature of 60°C and air velocity of 2.1m/s are 78, 46, 35.3, 30 and 26.8 min, respectively for bed inventories of 0.5 to 2.5 kg, whereas the corresponding values for θ= 15˚ are 72, 41, 30.7, 25.5 and 22.4 min. The corresponding reduction of drying time/kg paddy are 65.6% and 68.8% for θ = 0˚and 15˚, respectively when the inventory is increased from 0.5 to 2.5kg. The corresponding reductions of drying time/kg paddy for air velocity of 2.6 m/s for θ = 0˚ are 67.4% when the inventory is increased from 0.5 to 2.5kg. The drying time for an inventory of 2.5kg at the drying air temperature of 60˚C and air velocity of 1.1m/s for θ = 0˚ is 77 min, whereas the corresponding drying time is 62 min for air velocity of 2.6 m/s. It is observed that the percentage reduction of corresponding drying time/kg paddy is 19.4% when the velocity is increased from 1.1 to 2.6m/s. The drying time for an inventory of 2.5kg at

TH-1488_126103037

the drying air temperature of 60˚C and air velocity of 2.1m/s for θ = 0˚ is 67 min, whereas the corresponding drying time for θ = 15˚ is 56 min. It is observed that drying time/kg paddy decreases by 16.4% when the inclination is increased from 0˚ to 15˚. In all the above cases the time mentioned is to reach a moisture content of 12%.

Effect of drying air temperature on the drying time using STD plate for a bed inventory of 2.5 kg is shown in Table 4.4.

Table 4.4 Effect of drying air temperature on the drying time using STD plate for a bed inventory of 2.5 kg

Velocity (U) m/s	Bed inclination (Θ)	**Drying Time (min)**		
		55 °C	**60 °C**	**65 °C**
1.1	**0°**	87	77	67
	15°	76	66	56
	30˚	78	68	58
	45˚	92	82	72
1.6	**0°**	82	72	62
	15°	71	61	51
	30˚	73	63	53
	45˚	87	77	67
2.1	**0°**	77	67	57
	15°	66	56	46
	30˚	68	58	48
2.6	**0˚**	72	62	52

It is observed that drying time for an inventory of 2.5 kg at the air velocity of 2.1 m/s are 77, 67 and 57 min for θ = 0˚ and 66, 56 and 46 min for θ = 15˚ for air temperature of 55, 60 and 65˚C, respectively. It is found that the drying time/kg paddy decreases by 26% and 30.3%, respectively for θ = 0˚ and 15˚when the air temperature is increased from 55˚C to 65˚C. The drying time for an inventory of 2.5kg for θ = 0˚ at the air velocity of 1.1 m/s are 67 min and 52 min for 2.6 m/s for the air temperature of 65˚C. It is found that the drying time/kg paddy decreases by 22.4% when the air velocity is increased from 1.1 to 2.6 m/s. The drying time for an inventory of 2.5 kg at the air velocity of 2.1m/s and air temperature of 65˚C are 57min for θ = 0˚ and 46 min for θ = 15˚. It is found that the drying time/kg paddy decreases by 19.3%when the inclination is increased from 0˚ to 15˚

TH-1488_126103037

4.5 MOISTURE CONTENT VERSES DRYING TIME USING STD PLATE

Moisture content verses drying time of bubbling fluidized bed drying using standard distributor (STD) plate for θ = 0˚ and 15˚are presented and discussed. The moisture content verses drying time plots for θ=0˚are shown in Figs. 4.9 (a)-(c).

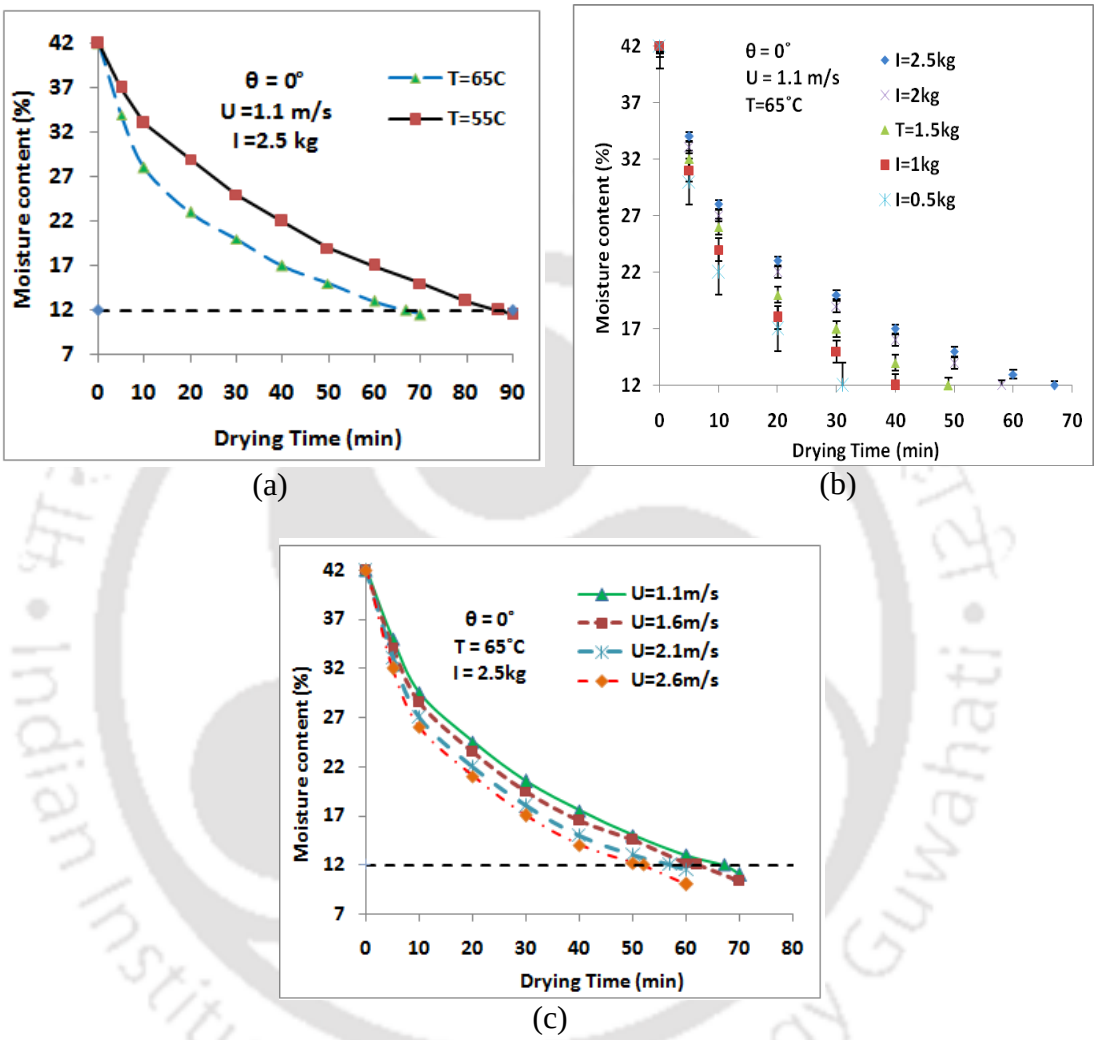

Figs. 4.9. Moisture content verses drying time plots using STD plate for θ= 0˚ at (a) different temperature (b) different inventory and (c) different velocity

The plots indicates high moisture removal rate at the beginning of the drying process and is attributed to the removal of the surface moisture of the paddy. The drying rate decreased with further drying time. The slow moisture removal rate during the later stages of drying process is due to the removal of the internal moisture from the paddy grains. In the Fig 4.9(a) the drying times for the inventory of 2.5kg at air velocity of 1.1m/s are 87 min and 67 min for the air temperature of 55˚C and 65˚C, respectively

TH-1488_126103037

to drop the final MC of 12% (w.b). It is observed that drying time/kg paddy decreases by 23% when the air temperature is increased from 55˚C to 65˚C.

In the Fig 4.9(b) the drying times at air velocity of 1.1m/s and air temperature of 65˚C are 31, 40, 49, 51 and 67 min respectively for the inventory 0.5 to 2.5kg, to drop the final MC of 12% (w.b). It is observed that drying time/kg paddy decreases by 56.7% when the inventory is increased from 0.5kg to 2.5kg. In the Fig. 4.9(c) the drying times at air temperature of 65˚C and an inventory of 2.5kg are 67, 62, 57 and 52 min, respectively for air velocity of 1.1, 1.6, 2.1 and 2.6 m/s to drop the final MC of 12% (w.b). It is observed that drying time/kg paddy decreases by 22.4% when the air velocity is increased from 1.1 to 2.6m/s. Figs. 4.10 (a)-(c) presents moisture content verses drying time plots using STD plate for $\theta = 15^{\circ}$ inclined bed.

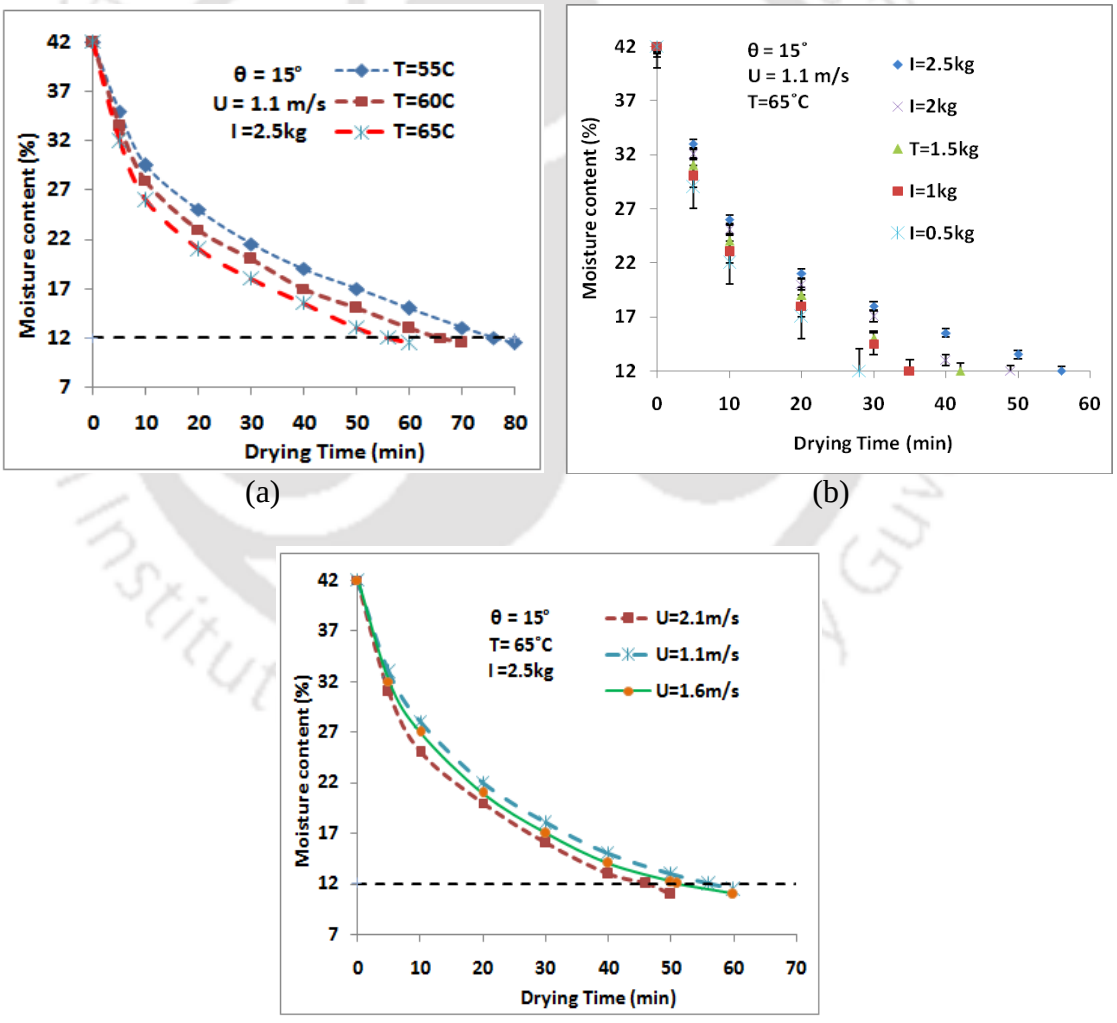

Figs. 4.10. Moisture content verses drying time plots using STD plate for $\theta = 15^{\circ}$ at (a) different temperature (b) different inventory and (c)different velocity

TH-1488_126103037

In the Fig. 4.10(a) the drying times for the inventory of 2.5kg at air velocity *U* =1.1m/s are 76 min, 66 min and 56 min for the drying air temperature of 55˚C, 60˚C and 65˚C, respectively to drop the final MC of 12% (w.b). It is observed drying time/kg paddy decreases by 26.3% when the air temperature is increased from 55˚C to 65˚C.In the Fig 4.10(b) the drying times/kg paddy at air velocity *U* = 1.1m/s and air temperature of 65˚C are 22, 25, 33, 40 and 56 min, respectively for the inventory 0.5 to 2.5kg to drop the final MC of 12% (w.b). It is observed that drying time/kg paddy decreases by 60.7% when the inventory is increased from 0.5kg to 2.5kg.

As shown in Figs. 4.9 (b) and 4.10 (b), uncertainty in measurement of moisture content (%) for the inventories of 0.5, 1, 1.5, 2 and 2.5 kg are calculated to be ±2%, ±1%, ±0.7%, ±5% and ±0.4%, respectively. Sample calculation in measurements of uncertainty is presented in Appendix. In the Fig 4.10(c) the drying times at air temperature of 65˚C and an inventory of 2.5kg are 56, 51 and 46 min, respectively for the air velocity of 1.1, 1.6 and 2.1m/s to drop the final MC of 12% (w.b). It is observed that drying time/kg paddy decreases by 17.9% when the air velocity is increased from 1.1m/s to 2.1 m/s. Fig. 4.11 presents moisture content verses drying time plots for different angles θ = 0˚, 15˚ and 30˚.

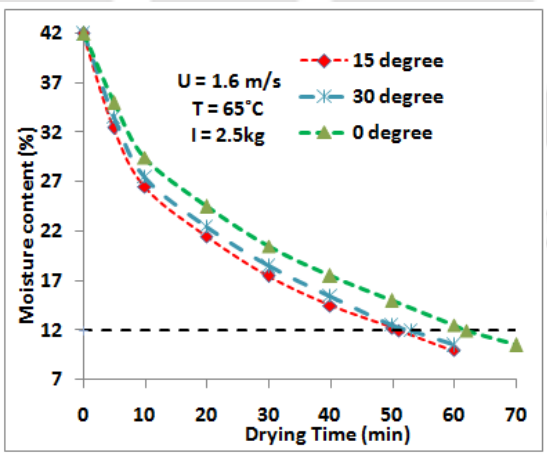

Fig. 4.11. Moisture content verses drying time plots using STD plate at different inclination

The drying times for the inventory of 2.5kg and air velocity of 1.6m/s and air temperature of 65˚C are 62 min, 51 min and 53 min, respectively for θ = 0˚, 15˚ and 30˚ to drop the final MC of 12% (w.b). Drying is found to be more efficient with θ =

TH-1488_126103037

15˚ and 30˚compared to $\theta = 0^{\circ}$. It is observed that drying time/kg paddy decreases by 17.7% when the inclination angle is increased from $\theta = 0^{\circ}$ to 15˚.It is observed that the variation of moisture content verses drying time plots for $\theta = 15^{\circ}$ and $\theta = 30^{\circ}$ are insignificant. Hence $\theta = 30^{\circ}$ is not expressed widely.

4.6 GRAIN QUALITY TEST

Two types of grain quality test have been performed for this research work.

1. Paddy Quality test during drying
2. Rice Quality test after drying

4.6.1 Paddy Quality test during drying (Uniformity of drying)

100 samples of paddy grains were taken out from the drying chamber during every 20 minute interval. The percentage moisture in the individual grains and bulk of the grain were determined to check whether the drying is uniform or not. Some of the tested results are shown in Fig. 4.12. It was found that percentage moisture content of the 80% of individual grains were same those of bulk grains in every 20 minutes. Hence the drying is uniform.

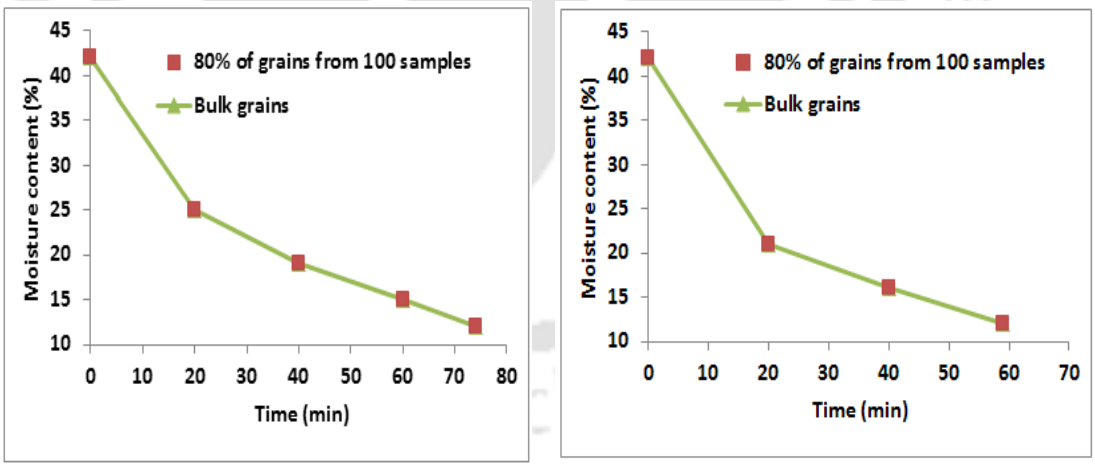

(a) (b)

Figs. 4.12 Moisture content verses drying time plots for quality test (a) $\theta = 0^{\circ}$ and (b) $\theta = 15^{\circ}$

4.6.2 Rice Quality test after drying (Milling quality)

Milling quality was checked by the percentage of milling recovery, percentage of head rice and percentage of broken. They were calculated by the following equations.

TH-1488_126103037

$$\% \text{ Head rice} = \frac{\text{Weight of whole grains after milling}}{\text{Weight of paddy samples}} \times 100 = 55\% \quad (4.1)$$

$$\% \text{ Broken} = \frac{\text{Weight of broken grains after}}{\text{Weight of paddy samples}} \times 100 = 15\% \quad (4.2)$$

$$\% \text{ Milling recovery} = \frac{\text{Weight of milled rice}}{\text{Weight of sample used}} \times 100 = 70\% \quad (4.3)$$

Weight of milled rice includes head rice and broken rice. 100 grams paddy sample was used to check the milling quality. Head rice is around 80% of whole grain. In Asia, head rice yield is 35% to 50% only. The percentage head rice yield of 55% obtained for the present system indicates good quality of rice obtained by the bubbling fluidized bed dryer.

4.7 PROCESS INTENSIFICATION (PI)

Any development that leads to a substantially smaller, cleaner, safer and more energy efficient chemical technology is known as process intensification. The PI for the systems 1 and 2 are shown in Table 4.5.

Table 4.5 PI for system 1and 2

1.Without heating system	2. With heating system (T=60°C)	PI
The drying time for 1 kg paddy is 120 min while using θ = 15˚fluidizer	The drying time for 1 kg paddy is only 45 min while using θ = 15˚fluidizer	0.375

.

$$\text{PI} = \frac{\text{Specific drying rate of system 1}}{\text{Specific drying rate of system 2}} \quad (4.4)$$

$$\text{Specific drying rate} = \frac{\text{Wt of evaporated water}}{\text{Drying time} \times \text{volume of set up}} \quad (4.5)$$

Volume of the set up = cross sectional area x height of dryer column (4.6)

$$MC_{wb} = \frac{(W_i - W_f)}{W_i} \times 100(\%), \quad (4.7)$$

$$MC_{db} = \frac{(W_i - W_f)}{W_f} \times 100(\%) \quad (4.8)$$

$$\text{PI} = \frac{\text{Specific drying rate of fluidized bed drying without heating system}}{\text{Specific drying rate of fluidized bed drying with heating system}} \quad (4.9)$$

TH-1488_126103037

PI = 0.375

i.e specific drying rate of the fluidized bed drying with heating system is only one third of those of without heating system.

4.8 SUMMARY

The results of the experiments viz., hydrodynamic behaviour and drying characteristics such as the effect of paddy bed inventory, drying air temperature, air velocity and dryer inclination on the time dependent moisture content of the grain using the standard distributor platein bubbling fluidized bed paddy drying without heating system (drying at room temperature), and with heating system are discussed in this chapter. The drying performance of the bubbling fluidized bed dryer using modified distributor plate, spirals insert and scale up effect will be discussed in next chapter.

TH-1488_126103037

CHAPTER 5

PERFORMANCE ENHANCEMENT OF BFBDRYER WITH DESIGN MODIFICATIONS

5.1 INTRODUCTION

In this chapter, drying performance of the bubbling fluidized bed (BFB) dryer (a) using the modified distributor (MD) plate for the inclined positions of the dryer, (b) using spiral inserts inside the dryer column which improves the contact between the solid and gas, thereby improving the mixing efficiency leading to higher heat transfer characteristics and (c) scale up effect are studied and discussed in subsequent subsections.

5.2 HYDRODYNAMIC BEHAVIOUROF PADDY DRYING USING TWO DIFFERENT DISTRIBUTOR PLATES

The results of comparison of hydrodynamic behaviour of paddy drying in bubbling fluidized drying using standard distributor (STD) plate and modified distributor (MD) plate for θ = 15˚ and 30˚are presented and discussed.Perforated distributor plate was used in this dryer. In the inclined dryer, it is observed that one side of the dryer is having higher amount of hot air compared to the other side. Hence, distributor plate is modified without changing the percentage opening area to improve the heat transfer and to reduce the drying time and experiment was carried out. From the experiment, pressure drop verses fluidization height, drying characteristics and energy consumption for drying are investigated. Variation of pressure along the top side (TS) and bottom side (LS) along the riser height are measured for different inputs like superficial air velocity, drying air temperature and different amount of bed inventory.

Figs. 5.1(a) and (b) presents comparison of pressure drop along the riser height using STD and MD plates for θ = 15˚ and 30˚. In the Figs. it is found that pressure drop fluctuation using MD plate slightly decreases than that of using STD plate. However, fluidization height for using STD plate and MD plate are same. Similar trend is observed at θ = 30˚exception fluidization heights of θ = 30˚are lower than that of θ = 15˚. Fluidization heights for the lower side and upper side of θ = 15˚are 36 cm and 40 cm, respectively whereas it was 32 cm and 36 cm for θ = 30˚. Variations of pressure

TH-1488_126103037

drop from both side of the riser column are different for the inclined beds. Hence it will be expressed as lower side and upper side separately for next investigations.

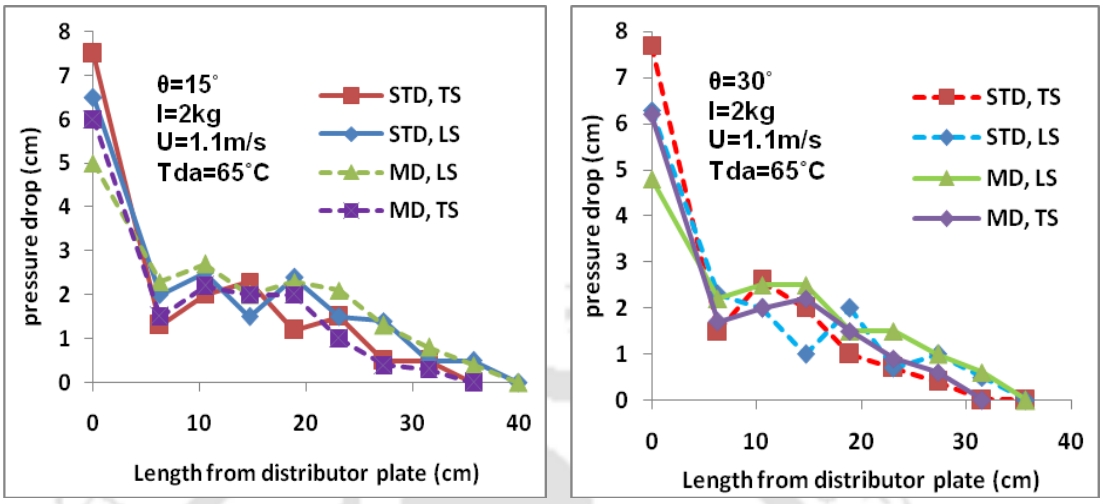

(a) (b)

Figs. 5.1 Pressure drop verses fluidization height using STD and MD plates for lower side and upper side of the riser column at (a) $\theta = 15^{\circ}$ and (b) $\theta = 30^{\circ}$

Figs. 5.2(a) and (b) present the pressure drop along the riser height of $\theta = 15^{\circ}$for lower side and upper side using STD plate and MD plate at different temperature. In the Figs. 5.2 (a) and (b) it is observed that pressure drop along the riser height using MD plate is higher than that of using STD plate for both temperatures 55˚C and 65˚C. However, fluidization heights for both plates are same. Fluidization heights are 40 cm at lower side and 36 cm at upper side for both plates.

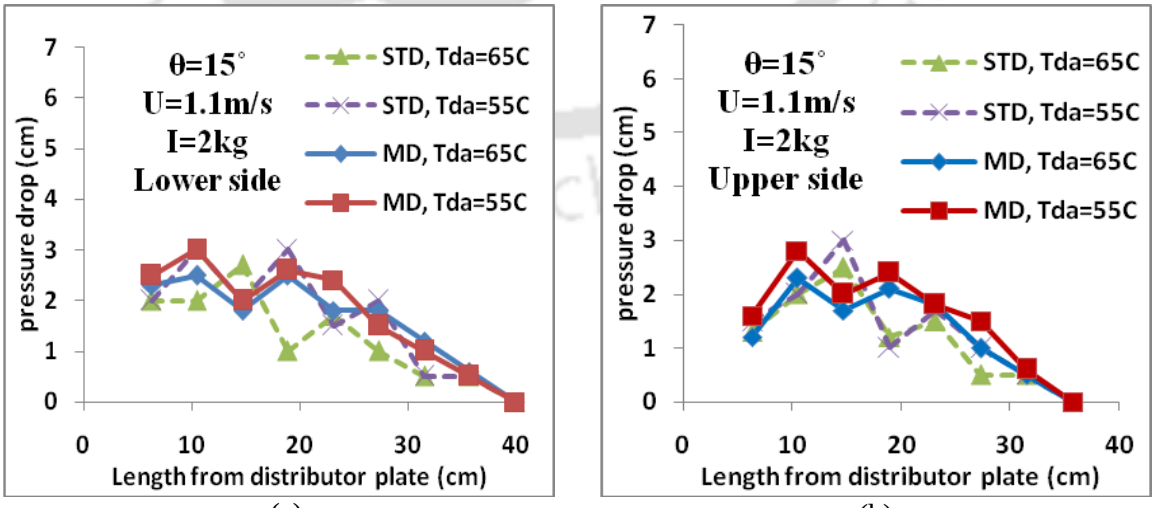

(a) (b)

Figs. 5.2 Pressure drop verses fluidization height using STD plate and MD plate for $\theta = 15^{\circ}$ at different temperature for (a) lower side and(b) upper side of riser column

TH-1488_126103037

Figs. 5.3(a) and (b) present the pressure drop along the riser height using STD and MD plates for θ = 15˚ at different inventory for lower side and upper side of riser column, respectively. In the Figs. 5.3(a) and (b) it is observed that pressure drop along the riser height using MD plate is higher than that of using STD plate for both inventories 0.5 kg and 2.5 kg. However, fluidization heights for both plates are same. Fluidization height for 2.5 kg is higher than that of 0.5kg for both plates. Fluidization heights for 2.5kg are 44 cm for lower side and 40 cm for upper side for both plates.

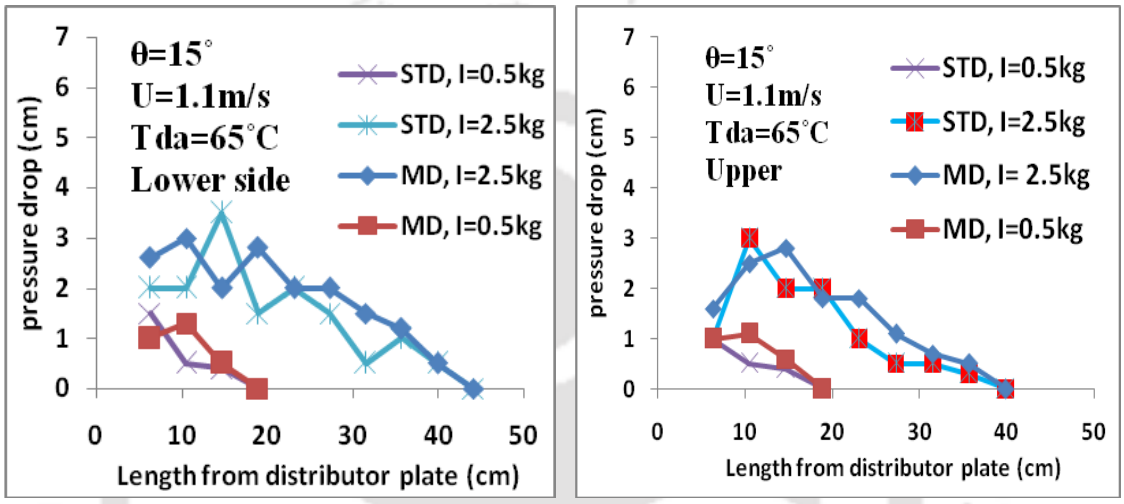

(a) (b)

Figs. 5.3 Pressure drop along the riser height using STD and MD plates for θ = 15˚ at different inventory for (a) lower side and (b) upper side of riser column

Figs. 5.4(a) and (b) presents the pressure drop verses fluidization height using STD and MD plates for θ = 15˚ at lower side and upper side of riser column for different velocity. In the Figs. 5.4(a) and (b) it is found that pressure drop along the riser height using MD plate is slightly higher than that of using STD plate. Pressure drop and fluidization height for 1.6 m/s is higher than that of 1.1m/s for both plates. Fluidization heights are 52 and 44 cm for lower side and 36 and 40 cm for upper side for 1.1 and 1.6 m/s, respectively for both plates.

5.3 DRYING CHARACTERISTICS OF FLUIDIZED BED USING MD PLATE

The results of the drying characteristics like various inventory, bed inclination, air velocity and drying air temperature on drying time of bubbling fluidized bed drying at room temperature and drying with heating system using modified distributor (MD) plate are presented and discussed in the subsequent sub-sections.

TH-1488_126103037

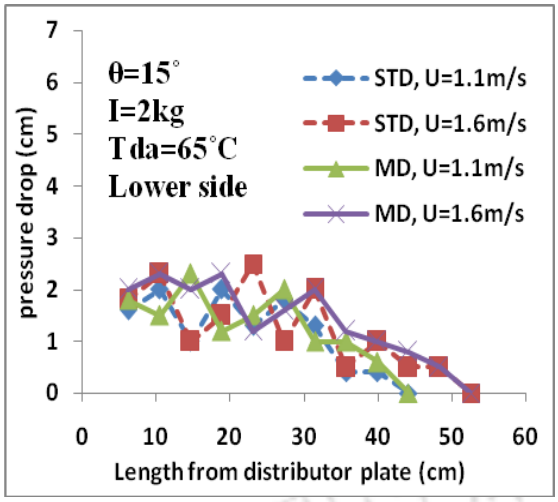

(a)

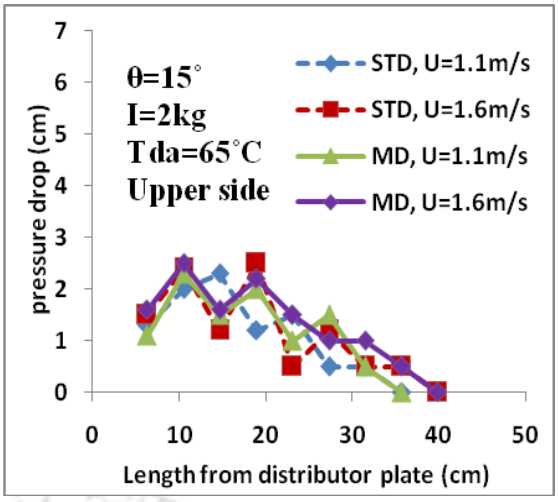

(b)

Figs. 5.4 Pressure drop verses fluidization height using STD and MD plates for θ = 15˚ at different velocity for (a) lower side and (b) upper side

5.3.1 Fluidized bed drying at room temperature using MD plate

The results of paddy drying at room temperature using MD plate are presented in Table 5.1.

Table 5.1 Time required for drying the paddy to attain a moisture level of 12% (w.b) for the experiments carried out at room temperature

Condition	Bed inclination (θ)	Drying Time (min)		
		1.5 kg	**1 kg**	**0.5 kg**
1.1m/s using MD plate	**15°**	135	110	85
	30˚	140	114	87
1.6 m/s using MD plate	**15°**	125	100	75
	30˚	130	104	77

In the Table 5.1 it is observed that drying time/kg paddy decreases by 7.4% when the velocity is increased from 1.1 to 1.6 m/s for an inventory of 1.5kg.Moreover, drying time/kg paddy decreases by 37% for θ = 15˚ and 37.8% for θ = 30˚for air velocity of 1.1 m/s and40% for θ = 15˚and 40.7% for θ = 30˚for air velocity of 1.6 m/s when the inventory is increased from 0.5 to 1.5 kg.

5.3.2Effect of inventory, temperature and velocity on drying time using MD plate

Time dependent moisture content of the grain of fluidized bed drying by the effect of load, temperature, velocity, inventory and inclination using the modified (MD) distributor plate are presented and discussed. Effect of load on the drying at an inlet

TH-1488_126103037

air temperature of 60°C and air velocity of 1.1, 1.6 and 2.1 m/s for θ = 15˚ and 30˚are shown in Table 5.2.

Table 5.2 Drying time (minutes) for different inventories at drying air temperature of 60°C and various operating conditions using MD plate

Air velocity (U) m.s^{-1}	Bed inclination (θ)	**Drying Time (min)**				
		0.5 kg	**1 kg**	**1.5 kg**	**2 kg**	**2.5 kg**
1.1	**15°**	37	43	49	55	61
	30˚	39	45	51	57	63
1.6	**15°**	36	41	46	51	56
	30˚	38	43	48	53	58
2.1	**15°**	35	39	43	47	51
	30˚	37	41	45	49	53

In the Table 5.2 it is observed that the time required for drying 1 kg of paddy at drying air temperature of 60˚C for θ = 15˚are 74, 43, 32.7, 27.5 and 24.4 min for air velocity of 1.1m/s,72, 41, 30.7, 25.5 and 22.4 min for air velocity of 1.6 m/s and 70, 39, 29, 23.5 and 20.4 min for air velocity of 2.1m/s, respectively for inventory of 0.5kg to 2.5 kg. It is observed that drying time/kg paddy decreases by 67% for 1.1 m/s and 68.9% for 1.6 m/s and 70.8% for 2.1 m/s, respectively when the inventory is increased from 0.5 kg to 2.5 kg. The drying time for an inventory of 2.5kg at air temperature of 60˚C and θ = 15˚ is 61min for air velocity of 1.1m/s and 51 min for 2.1 m/s. The corresponding reduction of drying time/kg paddy is 16.4% when the air velocity is increased from 1.1 m/s to 2.1 m/s for θ = 15˚.In all the above cases the time mentioned is to reach a moisture content of 12%.

Table 5.3 indicates the drying time at different velocities, different drying air temperatures, and with bed inclinations of 15° and 30˚ for an inventory of 2.5 kg. In the Table 5.3 it is observed that the drying time for an inventory of 2.5 kg at θ = 15˚ are 71, 61 and 51 min for air velocity of 1.1m/s, 66, 56 and 46 min for air velocity of 1.6 m/s and 61, 51 and 41 min for air velocity of 2.1m/s for the drying air temperature of 55˚C, 60˚C and 65˚C, respectively. The corresponding reductions of drying time/kg paddy are 28.2% for 1.1m/s and 30.3% for 1.6 m/s and 32.8% for 2.1m/s, respectively when the air temperature is increased from 55˚C to 65˚C. The drying time for an inventory of 2.5 kg at θ = 15˚ and air temperature of 65˚C are 51 min and 41 min for

TH-1488_126103037

air velocity of 1.1m/s and 2.1m/s, respectively. The corresponding drying time/kg paddy decreases by 19.6% when the air velocity is increased from 1.1 to 2.1 m/s.

Table 5.3 Effect of air temperature on drying time for an inventory of 2.5 kg using MD plate

Air velocity (U) m/s	Bed inclination (θ)	Drying Time (min)		
		55˚C	**60˚C**	**65˚C**
1.1	**15°**	71	61	51
	30˚	73	63	53
1.6	**15°**	66	56	46
	30˚	68	58	48
2.1	**15°**	61	51	41
	30˚	63	53	43

5.4 EFFECT OF MODIFICATION OF DISTRIBUTOR PLATE ON DRYING TIME

Effect of modification of distributor plate using the standard (STD) and modified (MD) distributor plates are shown in Tables 5.4, 5.5 and 5.6 for drying air velocity of 1.1, 1.6 and 2.1 m/s, respectively.

Table 5.4 indicates that the faster drying was obtained when the paddy was dried using MD plate in compared with STD plate. It is observed that the use of MD plate in the fluidized bed resulted in reductions of drying time/kg paddy for θ = 15˚ at air velocity of 1.1m/s for an inventory of 2.5kg are6.6, 7.6 and 9%, respectively for the drying air temperatures of 55, 60 and 65˚C.

From Table 5.5 it is observed that the use of modified distributor plate in the fluidized bed resulted in reductions of drying time/kg paddy for θ = 15˚ at air velocity of 1.6 m/s for an inventory of 2.5kg.are 7, 8.2 and 10% for drying air temperatures of 55, 60 and 65˚C, respectively.

From table 5.6 it is observed that the use of MD plate in the fluidized bed resulted in reductions of drying time/kg paddy for θ = 15˚ at air velocity of 2.1 m/s for an

TH-1488_126103037

inventory of 2.5kg.are7.6, 9 and 11% at the drying air temperatures of 55, 60 and 65˚C, respectively.

Table 5.4 Effect of distributor plate on drying time for air velocity of U = 1.1m/s at various temperatures

Condition	Bed inclination	Drying time (min)				
		0.5 kg	**1 kg**	**1.5 kg**	**2 kg**	**2.5 kg**
55°C,using STD plate	**0°**	51	60	69	78	87
	15°	48	55	62	69	76
	30°	50	57	64	71	78
55°C,using MD plate	**15°**	47	53	58	65	71
	30˚	49	55	60	67	73
60°C, using STD plate	**0°**	41	50	59	68	77
	15°	38	45	52	59	66
	30°	40	47	54	61	68
60°C, using MD plate	**15°**	37	43	49	55	61
	30°	39	45	51	57	63
65°C, using STD plate	**0°**	31	40	49	58	67
	15°	28	35	42	49	56
	30°	30	37	44	51	58
65°C,using MD plate	**15°**	27	33	39	45	51
	30°	29	35	41	47	53

Table 5.5 Effect of distributor plate on drying time for air velocity of U= 1.6ms^{-1} at various temperatures

Condition	Bed inclination	Drying time (min)				
		0.5kg	**1 kg**	**1.5kg**	**2 kg**	**2.5 kg**
55°C, using STD plate	**0°**	50	58	66	74	82
	15°	47	53	59	65	71
	30°	49	55	61	67	73
55°C, using MD plate	**15°**	46	51	56	61	66
	30˚	48	53	58	63	68
60°C, using STD plate	**0°**	40	48	56	64	72
	15°	37	43	49	55	61
	30°	39	45	51	57	63
60°C,using MD plate	**15°**	36	41	46	51	56
	30°	38	43	48	53	58
65°C,using STD plate	**0°**	30	38	46	54	62
	15°	27	33	39	45	51
	30°	29	35	41	47	53
65°C, using MD plate	**15°**	26	31	36	41	46
	30°	28	33	38	43	48

TH-1488_126103037

Table 5.6 Effect of distributor plate on drying time for air velocity U = 2.1 m/s at various temperatures

Condition	Bed inclination	Drying time (min)				
		0.5 (kg)	**1 (kg)**	**1.5 (kg)**	**2 (kg)**	**2.5 (kg)**
55°C, using STD plate	**0°**	49	56	63	70	77
	15°	46	51	56	61	66
	30°	48	53	58	63	68
55°C, using MD plate	**15°**	45	49	53	57	61
	30˚	47	51	55	59	63
60°C, using STD plate	**0°**	39	46	53	60	67
	15°	36	41	46	51	56
	30°	38	43	48	53	58
60°C,using MD plate	**15°**	35	39	43	47	51
	30°	37	41	45	49	53
65°C, using STD plate	**0°**	29	36	43	50	57
	15°	26	31	36	41	46
	30°	28	33	38	43	48
65°C, using MD plate	**15°**	25	29	33	37	41
	30°	27	31	35	39	43

5.5 MOISTURE CONTENT VERSES DRYING TIME USINGTWO DIFFERENT DISTRIBUTORPLATES

Comparison of moisture content verses drying time of bubbling fluidized bed drying using STD and MD plates for θ = 15˚are presented in Figs. 5.5 (a)-(c).In the Fig. 5.5 (a), drying time using STD distributor plate for an inventory of 2.5kg at air velocity of 1.1m/s are 76 and 56 min for the drying air temperature of 55˚C and 65˚C, respectively to drop the final MC of 12% (w.b). The corresponding drying times using MD plate are 71 min and 51 min. It is observed that drying time/kg paddy decreases by 6.6%and 8.9% for drying air temperature of 55˚C and 65˚C, respectively when MD plate is used. In the Fig. 5.5(b) the drying times/kg paddy using STD distributor plate at air velocity of 1.6 m/s and air temperature of 65˚C are 54 and 20.4 min, respectively for the inventory of 0.5 and 2.5kg to drop the final MC of 12% (w.b). The corresponding drying times/kg paddy using MD plate is 52 and 18.4 min. It is observed that drying time/kg paddy decreases by 3.7% and 9.8% for the inventory of 0.5 kg and 2.5 kg, respectively when MD plate is used.

TH-1488_126103037

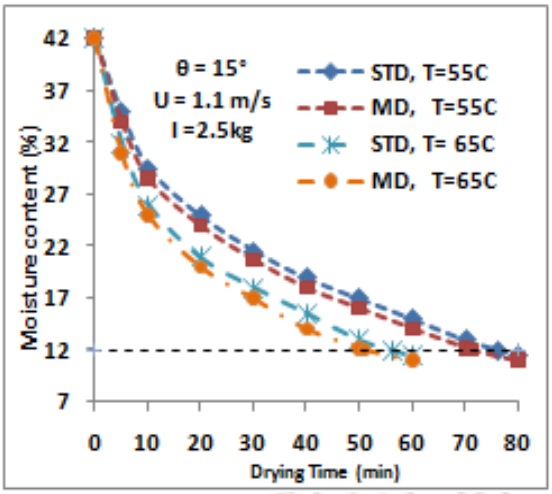

(a)

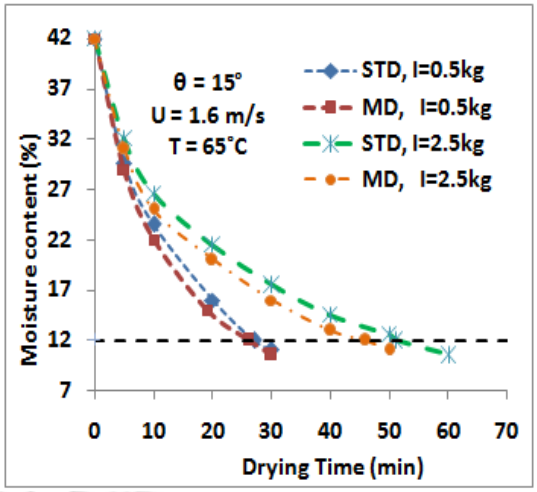

(b)

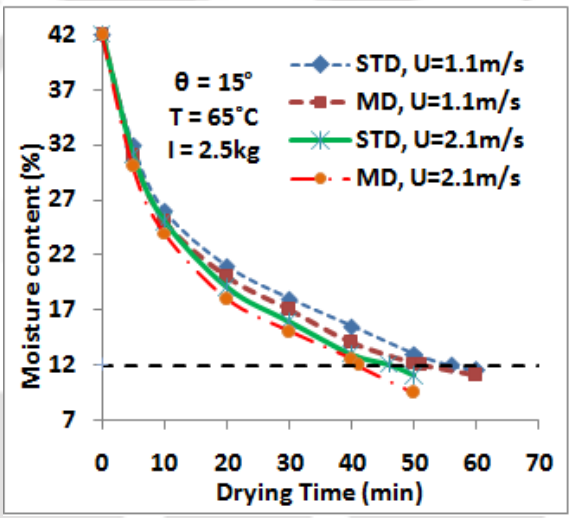

(c)

Figs. 5.5. Moisture content verses drying time plots using STD and MD plates for θ=15˚ at(a)different temperature (b) different inventory and (c)different velocity

In Fig. 5.5(c) the drying time using STD plate at air temperature of 65˚C and inventory of 2.5 kg are 56 and 46 min, respectively for air velocity of 1.1 m/s and 2.1 m/s to drop the final MC of 12% (w.b). The corresponding drying times using MD plate are 51 and 41 min. It is observed that drying time/kg paddy decreases by 8.9% and 10.9%, respectively for air velocity of 1.1m/s and 2.1 m/s when MD plate is used. Fig. 5.6 presents moisture content verses drying time plots for different angles θ = 0˚, 15˚ and 30˚.

TH-1488_126103037

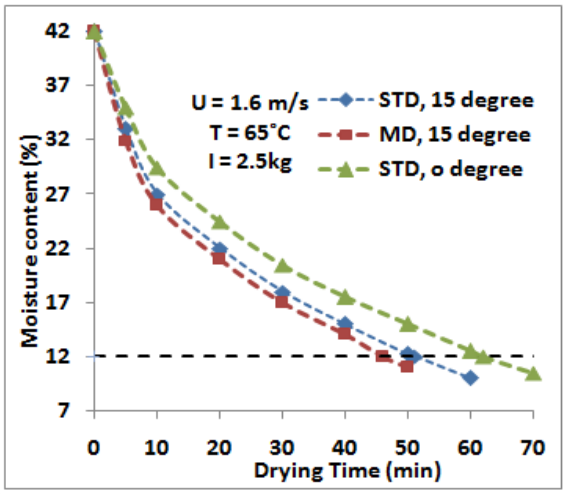

Fig. 5.6. Moisture content verses drying time plot using STD and MD plates at different inclination

In the Fig. 5.6 the drying times using STD plate for an inventory of 2.5kg at air velocity of 1.6m/s and air temperature of 65˚C are 62 min and 51 min, respectively for θ= 0˚ and 15˚to drop the final MC of 12% (w.b). The corresponding drying time using MD plate is 46 min for θ = 15˚.It is observed that drying time/kg paddy decreases by 9.8% for θ = 15˚ when MD plate is used.

5.6 PERFORMANCE ENHANCEMENT OF BFB DRYING USING SPIRALS

Paddy drying process consumes high energy due to the removal of internal moisture. The main objective for a sustainable dryer is to reduce required energy input by means of designing an efficient drying system which can provide the dried products with acceptable quality level. The drying performance of the bubbling fluidized bed dryer can be improved by installing spirals inside the dryer column which improves the contact between the solid and gas, thereby improving the mixing efficiency leading to higher heat transfer characteristics. The effect of spirals in bubbling fluidized bed drying on hydrodynamic behaviour, moisture removal rate and drying time are presented and discussed in subsequent subsections. Figs. 5.7(a) and (b) show the photograph of fluidized bed dryer column with spirals and photograph of spiral.The detail dimensions of spiral inserts are: length of spiral is 570mm, diameter of spiral is 5mm, length of spiral taps is 35 mm, number of taps is 18, pitch of taps is 30 mm and number of spiral is 2.

TH-1488_126103037

(a) (b)

Figs. 5.7 Photographs of (a) fluidized bed dryercolumn and (b) spiral

5.7 HYDRODYNAMIC BEHAVIOUR OF PADDY DRYINGWITH AND WITHOUT THE USE OF SPIRALS

Variation of pressure drop along the riser height for $\theta = 0^0$ with the use of spirals (SP) and without the use of spirals (XSP)at different temperatures is presented in Fig. 5.8. In the Fig. it is observed that pressure drop along the riser height using spirals is slightly higher than that of without the use of spirals for both temperature. Pressure drop for 55˚C is higher than that of 65˚C for both cases. Fluidization height with and without the use of spirals are 44cm. Pressure drop fluctuation decreases significantly when spiral inserts are used.

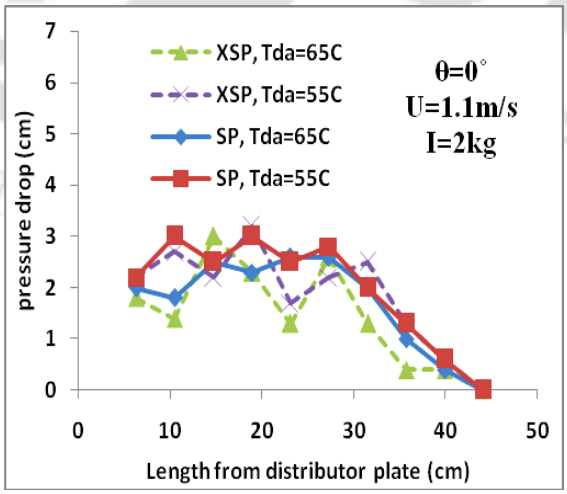

Fig. 5.8 Pressure drop verses fluidization height with and without the use of spirals at different temperature for $\theta = 0^{\circ}$

TH-1488_126103037

Figs. 5.9 (a) and (b) present the pressure drop along the riser height with and without the use of spirals for $\theta = 0^{\circ}$ at different inventory and different velocity, respectively. In the Figs. it is observed that pressure drop fluctuation decreases significantly with the use of spirals in compared without the use of spirals. Moreover, pressure drop along the riser height also increases when spirals inserts are used. However, fluidization heights for with and without the use of spirals are same. Fluidization height for inventory 2.5kg is 48 cm and inventory 0.5 kg is 23 cm for both cases in Fig. 5.9 (a). Fluidization heights are 44 cm for air velocity of 1.1m/s and 52 cm for 1.6m/s, respectively for with and without the use of spirals in Fig. 5.9 (b).

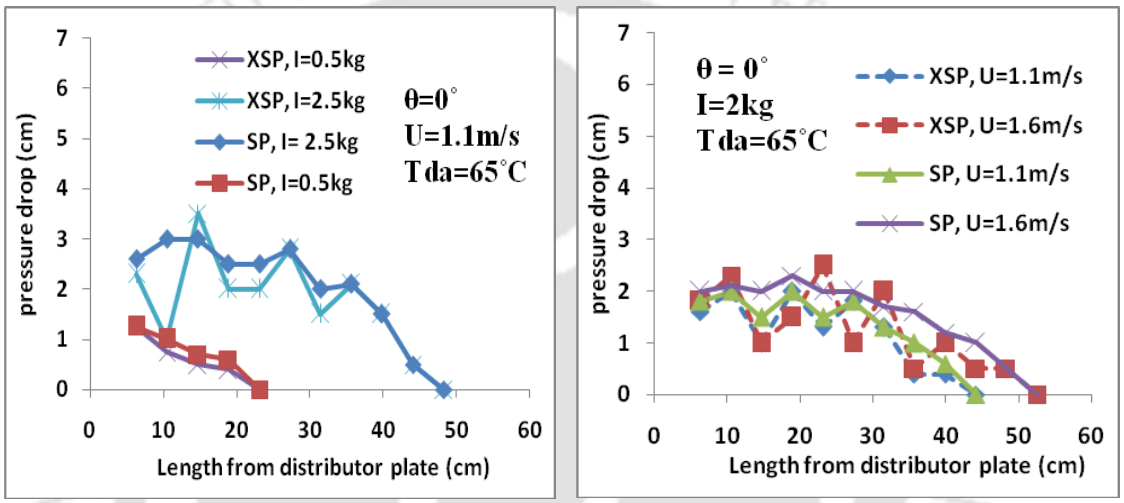

(a) (b)

Figs. 5.9 Pressure drop verses fluidization height for $\theta = 0^{\circ}$ with and without the use of spirals at (a) different inventory and (b) different velocity

Figs. 5.10(a) and (b) present the pressure drop along the riser height with and without the use of spirals for $\theta = 15^{\circ}$ and 30°.In the Figs. 5.10(a) and (b) it is found that pressure drop with the use of spirals is slightly higher than that of without the use of spirals. However pressure drop fluctuation decreases significantly when spiral inserts are used. Fluidization height for with and without the use of spirals are same. Fluidization heights are 40 cm and 36 cm for $\theta = 15^{\circ}$ and36 and 32 cm for $\theta = 30^{\circ}$, respectively for lower side and upper side.

TH-1488_126103037

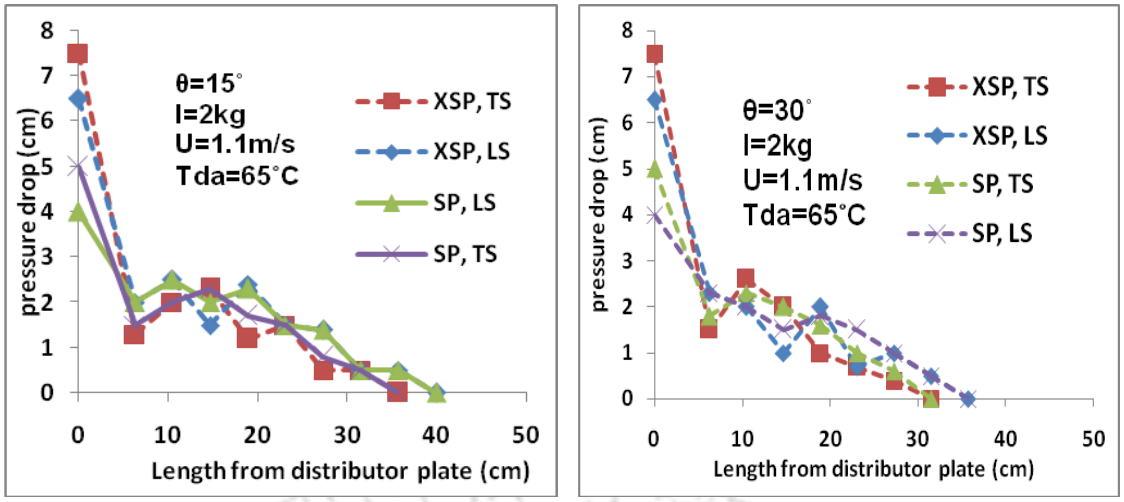

(a) (b)

Figs. 5.10 Pressure drop verses fluidization height with and without the use of spirals for lower side and upper side of the riser column at (a) $\theta = 15^{\circ}$ and (b) $\theta = 30^{\circ}$

Variations of pressure drop from both side of the riser column are different for the inclined beds. Hence it will be expressed as lower side and upper side separately for next investigations. Figs. 5.11(a) and (b) present the pressure drop along the riser column for lower side and upper side with and without the use of spirals for $\theta = 15^{\circ}$ at different temperature.

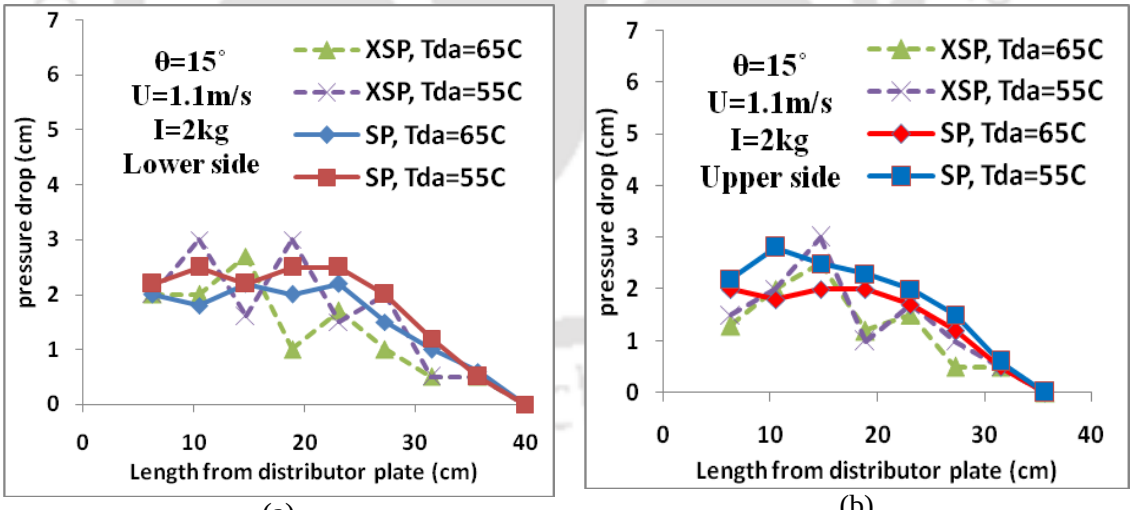

(a) (b)

Figs. 5.11 Pressure drop verses fluidization height with and without the use of spirals for $\theta = 15^{\circ}$ at different temperature for (a) lower side and (b) upper side of riser column

In the Figs. 5.11(a) and (b) it is observed that pressure drop fluctuation becomes smooth when spirals inserts are used in compared without the use of spirals. Moreover, pressure drop with the use of spirals is higher than that of without the use

TH-1488_126103037

of spirals. However, fluidization heights for with and without the use of spirals are same. Fluidization height for lower side is 40 cm and 36 cm for upper side. Pressure drop at 55˚C is higher than that of 65˚C for both cases. Figs. 5.12 (a) and (b) present the pressure drop along the riser height for lower side and upper side with and without the use of spirals for $\theta = 15^{\circ}$ at different inventory.

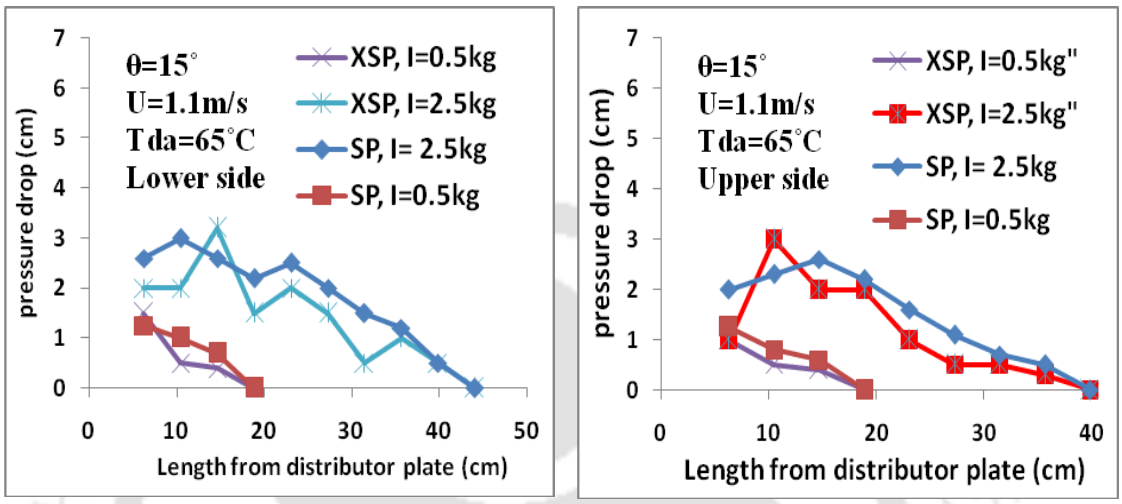

(a) (b)

Figs. 5.12 Pressure drop verses fluidization height with and without the use of spirals for $\theta = 15^{\circ}$ at different inventory for (a) lower side and (b) upper side of riser column.

In the Figs. 5.12(a) and (b) it is observed that pressure drop and fluidization height are high at an inventory of 2.5 kg whereas it is low at 0.5kg for with and without the use of spirals. Fluidization heights are 20 cm and 44cm for lower side and 20 cm and 40 cm for upper side for both cases. Pressure drop fluctuation decreases significantly when spirals inserts are used.

Figs. 5.13(a) and (b) presents the pressure drop along the riser height with and without the use of spirals for $\theta = 15^{\circ}$ at lower side and upper side of riser column at different velocity. It is found that pressure drop and fluidization height at the velocity of 1.6 m/s is higher than that of 1.1m/s for with and without the use of spirals. Fluidization heights are 44 and 40 cm for lower side and 40 and 32 cm for upper side for the air velocity of 1.6 m/s and 1.1m/s, respectively for with and without the use of spirals. Pressure drop increases when spirals inserts are used. However, fluidization heights are same for with and without the use of spirals.

TH-1488_126103037

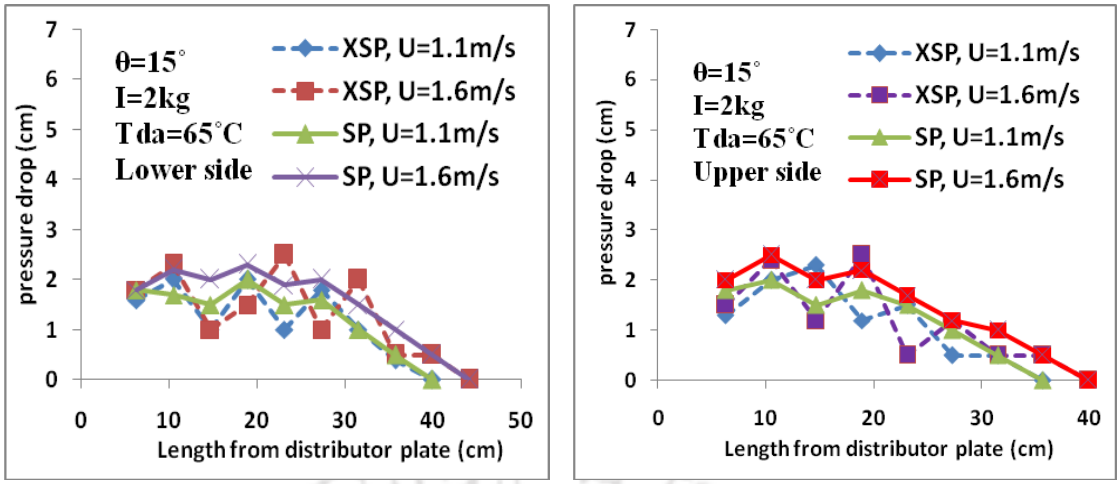

(a) (b)

Figs. 5.13 Pressure drop verses fluidization height with and without the use of spirals for $\theta = 15^{\circ}$ at different velocity for (a) lower side (b) upper side of riser column

Figs. 5.14(a) and (b) present the pressure drop along the riser height with and without the use of spirals for $\theta = 0^{\circ}$, 15° and 30° at the drying air temperature of 65˚C, superficial air velocity of 1.6 m/s and the inventory of 2kg.In the Figs. 5.14(a) and (b) it is observed that pressure drop fluctuation decreases when spirals inserts are used. Pressure drop and fluidization height are higher at $\theta = 0^{\circ}$ than $\theta = 15^{\circ}$ and 30° for with and without the use of spirals. Fluidization heights are 52, 44 and 40 cm for lower side and 52, 40 and 36 cm for upper side for $\theta = 0^{\circ}$. 15° and 30°, respectively for with and without spirals inserts.

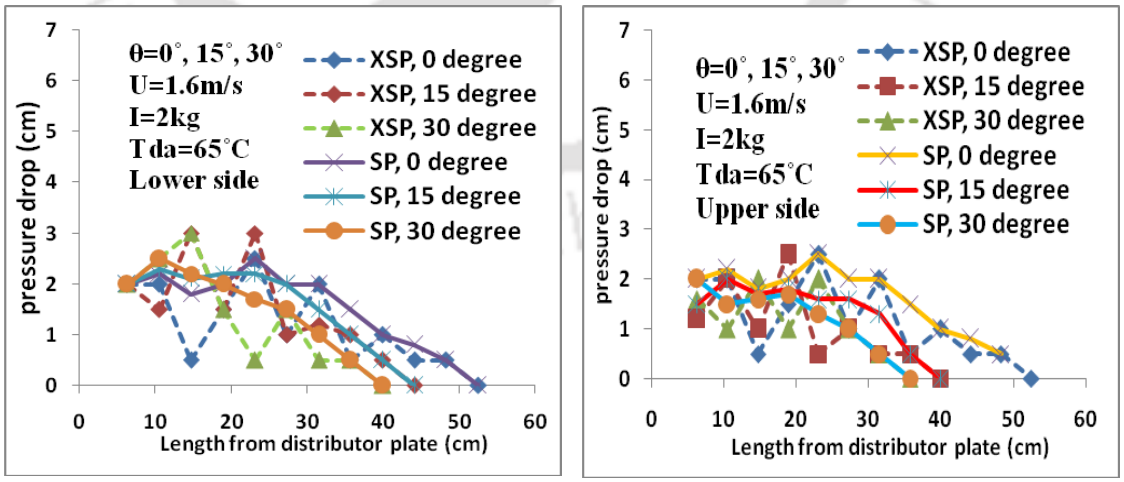

(a) (b)

Figs. 5.14 Pressure drop verses fluidization height with and without the use of spirals for different inclination angles of $\theta = 0^{\circ}$. 15° and 30° (a) lower side and (b) upper side of the riser column

TH-1488_126103037

5.8 EFFECT OF LOAD, TEMPERATURE AND VELOCITY ON DRYING TIME USING SPIRALS

Effect of load, temperature and velocity on time dependent moisture content of the grain of fluidized bed drying using spirals are shown in Table 5.7.

Table 5.7 Drying time (minutes) for different bed inventories at drying air temperature of 60°C and various operating conditions using spirals

Bed inclination (Θ)	Air velocity (U) m.s^{-1}	**Drying Time (min)**				
		0.5 kg	**1 kg**	**1.5 kg**	**2 kg**	**2.5 kg**
0°	**U = 1.1**	29	36	43	50	57
15°		25	29	33	37	41
30˚		27	31	35	39	43
0°	**U = 1.6**	28	34	40	46	52
15°		24	27	30	33	36
30˚		26	29	32	35	38
0°	**U = 2.1**	27	32	37	42	47
15°		23	25	27	29	31
30˚		25	27	29	31	33
0˚	**U = 2.6**	26	30	34	38	42

In the Table 5.7 it is observed that the time required for drying 1 kg of paddy for θ = 0˚ at drying air temperature of 60°C and air velocity of 2.1m/s are 54 and 18.8 min for 0.5 kg and 2.5 kg, whereas the corresponding drying time/kg paddy for θ = 15˚ are 46min and 12.4 min, respectively. It is observed that drying time/kg paddy decreases by 65.2% for θ = 0˚ and 73% for θ = 15˚ when the inventory is increased from 0.5 to 2.5kg. Drying time for an inventory of 2.5kg at drying air temperature of 60˚C for θ = 0˚ are 57 and 42 min, respectively for the air velocity of 1.1 m/s and 2.6 m/s. The corresponding reduction of drying time/kg paddy is 26.3% when the air velocity is increased from 1.1 to 2.6 m/s. Drying time for an inventory of 2.5kg at drying air temperature of 60˚C for the air velocity of 2.1 m/s are 47 and 31 min, respectively for θ = 0˚ and 15˚. The corresponding reduction of drying time/kg paddy is 34% when the inclination is increased from θ = 0˚ to 15˚.

Table 5.8 indicates the drying time at different velocities and temperatures with bed inclinations of θ = 0°, 15° and 30˚ for an inventory of 2.5 kg.

TH-1488_126103037

Table 5.8 Effect of air temperature on the drying time for an inventory of 2.5 kg using spirals

Velocity (U) m/s	Bed inclination (Θ)	Drying Time (min)		
		55˚C	**60˚C**	**65˚C**
1.1	**0˚**	67	57	47
	15˚	51	41	31
	30˚	53	43	33
1.6	**0˚**	62	52	42
	15˚	46	36	26
	30˚	48	38	28
2.1	**0˚**	57	47	37
	15˚	41	31	21
	30˚	43	33	23
2.6	**0˚**	52	42	32

In the Table 5.8, it is observed that drying time for an inventory of 2.5 kg at air velocity of 2.1 m/s are 57, 47 and 37 min for θ = 0˚and 41, 31 and 21 min for θ = 15˚for the drying air temperature of 55, 60 and 65°C, respectively. The corresponding drying time/kg paddy decreases by 35% and 48.8% for θ = 0˚ and 15˚, respectively when the air temperature is increased from 55 to 65˚C.The drying time for an inventory of 2.5 kg at drying air temperature of 65˚Cfor θ = 0˚are 47 min for the air velocity of 1.1 m/sand 32 min for 2.6 m/s, respectively. The corresponding reduction of drying time/kg paddy is 31.9% when the air velocity is increased from 1.1m/s to 2.6 m/s. The drying time for an inventory of 2.5 kg at drying air temperature of 65˚C and air velocity of 2.1 m/s are 37 min and 21 min for θ = 0˚and 15˚, respectively. The corresponding drying time/kg paddy decreases by 43.2% when the inclination is increased from 0˚ to 15˚.

5.9 EFFECT OF SPIRALS ON DRYING TIME

Spirals are used inside the drying chamber to reduce the drying time and energy consumptions by improving particles mixing properly and heat transfer from the hot air to particles. Effect of spirals on drying time at air velocities of 1.1, 1.6, 2.1 and 2.6 m/s are shown in Tables 5.9 to 5.12, respectively.

TH-1488_126103037

Table 5.9 Effect of spirals on drying time for air velocity of 1.1m/s

Condition	Bed inclination	Drying time (min)				
		0.5 (kg)	**1 (kg)**	**1.5 (kg)**	**2 (kg)**	**2.5 (kg)**
55°C, without spirals	**0°**	51	60	69	78	87
	15°	47	53	58	65	71
	30°	49	55	60	67	73
55°C, with spirals	**0°**	39	46	53	60	67
	15°	35	39	42	47	51
	30˚	37	41	44	49	53
60°C, without spirals	**0°**	41	50	59	68	77
	15°	37	43	49	55	61
	30°	39	45	51	57	63
60°C, with spirals	**0°**	29	36	43	50	57
	15°	25	29	33	37	41
	30°	27	31	35	39	43
65°C, without spirals	**0°**	31	40	49	58	67
	15°	27	33	39	45	51
	30°	29	35	41	47	53
65°C, with spirals	**0°**	19	26	33	40	47
	15°	15	19	23	27	31
	30°	17	21	25	29	33

Table 5.10 Effect of spirals on drying time for air velocity of 1.6 m/s

Condition	Bed inclination	Drying time (min)				
		0.5 (kg)	**1 (kg)**	**1.5 (kg)**	**2 (kg)**	**2.5 (kg)**
55°C, without spirals	**0°**	50	58	66	74	82
	15°	46	51	56	61	66
	30°	48	53	58	63	68
55°C, with spirals	**0°**	38	44	50	56	62
	15°	34	37	40	43	46
	30˚	36	39	42	45	48
60°C, without spirals	**0°**	40	48	56	64	72
	15°	36	41	46	51	56
	30°	38	43	48	53	58
60°C, with spirals	**0°**	28	34	40	46	52
	15°	24	27	30	33	36
	30°	26	29	32	35	38
65°C, without spirals	**0°**	30	38	46	54	62
	15°	26	31	36	41	46
	30°	28	33	38	43	48
65°C, with spirals	**0°**	18	24	30	36	42
	15°	14	17	20	23	26
	30°	16	19	22	25	28

TH-1488_126103037

Table 5.11 Effect of spirals on drying time for air velocity of 2.1 m/s

Condition	Bed inclination	Drying time (min)				
		0.5 (kg)	**1 (kg)**	**1.5 (kg)**	**2 (kg)**	**2.5 (kg)**
55°C, without spirals	**0°**	49	56	63	70	77
	15°	45	49	53	57	61
	30°	47	51	55	59	63
55°C, with spirals	**0°**	37	42	47	52	57
	15°	25	28	31	34	41
	30˚	27	30	33	36	43
60°C, without spirals	**0°**	39	46	53	60	67
	15°	35	39	43	47	51
	30°	37	41	45	49	53
60°C, with spirals	**0°**	27	32	37	42	47
	15°	23	25	27	29	31
	30°	25	27	29	31	33
65°C, without spirals	**0°**	29	36	43	50	57
	15°	25	29	33	37	41
	30°	27	31	35	39	43
65°C, with spirals	**0°**	17	22	27	32	37
	15°	13	15	17	19	21
	30°	15	17	19	21	23

Table 5.9 indicates that the faster drying was obtained when the paddy was dried using spirals inside the fluidized bed. The use of spirals in the fluidized bed resulted in the reductions in drying time/kg paddy for air velocity of 1.1 m/s and an inventory of 2.5kg are 22.9, 25.9 and 29.9% for θ = 0˚ and 28.2, 32.8 and 39.2% for θ = 15˚ at the air temperatures of 55, 60 and 65˚C, respectively in compared without the use of spirals.

In the Table 5.10 it is observed that the reductions in drying time/kg paddy using spirals at air velocity of 1.6 m/s for an inventory of 2.5kg are 24.4, 27.8 and 32.3% at θ = 0˚ and 30.3, 35.7 and 43.8% at θ = 15˚for the air temperatures of 55, 60 and 65˚C, respectively in compared without the use of spirals.

In the Table 5.11it is observed that the reductions in drying time/kg paddy using spirals for air velocity of 2.1 m/s and an inventory of 2.5kg are 25.9, 29.8 and 35.1% at θ = 0˚ and 32.8, 39.2 and 48.8 % at θ = 15˚at the air temperatures of 55, 60 and 65˚C, respectively in compared without the use of spirals. The minimum drying time

TH-1488_126103037

per kg paddy is 8.4 min at an inventory of 2.5 kg, air temperature is 65˚C, air velocity of 2.1 m/s, an inclination angle of 15˚ using modified distributor plate with the use of spiral inserts.

Table 5.12 Effect of spirals on drying time for air velocity of 2.6 m/s

Condition	Bed inclination	Drying time (min)				
		0.5 (kg)	**1 (kg)**	**1.5 (kg)**	**2 (kg)**	**2.5 (kg)**
55°C, without spirals	**0°**	48	54	60	66	72
55°C, with spirals	**0°**	36	40	44	48	52
60°C, without spirals	**0°**	38	44	50	56	62
60°C, with spirals	**0°**	26	30	34	38	42
65°C, without spirals	**0°**	28	34	40	46	52
65°C, with spirals	**0°**	16	20	24	28	32

In the Table 5.12 it is observed that the reductions in drying time/kg paddy using spirals for air velocity of 2.6 m/s for an inventory of 2.5kg are 27.8, 32.3 and 38.5% at θ = 0˚for the air temperatures of 55, 60 and 65˚C, respectively in compared without the use of spirals.

5.10 MOISTURE CONTENT VERSES DRYING TIME WITH AND WITHOUT THE USE OF SPIRALS

The moisture content verses drying time plots for the fluidized bed dryer with the use of spirals (SP) and without the use of spirals (XSP) for θ = 0˚ are shown in Figs. 5.15(a)-(c).From the Fig. 5.15(a) it is evident that use of spirals increased the moisture removal at a faster rate compared to the case without spirals. Providing the spiral in the drying bed promoted better solid gas mixing resulting in higher heat transfer rate from the hot air to particles. In the Fig. 5.15(a) the drying times for an inventory of 2.5kg at air velocity of 1.1m/s are 87, 77, and 67 min for without spirals inserts for drying air temperature of 55, 60 and 65˚C, respectively to drop the final MC of 12% (w.b), whereas the corresponding drying time are 67, 57 and 47 min for with spiral inserts. It is observed that drying time/kg paddy decreases by 22.9, 25.9 and 29.9%, respectively for air temperature of 55, 60 and 65˚C when spiral inserts are used.

TH-1488_126103037

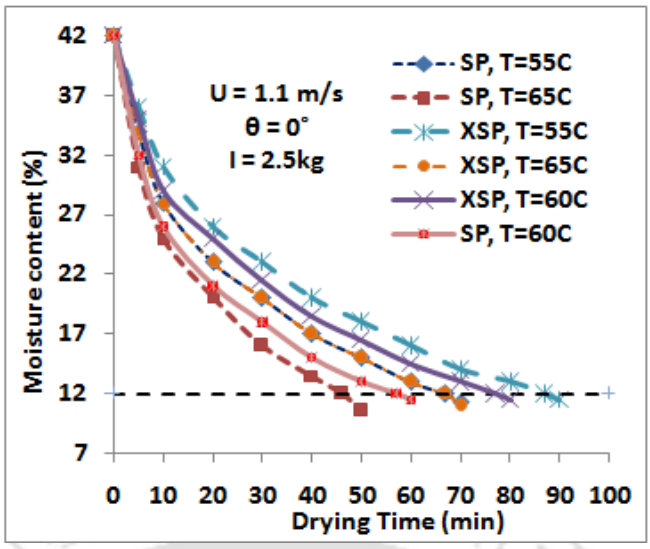

Fig. 5.15(a) Moisture content verses drying time plotwith and without the use of spirals for $\theta = 0^{\circ}$ at different temperature

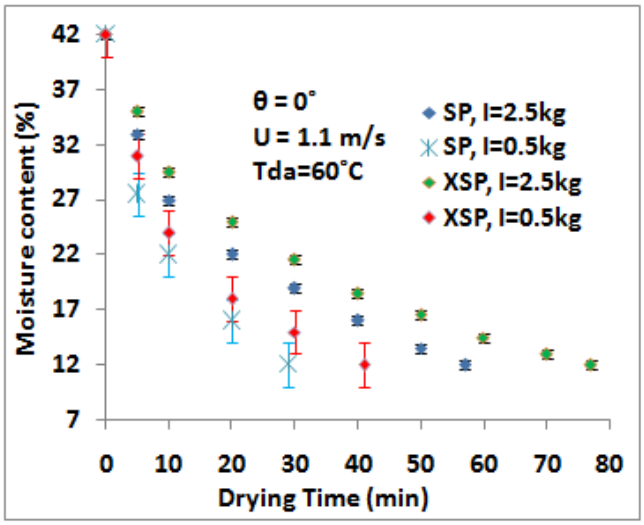

Fig 5.15(b) Moisture content verses drying time plot with and without the use of spirals for $\theta = 0^{\circ}$ at different inventory

In the Fig. 5.15(b) the drying times/kg paddy without spiral inserts at air velocity of1.1m/s and air temperature of 60˚C are 82 and 30.8 min, respectively for the inventory 0.5 to 2.5kg to drop the final MC of 12% (w.b), whereas the corresponding drying time with spiral inserts are 58 and 22.8 min. It is observed that drying time/kg paddy decreases by 29.3% and 25.9% for the inventory of 0.5kg and 2.5kg, respectively when spiral inserts are used.

TH-1488_126103037

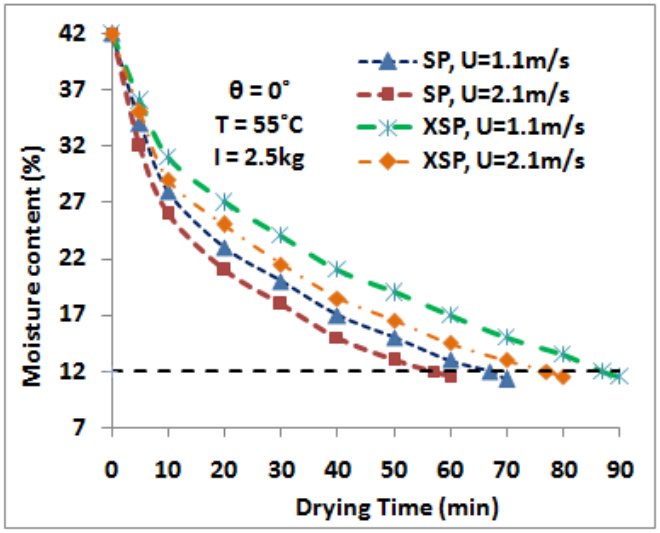

Fig. 5.15(c) Moisture content verses drying time plot with and without the use of spirals for $\theta = 0^{\circ}$ at different velocity

In the Fig. 5.15(c) the drying times without spiral inserts at air temperature of 55˚C and an inventory of 2.5kg are 87 and 77 min respectively for the air velocity of 1.1m/s and 2.1 m/s to drop the final MC of 12% (w.b). The corresponding drying times with spiral inserts are 67 and 57 min. It is observed that drying time/kg paddy decreases by 22.9% and 25.9% for air velocity of 1.1 m/s to 2.1 m/s, respectively when spiral inserts are used. The moisture content verses drying time plots for the fluidized bed dryer with the use of spirals (SP) and without the use of spirals (XSP) for $\theta = 15^{\circ}$ are shown in Figs. 5.16(a)-(c).

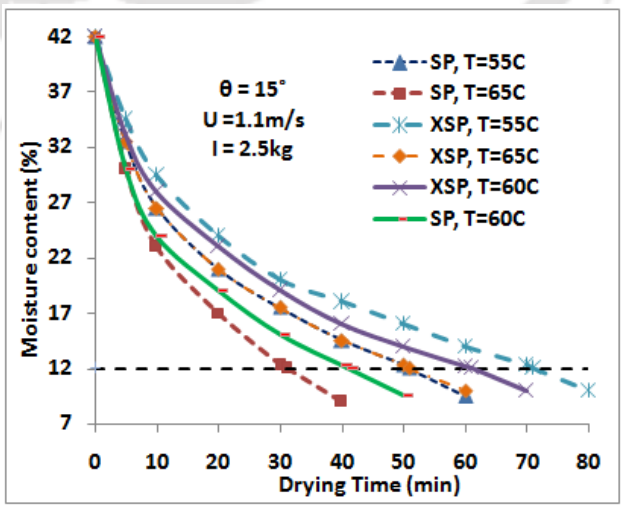

Fig. 5.16(a) Moisture content verses drying time plotwith and without the use of spirals for $\theta = 15^{\circ}$ at different temperature

TH-1488_126103037

In the Fig. 5.16(a) the drying times without spiral inserts for the inventory of 2.5kg at air velocity of1.1m/s are 71, 61 and 51 min for the drying air temperature of 55, 60 and 65˚C, respectively to drop the final MC of 12% (w.b). The corresponding drying times with spiral inserts are 51 min, 41 min and 31 min. It is observed that drying time/kg paddy decreases by 28.2%, 32.8% and 39.2%, respectively for air temperature of 55, 60and 65˚C when spiral inserts are used.

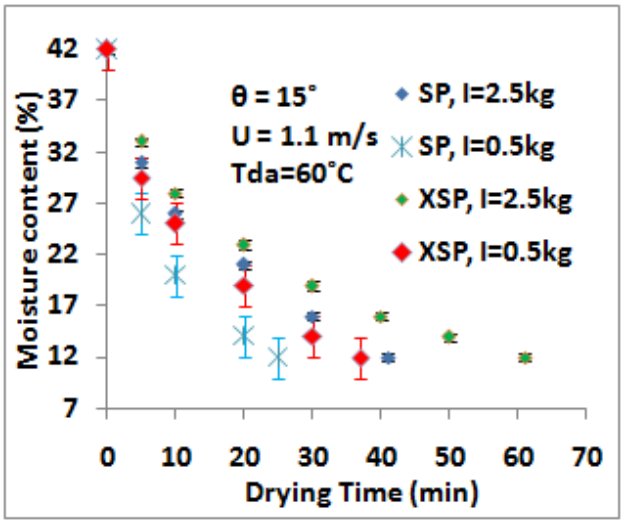

Fig. 5.16(b) Moisture content verses drying time plot with and without the use of spirals for θ = 15˚ at different inventory

In the Fig. 5.16(b) the drying times/kg paddy without spiral inserts at air velocity of 1.1m/s and air temperature of 60˚C are 74 and 24.4 min, respectively for the inventory 0.5 and 2.5kg to drop the final MC of 12% (w.b), whereas the corresponding drying time/kg paddy with spiral inserts are 50 and 16.4 min. It is observed that drying time/kg paddy decreases by 32.4% and 32.8% for the inventory of 0.5kg and 2.5kg, respectively when spiral inserts are used. As shown in Figs. 5.15(b) and 5.16(b), uncertainty in measurement of moisture content (%) for the inventories of 0.5 and 2.5kg are calculated to be ±2% and ±0.4%, respectively.

TH-1488_126103037

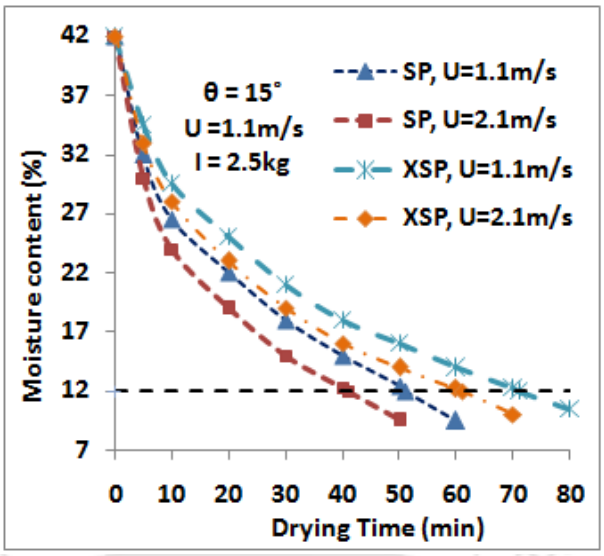

Fig. 5.16(c) Moisture content verses drying time plot with and without the use of spirals for $\theta = 15^{\circ}$ at different velocity

In the Fig. 5.16(c) drying times without spiral inserts at air temperature of 55˚C and inventory of 2.5kg are 71 and 61 min, respectively for the air velocity of 1.1 m/s and 2.1 m/s to drop the final MC of 12% (w.b), whereas the corresponding drying time with spiral inserts are 51 and 41 min. It is observed that drying time/kg paddy decreases by 28.2% and 32.8%, respectively for the air velocity of 1.1 and 2.1 m/s when spiral inserts are used. Fig. 5.17 presents moisture content verses drying time with and without the use of spiral inserts for $\theta = 15^{\circ}$ at different inclination.

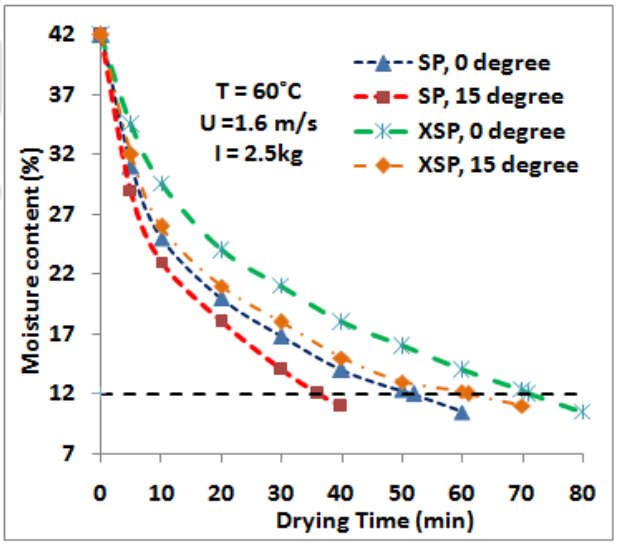

Fig. 5.17 Moisture content verses drying time with and without the use of spiral inserts at different inclination

TH-1488_126103037

In the Fig. 5.17 drying times without spiral inserts for an inventory of 2.5kg, air velocity of 1.6 m/s and air temperature of 60˚C are 72 and 56 min, respectively for θ = 0˚, and 15˚ to drop the final MC of 12% (w.b), whereas the corresponding drying time are 52 and 36 min when spiral inserts are used. It is observed that drying time/kg paddy decreases by 27.8% and 35.7%, respectively for θ = 0˚ and 15˚when spiral inserts are used.

5.11 EFFECT OF SCALE UP ON DRYING TIME USING STD PLATE

The comparison results of drying time of small setup and large set up, i.e., dryer cross sectional area of 150 mm × 150 mm are shown in Tables 5.13 and 5.14.From Tables 5.13 and 5.14, it is observed that drying time per kg paddy decreases by average 10% by the effect of scale up. The maximum reduction in drying time per kg paddy by the effect of scale up using STD plate is 11% at air temperature of 65˚C, air velocity of 2.1 m/s, an inclination angle of 15˚ and an inventory of 2.5 kg.

Table 5.13 Effect of scale up on drying time (minutes) using STD plate at air temperature of 60˚Cfor different inventory

Bed inclination (Θ)	Air velocity (U)	**Drying Time (min)**				
		0.5 kg	**1 kg**	**1.5 kg**	**2 kg**	**2.5 kg**
0°	Small setup U = 1.1 ms^{-1}	41	50	59	68	77
15°		38	45	52	59	66
30˚		40	47	53	61	68
0°	Large setup U= 1.1 ms^{-1}	36	45	54	68	72
15°		33	40	47	59	61
30˚		35	42	49	61	63
0°	Small setup U = 1.6 ms^{-1}	40	48	56	64	72
15°		37	43	49	55	61
30˚		39	45	51	57	63
0°	Large setup U = 1.6 ms^{-1}	35	43	51	59	67
15°		32	38	44	50	56
30˚		34	40	46	52	58
0°	Small setup U = 2.1 ms^{-1}	39	46	53	60	67
15°		36	41	46	51	56
30˚		38	43	48	53	58
0°	Large setup U = 2.1 ms^{-1}	34	41	48	55	62
15°		31	36	41	46	51
30°		33	38	43	48	53

TH-1488_126103037

Table 5.14Effect of scale up on drying time (minutes) using STD plate for an inventory of 2.5 kg at different temperature

Bed inclination (Θ)	Air velocity (U)	**Drying Time (min)**		
		55˚C	**60˚C**	**65˚C**
0°	Small setup U = 1.1 ms^{-1}	87	77	67
15°		76	66	56
30˚		78	68	58
0°	Large setup U = 1.1 ms^{-1}	82	72	62
15°		71	61	51
30˚		73	63	53
0°	Small setup U= 1.6 ms^{-1}	82	72	62
15°		71	61	51
30˚		73	63	53
0°	Large setup U = 1.6 ms^{-1}	77	67	57
15°		66	56	46
30˚		68	58	48
0°	Small setup U = 2.1 ms^{-1}	77	67	57
15°		66	56	46
30˚		68	58	48
0°	Large setup U= 2.1 ms^{-1}	72	62	52
15°		61	51	41
30˚		63	53	43

5.12 SUMMARY

The comparison results of the hydrodynamic behaviour and drying characteristics such as moisture content verses drying time of paddy drying in fluidized bed using standard as well as modified distributor plate, with and without the use of spirals and effect of scale up are presented and discussed in this chapter. Blower as well as thermal energy consumptions of the bubbling fluidized bed dryer for various combinations using standard as well as modified distributor plates, with and without the use of spirals, vertical and inclined beds and scale up effect will be discussed in chapter 6.

TH-1488_126103037

CHAPTER 6

ENERGY CONSUMPTIONS OF THE BFB DRYER

6.1 INTRODUCTION

Energy consumptions of the bubbling fluidized bed dryer for various combinations using standard and modified distributor plates, with and without the use of spirals, vertical and inclined bed, at different air velocity, three air temperatures and various paddy bed inventories are presented and discussed in this chapter. The discussion is mainly the following:

a) Electrical as well as thermal energy consumptions of the fluidized bed dryer using standard distributor plate.
b) Comparison of energy consumptions using standard distributor plate and modified distributor plate
c) Comparison of energy consumptions with and without the use of spiral
d) Comparison of energy consumptions of two BFB dryers with different bed cross-sectional area

Energy consumptions are measured for different inputs like superficial air velocity, drying air temperature and bed inventories.

6.2 ENERGY CONSUMPTIONS USING STD PLATE

Figs. 6.1(a)-(c) present the electrical (blower) energy consumption using standard distributor (STD) plate at different inventory, temperature and velocity.

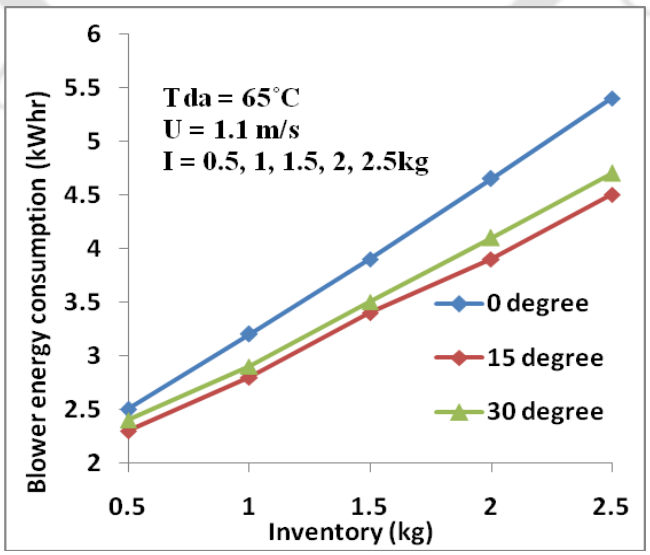

Fig. 6.1(a) Blower energy consumption using STD plate at different inventory

TH-1488_126103037

In the Fig. 6.1 (a) blower energy consumption per kg paddy for θ = 0˚ at drying air temperature of 65˚C and air velocity of 1.1m/s are 5, 3.2, 2.6, 2.35 and 2.16 kWhr/kg, respectively for inventory of 0.5 kg to 2.5 kg, whereas the corresponding values are 4.6, 2.8, 2.27, 1.95 and 1.8 kWhr/kg for θ = 15˚ and 4.8, 2.9, 2.3, 2.05 and 1.88 kWhr/kg for θ = 30˚, respectively. It is observed that the corresponding blower energy consumption per kg paddy decreases by 56.8%, 60.9% and 60.8% for θ = 0˚, 15˚ and 30˚, respectively when inventory is increased from 0.5 to 2.5kg.

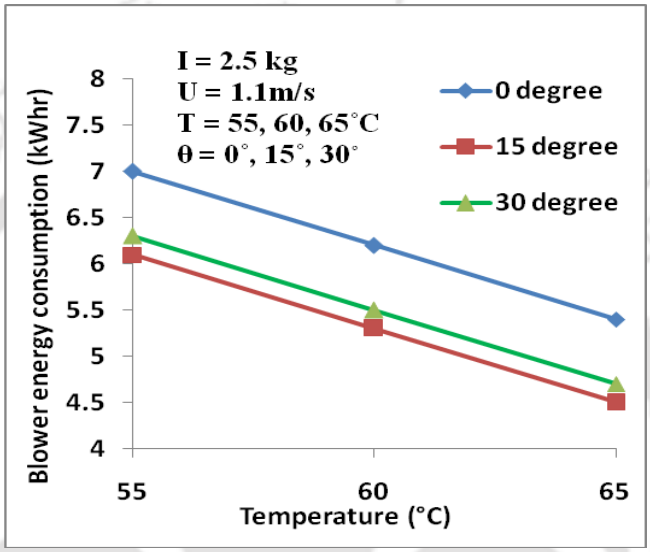

Fig. 6.1(b) Blower energy consumption using STD plate at different temperature

In the Fig 6.1 (b) blower energy consumption for θ = 0˚ dryer at air velocity of 1.1m/sand an inventory of 2.5 kg are 7, 6.2 and 5.4 kWhr for drying air temperatures of 55˚C, 60˚C and 65˚C, respectively whereas the corresponding values are 6.1, 5.3 and 45 kWhr for θ = 15˚ and 6.3, 5.5 and 4.7 kWhr for θ = 30˚. It is observed that blower energy consumption per kg paddy decreases by 22.9%, 26.2% and 25.4% for θ = 0˚, 15˚ and 30˚, respectively when drying air temperature is increased from 55˚C to 65˚C.

Fig. 6.2 presents the blower energy consumption using STD plate at different air velocity.

TH-1488_126103037

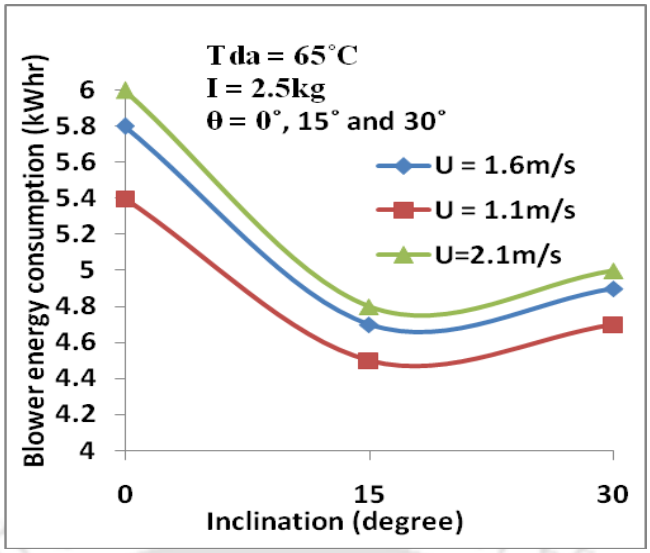

Fig. 6.1(c) Blower energy consumption using STD plate at different velocity

In the Fig. 6.1(c) blower energy consumptions at drying air temperature of 65˚Cand an inventory of 2.5 kg are 5.4, 4.5 and 4.7 kWhr for θ = 0˚, 15˚ and 30˚, respectively for air velocity of 1.1 m/s, whereas the corresponding values for air velocity of 2.1 m/s are 6, 4.8 and 5 kWhr. It is observed that blower energy consumption per kg paddy increases by 10%, 6.2% and 6% for θ = 0˚, 15˚ and 30˚, respectively when air velocity is increased from 1.1m/s to 2.1m/s. Figs. 6.2(a)-(b) present thermal energy consumption using STD plate at different inventory and different temperature.

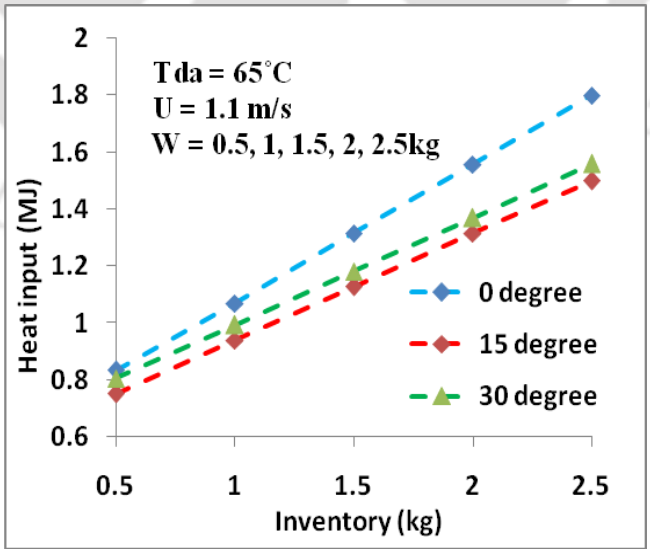

Fig. 6.2(a) Thermal energy consumption using standard distributor plate at different inventory

TH-1488_126103037

In the Fig. 6.2 (a) thermal energy consumption per kg paddy for θ = 0˚ at drying air temperature of 65˚C and air velocity of 1.1m/s are 1.66, 1.07, 0.87, 0.78 and 0.72MJ/kg, respectively for bed inventories of 2.5 kg to 0.5 kg, whereas the corresponding values are 1.5, 0.94, 0.75, 0.628 and 0.6 MJ/kg for θ = 15˚ and 1.61, 0.99, 0.79, 0.68 and 0.62 MJ/kg for θ = 30˚, respectively. It is observed that thermal energy consumption per kg paddy decreases by 56.8%, 60.1% and 61.3% for θ = 0˚, 15˚ and 30˚, respectively when inventory is increased from 0.5 to 2.5kg.

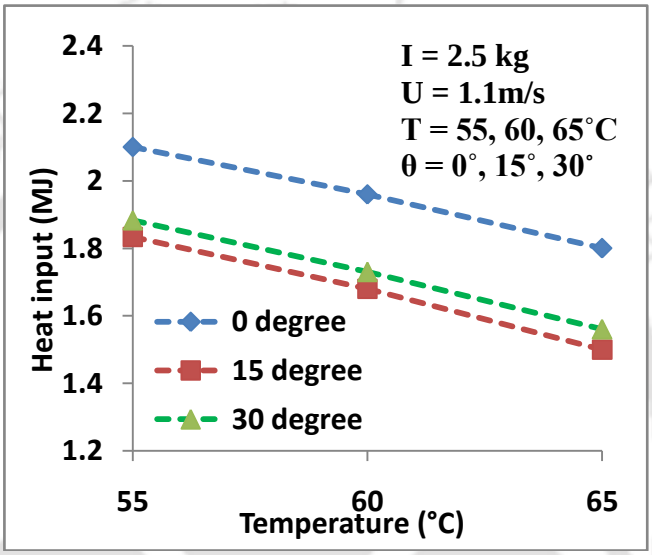

Fig. 6.2(b) Thermal energy consumption using standard distributor plate at different temperature

In the Fig 6.2(b) thermal energy consumption for θ = 0˚ dryer at air velocity of 1.1m/sand an inventory of 2.5 kg are 2.1, 1.96 and 1.8 MJ for air temperatures of 55˚C, 60˚C and 65˚C, respectively whereas the corresponding values are 1.83, 1.68 and 1.5 MJ for θ = 15˚ and 1.88, 1.73 and 1.56 MJ for θ = 30˚. It is observed that thermal energy consumption per kg paddy decreases by 14.3%, 18% and 17%, respectively for θ = 0˚, 15˚ and 30˚ when drying air temperature is increased from 55 to 65˚C.

Fig. 6.2(c) presents the thermal energy consumption using STD plate at different air velocity. In the Fig. 6.4 thermal energy consumptions at drying air temperature of 65˚Cand an inventory of 2.5 kg are 1.74, 1.45 and 1.51 MJ for θ = 0˚, 15˚ and 30˚, respectively for air velocity of 1.1 m/s, whereas the corresponding values are 1.71,

TH-1488_126103037

1.38 and 1.44 MJ for air velocity of 2.1 m/s. It is observed that thermal energy consumption per kg paddy decreases by 2%, 4.8% and 4.6% for θ = 0˚, 15˚ and 30˚, respectively when air velocity is increased from 1.1 to 2.1m/s.

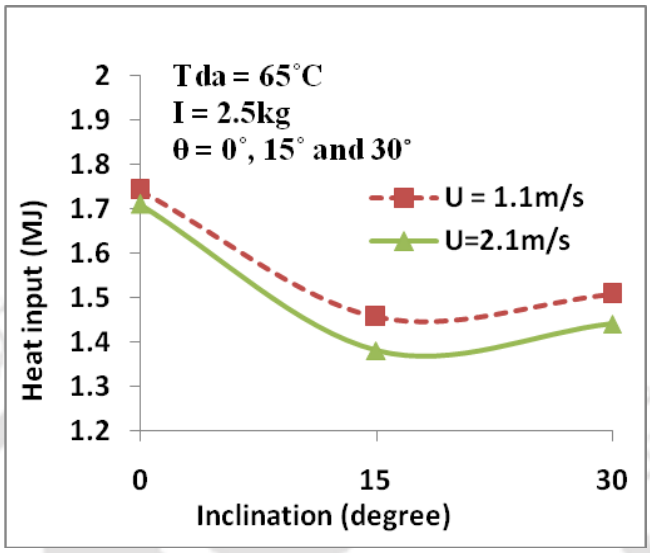

Fig. 6.2(c) Thermal energy consumption using STD plate at different velocity

6.3 COMPARISON OF ENERGY CONSUMPTIONS USING TWO DIFFERENT DISTRIBUTOR PLATES

Blower energy consumption using STD plate and MD plate at different inventory, temperature and velocity are shown in Figs. 6.3(a)-(b).

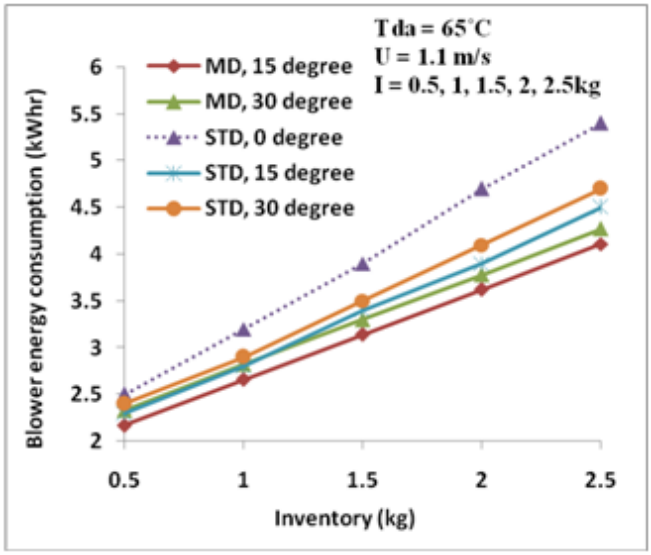

Fig. 6.3(a) Blower energy consumption using STD plate and MD plate at different inventory

TH-1488_126103037

In the Fig 6.3 (a) blower energy consumption per kg paddy using STD plate at drying air temperature of 65˚C and air velocity of 1.1m/s are 5, 3.2, 2.6, 2.35 and 2.16 kWhr/kg for θ = 0˚, 4.6, 2.8, 2.27, 1.95 and 1.8 kWhr/kg for θ = 15˚ and 4.8, 2.9, 2.3, 2.05 and 1.88 kWhr/kg for θ = 30˚, respectively for inventory of 0.5 kg to 2.5kg. The corresponding drying time using MD plate are 4.34, 2.66, 2.1, 1.81 and 1.64 kWhr/kg for θ = 15˚and 4.66, 2.82, 2.2, 1.89 and 1.71 kWhr/kg for θ = 30˚, respectively for the inventory of 0.5 to 2.5 kg. It is observed that blower energy consumption per kg paddy decreases by 5.7% for 0.5 kg and 8.9% for 2.5kg for θ = 15˚ and3% for 0.5 kg and9% for 2.5 kg for θ = 30˚, respectively when MD plate is used.

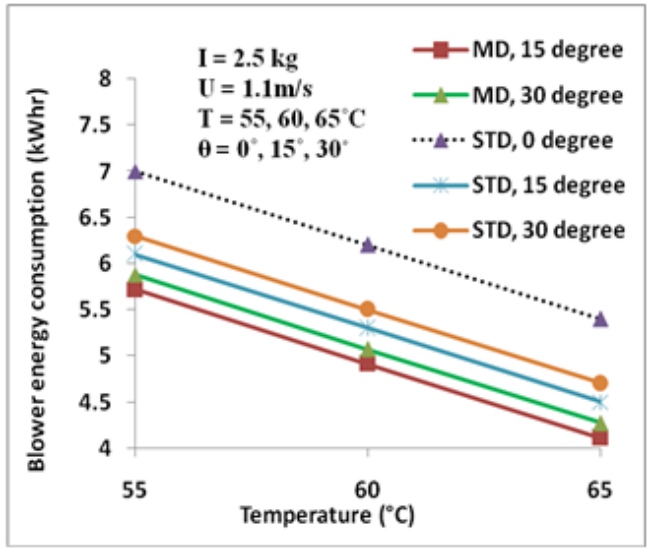

Fig. 6.3(b) Blower energy consumption using STD plate and MD plate at different temperature

In the Fig 6.3 (b) blower energy consumptions using STD plate at air velocity of 1.1m/sand an inventory of 2.5 kg, are 7, 6.2 and 5.4 kWhr for θ = 0˚, 6.1, 5.3 and 45 kWhr for θ = 15˚ and 6.3, 5.5 and 4.7 kWhr for θ = 30˚, respectively for drying air temperature of 55˚C, 60˚C and 65˚C,whereas the corresponding values using MD plate are5.72, 4.91 and 4.11 kWhr for θ = 15˚ and 5.88, 5.07 and 4.27 kWhr for θ = 30˚. It is observed that blower energy consumption per kg paddy decreases by 6.2% and 8.7% for θ = 15˚ and 6.7%and 9.1% for θ =30˚, respectively for 55˚C and 65˚C when MD plate is used.

TH-1488_126103037

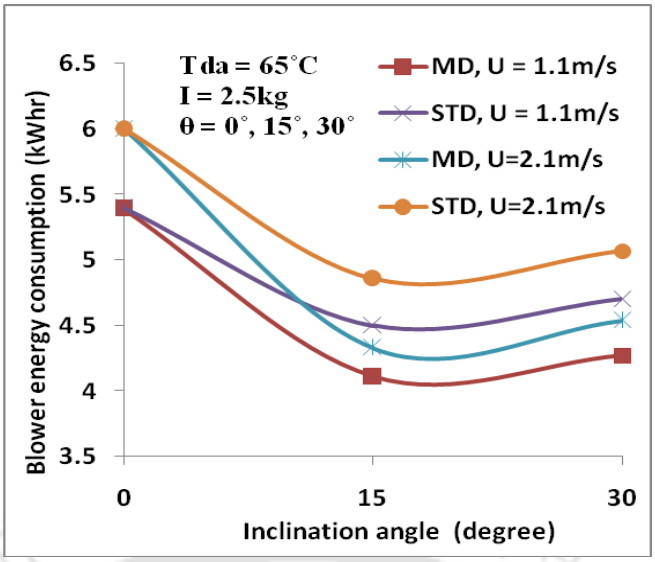

Fig. 6.3(c) Blower energy consumption using STD and MD plates at different velocity

In the Fig. 6.3(c) blower energy consumptions using STD plate at drying air temperature of 65˚Cand an inventory of 2.5 kg are 5.4, 4.5 and 4.7 kWhr for θ = 0˚, 15˚ and 30˚, respectively for air velocity of 1.1 m/s and 6, 4.8 and 5.1 kWhr for air velocity of 2.1 m/s. The corresponding blower energy consumptions using MD plate are 4.11 and 4.27 kWhr for θ =15˚ and 30˚, respectively for air velocity of 1.1 m/s and 4.32 and 4.54 kWhr for air velocity of 2.1 m/s. It is observed that blower energy consumption per kg paddy decreases by 8.7% and 9.2% for 1.1m/s and 11% and 10.4% for 2.1 m/s for θ = 15˚ and 30˚, respectively when MD plate is used.

Figs. 6.4(a)-(c) present the thermal energy consumption using standard distributor plate and modified distributor plate at different inventory, temperature and velocity. In the Fig 6.4(a) thermal energy consumption per kg paddy using STD plate at the drying air temperature of 65˚C and air velocity of 1.1m/s are 1.66, 1.07, 0.87, 0.78 and 0.72MJ/kg for θ = 0˚, 1.5, 0.94, 0.75, 0.628 and 0.6 MJ/kg for θ = 15˚ and 1.61, 0.99, 0.79, 0.68 and 0.62 MJ/kg for θ = 30˚, respectively for the inventory of 0.5 kg to 2.5kg. The corresponding values using MD plate are 1.45, 0.88, 0.69, 0.60 and 0.54 MJ/kg for θ = 15˚ and 1.56, 0.94, 0.73, 0.63 and 0.57 MJ/kg for θ = 30˚ for 0.5 kg to 2.5 kg, respectively. It is observed that thermal energy consumption per kg paddy decreases by 3.6% for 0.5kg and 8.3% for 2.5 kg for θ = 15˚ and 3.1% for 0.5 kg and 8.7% for 2.5kg for θ =30˚, respectively when MD plate is used.

TH-1488_126103037

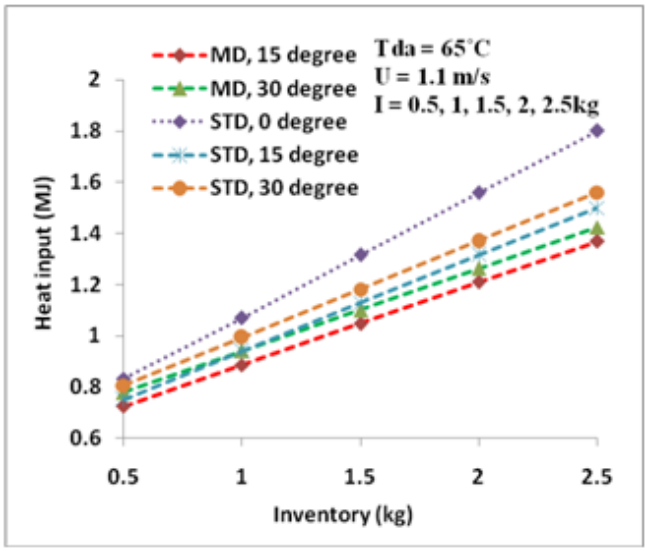

Fig. 6.4(a) Thermal energy consumption using STD plate and MD plates at different inventory

.

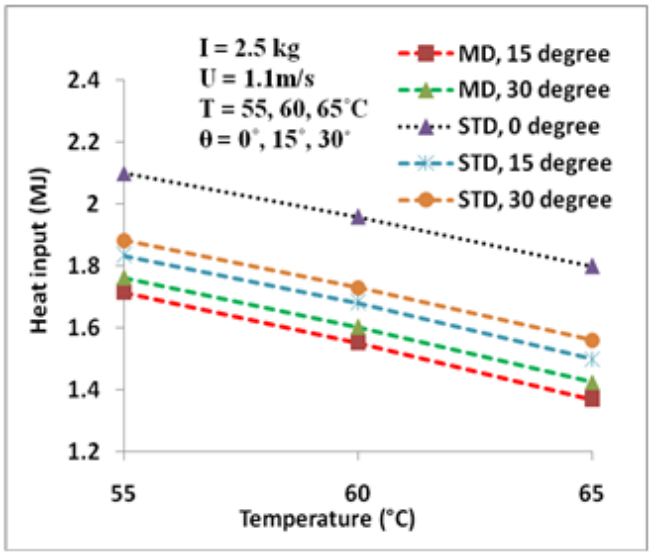

Fig. 6.4(b) Thermal energy consumption using STD plate and MD plates at different temperature

In the Fig 6.4 (b)at air velocity of 1.1m/sand an inventory of 2.5 kg, thermal energy consumption values using STD plate are 2.1, 1.96 and 1.8 MJ for θ = 0˚, 1.83, 1.68 and 1.5 MJ for θ = 15˚, 1.88, 1.73 and 1.56 MJ for θ = 30˚, respectively for air temperatures of 55˚C, 60˚C and 65˚C. The corresponding values using MD plate are 1.71, 1.55 and 1.37 MJ for air temperatures of 55˚C, 60˚C and 65˚C, respectively for θ = 15˚ and 1.76, 1.6 and 1.42 MJ for θ = 30˚. It is observed that thermal energy

TH-1488_126103037

consumption per kg paddy decreases by 6.5% for 55˚C and 8.7% for 65˚C for θ = 15˚ and 6.4% for 55˚C and 8.7% for 65˚C for θ = 30˚ when MD plate is used.

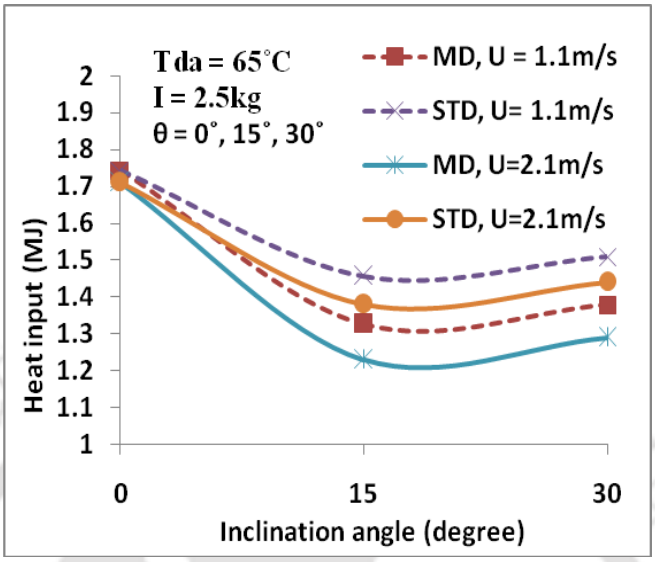

Fig. 6.4(c) Thermal energy consumption using STD and MD plates at different velocity

In the Fig. 6.4(c),thermal energy consumptions using STD plate at drying air temperature of 65˚Cand an inventory of 2.5 kg are 1.74, 1.45 and 1.51 MJ for θ = 0˚, 15˚ and 30˚, respectively for air velocity of 1.1 m/s and 1.71, 1.38 and 1.44 MJ for air velocity of 2.1 m/s. The corresponding values using MD plate are 1.45 and 1.51 MJ for θ = 15˚ and 30˚, respectively for air velocity of 1.1 m/s and 1.38 and 1.44 MJ for 2.1 m/s. It is observed that thermal energy consumption per kg paddy decreases by 9% and 9.2% for 1.1m/s and 11% and 10.4% for 2.1 m/s, respectively for θ = 15˚ and 30˚when MD plate is used.

6.4 COMPARISON OF ENERGY CONSUMPTIONS WITH AND WITHOUT THE USE OF SPIRALS

Blower energy consumption with and without the use of spiral insert at different inventory and different temperature are shown in Figs. 6.5(a)-(c). In the Fig. 6.5 (a) blower energy consumption per kg paddy without the use of spirals at drying air temperature of 65˚C and air velocity of 1.1m/s are 5, 3.2, 2.6, 2.35 and 2.16 kWhr/kg for θ = 0˚, 4.6, 2.8, 2.27, 1.95 and 1.8 kWhr/kg for θ = 15˚ and 4.8, 2.9, 2.3, 2.05 and 1.88 kWhr/kg for θ = 30˚, respectively for the inventory of 0.5 kg to 2.5 kg. The

TH-1488_126103037

corresponding values with the use of spirals are 3.06, 2.1, 1.77, 1.61 and 1.51 kWhr/kg for θ = 0˚, 2.42, 1.53, 1.23, 1.08 and 0.99 kWhr/kg for θ = 15˚ and 2.74, 1.69, 1.34, 1.16 and 1.06 kWhr/kg for θ = 30˚, respectively for bed inventories of 0.5 kg to 2.5 kg. It is observed that blower energy consumption per kg paddy decreases by 38.8%, 47.4% and 42.9% for 0.5kg and 30.1%, 44.7% and 43.6% for 2.5kg for θ = 0˚, 15˚ and 30˚, respectively when spiral inserts are used.

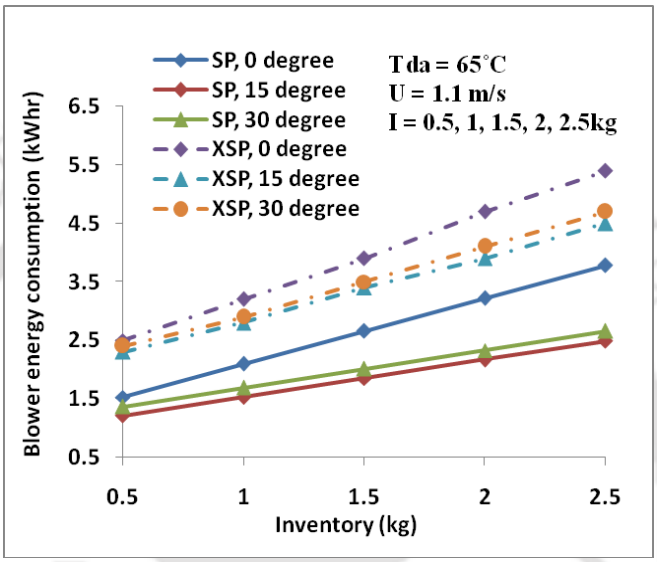

Fig. 6.5(a) Blower energy consumption with and without the use of spirals at different inventory

.

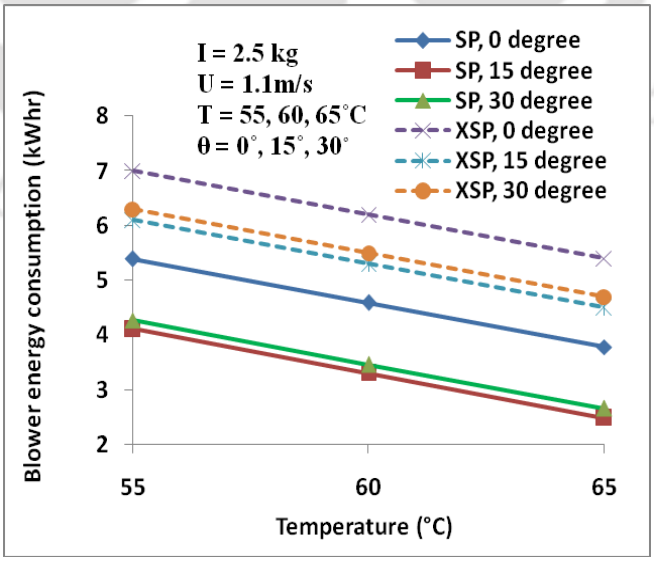

Fig. 6.5(b) Blower energy consumption with and without the use of spirals at different temperature

TH-1488_126103037

In the Fig 6.5 (b) blower energy consumptions without the use of spirals at air velocity of 1.1m/sand an inventory of 2.5 kg are 7, 6.2 and 5.4 kWhr for θ = 0˚, 1, 5.3 and 4.5 kWhr for θ = 15˚ and 6.3, 5.5 and 4.7 kWhr for θ = 30˚, respectively for drying air temperatures of 55˚C, 60˚C and 65˚C. The corresponding values with the use of spirals are 5.39, 4.59 and 3.78kWhr for θ = 0˚, 4.11, 3.3 and 2.49 kWhr for θ = 15˚ and 4.27, 3.46 and 2.66 kWhr for θ = 30˚, respectively for drying air temperatures of 55˚C, 60˚C and 65˚C. It is observed that blower energy consumption per kg paddy decreases by 23%, 32.6% and 32.2% for 55˚C, 25.9%, 37.7% and 37.1% for 60˚C and 30%, 44.7% and 43.4% for 65˚C for θ = 0˚, 15˚ and 30˚, respectively when spiral inserts are used.

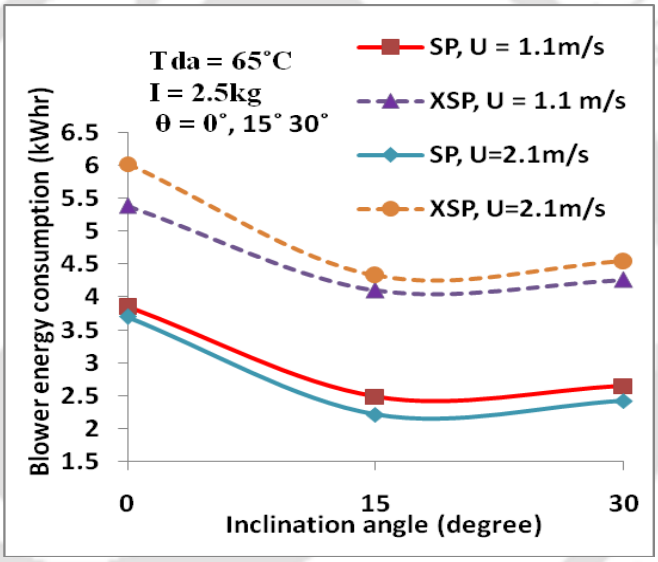

Fig. 6.5(c)Blower energy consumption with and without the use of spiral at different velocity

In the Fig 6.5(c)blower energy consumptions without the use of spirals at drying air temperature of 60˚Cand an inventory of 2.5 kg are 5.39, 4.1 and 4.26 kWhr for air velocity of 1.1 m/s and 6.02, 4.32 and 4.54 kWhr for air velocity of 2.1 m/s, respectively for θ = 0˚, 15˚ and 30˚. The corresponding values with the use of spirals are 3.85, 2.49 and 2.65 kWhr for air velocity of 1.1 m/s and 3.7, 2.21 and 2.42 kWhr for air velocity of 2.1 m/s, respectively for θ = 0˚, 15˚ and 30˚. It is observed that blower energy consumption per kg paddy decreases by 28.5%, 39.2% and 37.8% for

TH-1488_126103037

1.1m/s and 38.3%, 48.8% and 46.7% for 2.1 m/s for θ = 0˚, 15˚ and 30˚, respectively when spiral inserts are used.

Figs. 6.6(a)-(c) present the thermal energy consumption using spiral inserts at different inventory and different temperature. In the Fig 6.6(a) thermal energy consumption per kg paddy without the use of spirals at drying air temperature of 65˚C and air velocity of 1.1m/s are 1.66, 1.07, 0.87, 0.78 and 0.72MJ/kg for θ = 0˚, 1.5, 0.94, 0.75, 0.628 and 0.6 MJ/kg for θ = 15˚ and 1.61, 0.99, 0.79, 0.68 and 0.62 MJ/kg for θ = 30˚, respectively for bed inventories of 2.5 kg to 0.5 kg. The corresponding values with the use of spirals are1.02, 0.69, 0.59, 0.54 and 0.5MJ/kg for θ = 0˚, 0.81, 0.51, 0.41, 0.36 and 0.33 MJ/kg for θ = 15˚ and 0.91, 0.56, 0.45, 0.39 and 0.35 MJ/kg for θ = 30˚, respectively for bed inventories of 0.5 kg to 2.5 kg. It is observed that thermal energy consumption per kg paddy decreases by 38.6%, 46.3% and 43.5% for inventory of 0.5 kg and 30.6%, 45% and 43.5% for inventory of 2.5 kg for θ = 0˚, 15˚ and 30˚, respectively when spiral inserts are used.

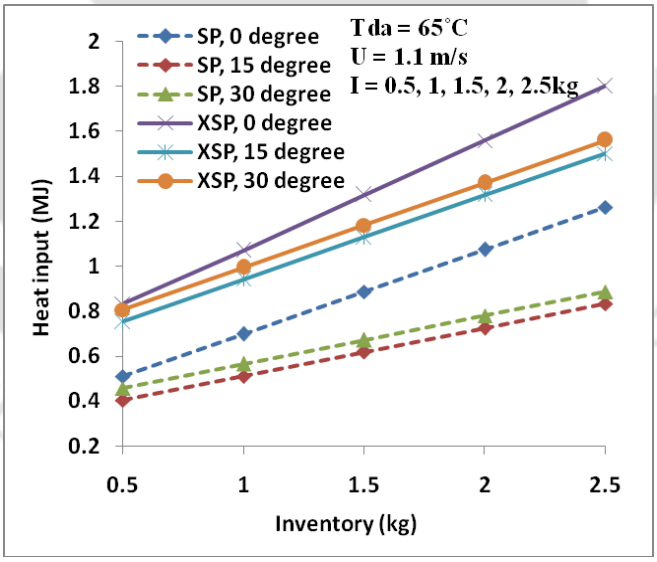

Fig. 6.6(a) Thermal energy consumption with and without the use of spiral at different inventory

In the Fig. 6.6(b) thermal energy consumption values without the use of spirals at air velocity of 1.1m/sand an inventory of 2.5 kg, are 2.1, 1.96 and 1.8 MJ for θ = 0˚, 1.83, 1.68 and 1.5 MJ for θ = 15˚ and 1.88, 1.73 and 1.56 MJ for θ = 30˚, respectively for air temperatures of 55˚C, 60˚C and 65˚C. The corresponding values using spiral

TH-1488_126103037

inserts are 1.62, 1.45 and 1.26 MJ for θ = 0˚, 1.23, 1.04 and 0.83 MJ for θ = 15˚ and 1.28, 1.09 and 0.89 MJ for θ = 30˚, respectively for air temperatures of 55˚C, 60˚C and 65˚C.It is observed that thermal energy consumption per kg paddy decreases by 23.3%, 32.9% and 32.1% for 55˚C, 26%, 37.9% and 36.8% for 60˚C and 29.9%, 44.5% and 43.2% for 65˚C respectively for θ = 0˚, 15˚ and 30˚ when spiral inserts are used.

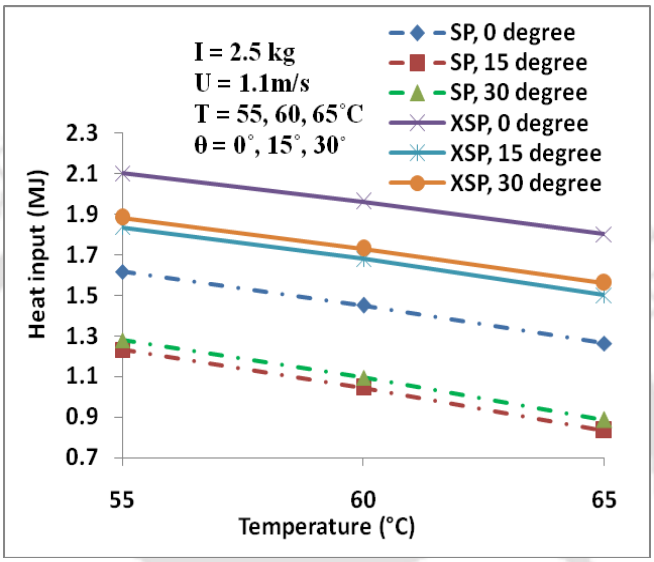

Fig. 6.6(b) Thermal energy consumption with and without the use of spiral at different temperature

.

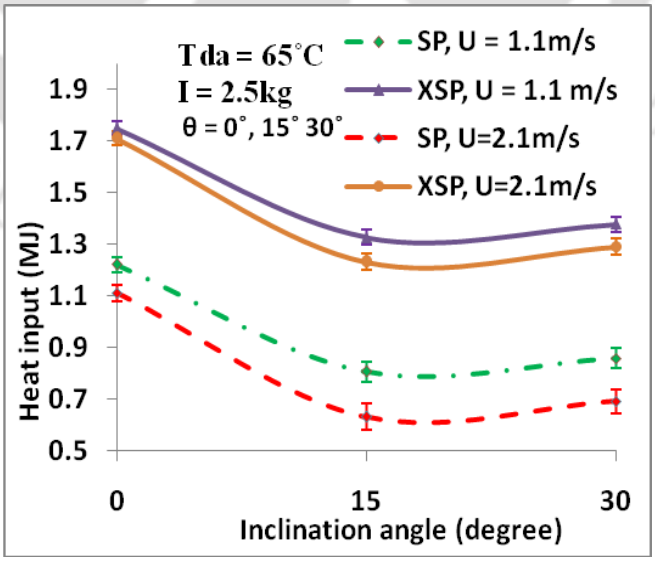

Fig. 6.6(c) Thermal energy consumption with and without the use of spiral at different velocity

TH-1488_126103037

In the Fig. 6.6(c) thermal energy consumptions without the use of spirals at drying air temperature of 65˚Cand an inventory of 2.5 kg are 1.75, 1.32 and 1.37 MJ for air velocity of 1.1 m/s and 1.71, 1.23 and 1.29 MJ for air velocity of 2.1 m/s, respectively for θ = 0˚, 15˚ and 30˚. The corresponding values with the use of spirals are 1.22, 0.806 and 0.858 MJ for air velocity of 1.1 m/s and 1.11, 0.63 and 0.69 MJ for air velocity of 2.1 m/s, respectively for θ = 0˚, 15˚ and 30˚. It is observed that thermal energy consumption per kg paddy decreases by 30.3%, 39% and 37.7% for 1.1m/s and 35.1%, 48.8% and 46.5% for 2.1 m/s for θ = 0˚, 15˚ and 30˚, respectively when spiral inserts are used.

As shown in Fig. 6.6(c), uncertainty in measurement of thermal energy consumption for the inventory of 2.5 kg, air temperature of 65˚C air velocity of 1.1m/s for without the use of spirals are calculated to be ±2.6%, ±2.9%, and ±2.9% and with the use of spirals are ±3%, ±3.9% and ±3.7%, respectively for θ = 0˚, 15˚ and 30˚. Uncertainty in measurement of thermal energy consumption for the inventory of 2.5 kg, air temperature of 65˚C air velocity of 2.1m/s for without the use of spirals are calculated to be ±2.7%, ±3.2% and ±3.1% and with the use of spirals are ±3.4%, ±5.2% and ±4.8%, respectively for θ = 0˚, 15˚ and 30˚. Sample calculation in measurements of uncertainty is presented in Appendix.

6.5 OPTIMUM CONDITION

The input parameters of an inventory of 2.5 kg, air temperature of 65˚C, an inclination angle of 15˚, superficial air velocity of 2.1 m/s using modified distributor plate and the use of spiral inserts gives the least drying time and energy consumptions/kg paddy for the paddy drying under the conditions investigated. The least blower energy consumption/kg paddy is 0.884 kWhr/kg (see Fig 6.5c), the least thermal energy consumption/kg paddy is 0.252 MJ/kg (0.07 kWhr/kg) (see Fig 6.6c). The overall drying energy consumption is 0.954 kWhr/kg of paddy. Under this condition the minimum drying rate is 8.4 min/kg (see table 5.10).

TH-1488_126103037

6.6 EFFECT OF SCALE UP

Comparison of blower as well as thermal energy consumptions of small set up and large set up using STD plate at the drying air temperature of 65˚C, air velocity of 1.1 m/s, an inventory of 2.5 kg and inclination of 0˚, 15˚ and 30˚ and are shown in Figs. 6.7 and 6.8. i.e., dryer cross sectional area of large set up, $A_{c\ large}$ = 15 cm × 15 cm

dryer cross sectional area of small set up $A_{c\ small}$= 10 cm × 10 cm

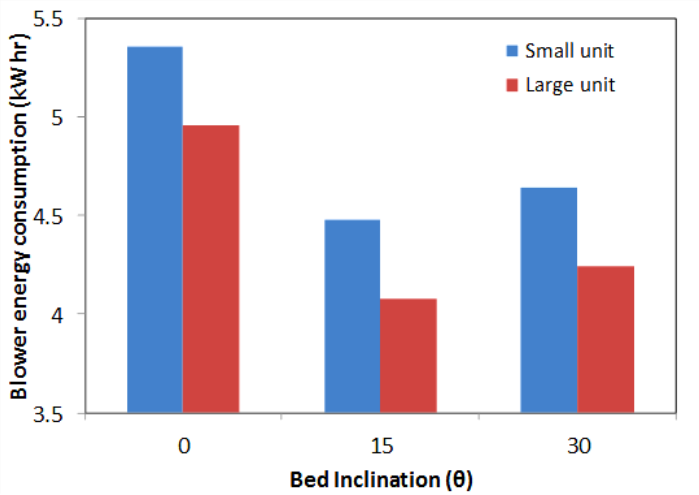

Fig. 6.7 Blower energy consumption of small setup and large setup at air temperature of 65 °C, air velocity of1.1 m/s and an inventory of 2.5 kg.

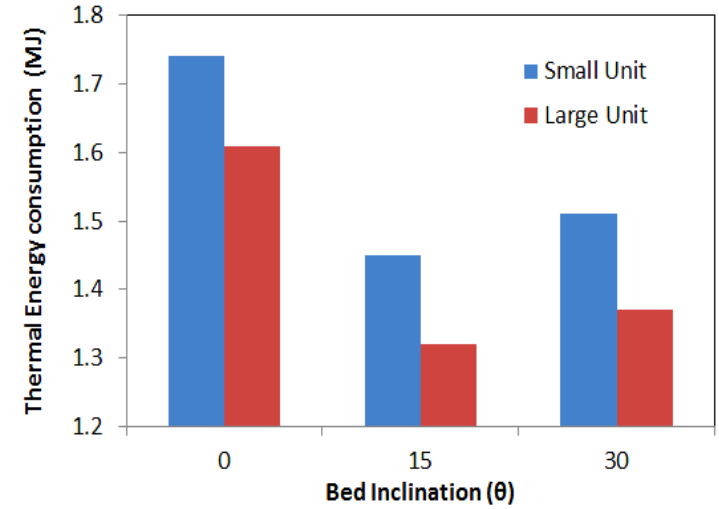

Fig. 6.8 Thermal energy consumption of small setup and large setup at air temperature of 65 °C, air velocity of1.1 m/s and an inventory of 2.5 kg

From the Figs. 6.7 and 6.8, it is observed that blower as well as thermal energy consumption per kg paddy decreases by 10 % by the effect of scale up.

TH-1488_126103037

6.7 SUMMARY

Blower as well as thermal energy consumptions of fluidized bed dryer using standard as well as modified distributor plates, with and without the use of spiral inserts at vertical and inclined positions of dryer, various inventories, different temperature and different air velocities, optimum condition and scale up effect are presented and discussed. Conclusion of the experimental results will be described in chapter 7.

भारतीय प्रौद्योगिकी संस्थान गुवाहाटी • Indian Institute of Technology Guwahati •

TH-1488_126103037

CHAPTER 7

CONCLUSIONS AND FUTURE SCOPE OF INVESTIGATION

7.1 CONCLUSIONS

In the present work a bubbling fluidized bed paddy dryer system with provision for varying the inclination was designed and developed. Experiments were carried out to investigate the hydrodynamic behaviour, drying characteristics and energy consumptions under various conditions of drying viz., bed inclination, bed inventories, air temperatures, air velocities. Attempts were made to improve the performance of the dryer with the modification of distributor plate and provision of spirals inserts in the dryer column. In addition, scale up effect is also studied. Following are the major conclusions drawn from the study:

7.1.1 Hydrodynamic behaviour

- The minimum fluidization velocity for the vertical bed ($\theta = 0^{\circ}$) was observed to be 0.5 m/s. However, bed could be maintained in the bubbling fluidization mode in the range of 0.9 m/s to 2.6 m/s for $\theta = 0^{\circ}$. Same configuration was showing pneumatic conveying mode for the superficial velocity of air above 3 m/s.
- With increase in inclination with respect to the vertical bed, fast fluidization and pneumatic conveying mode was achieved at a lower superficial velocity (as low as 2.5 m/s). Hence experiments were conducted in the superficial air velocity range of 1.1 – 2.1 m/s for $\theta = 15^{\circ}$ and 30°.
- It was observed that the pressure drop on the two opposite sides of the riser column remain same for the vertical bed irrespective of the superficial velocity, air temperature and bed inventory.
- Pressure drop on the two opposite sides of the riser column was observed to be varying when the bed is inclined at an angle from the vertical. This variation in pressure attributes to a swirling motion of gas-solid mixture in a plane perpendicular to the bed axis assisting better gas-solid mixing. This swirling motion enhances heat and moisture transfer from the solid to be dried.
- It was observed that with increase in the angle of inclination (from the vertical) the swirling motion increases improving drying rate. However, inclination

TH-1488_126103037

beyond 30˚ reduces fluidization behaviour. It was observed that fluidization phenomenon fails at the bed inclination of 45˚.

- Variation in pressure drops on both the upper and lower sides of the drying bed are almost similar for bed inclination of 15° and 30˚. However, the fluidization stops for the bed inclination of 45°.
- Pressure drop fluctuations along the riser height are so high when standard distributor plate is used. These fluctuations slightly decrease when modified distributor plate is used. Pressure drop fluctuations along the riser column of the dryer could be reduced significantly by the use of spirals.

7.1.2 Moisture removal rate and drying time

- Moisture removal rate is high at the beginning of the drying process for removing surface moisture and it is low at the later process of drying for removing internal moisture of grains. The input parameters of the drying process are inventory of 0.5 kg to 2.5 kg, air temperature of 55, 60 and 65˚C, air velocity of 1.1, 1.6, 2.1 and 2.6 m/s and inclination of 0˚, 15˚, 30˚ and 45˚.
- The maximum reduction of drying time per kg paddy is 11% at the drying air temperature of 65˚C, air velocity of 2.1 m/s, an inventory of 2.5 kg and an inclination of 15˚when modified distributor plate is used.
- The maximum reduction of drying time per kg paddy is 48.8% at the drying air temperature of 65˚C, air velocity of 2.1 m/s, an inventory of 2.5 kg and an inclination of 15˚ when spiral inserts are used.
- Uncertainty in moisture measurement is found to be ±2%, ±1%, ±0.7%, ±5% and ±0.4%, respectively for the inventories of 0.5, 1, 1.5, 2 and 2.5 kg.
- Best performance with a combination of minimum drying time and faster moisture removal rate was obtained with a bed inclination of 15˚, an inventory of 2.5 kg, air velocity of 2.1 ms^{-1}, air temperature of 65˚C using modified distributor plate with the use of spirals inserts.
- The maximum reduction of drying time per kg paddy is 67.7% when the inventory is increased from 0.5 kg to 2.5kg, 48.8% when the temperature is increased from 55˚C to 65˚C, 43.2% when the inclination is increased from 0˚ to 15˚ and 32.3% when the velocity is increased from 1.1 m/s to 2.1 m/s.

TH-1488_126103037

- In addition, the maximum reduction of drying time per kg paddy by the effect of scale up using STD plate is 11% at drying air temperature of 65˚C, air velocity of 2.1 m/s, an inclination angle of 15˚ and an inventory of 2.5 kg.

7.1.3 Energy consumptions

- The maximum reduction of energy consumptions per kg paddy is 12.2% at air temperature of 65˚C, air velocity of 2.1 m/s, an inventory of 2.5 kg and an inclination of 15˚ when modified distributor plate is used.
- The maximum reduction of energy consumptions per kg paddy is 48.8% at air temperature of 65˚C, air velocity of 2.1 m/s, an inventory of 2.5 kg and an inclination of 15˚ when spiral inserts are used.
- Best performance with a combination of minimum blower as well as thermal energy consumptions was obtained with a bed inclination of 15˚, an inventory of 2.5 kg, air velocity of 2.1 ms^{-1}, air temperature of 65˚C using modified distributor plate with the use of spirals inserts.
- Energy consumptions per kg paddy decrease by 67.7% when the inventory is increased from 0.5 kg to 2.5kg, 48.8% when the temperature is increased from 55˚C to 65˚C, 43.2% when the inclination is increased from 0˚ to 15˚ and 32.3% when the velocity is increased from 1.1 m/s to 2.1 m/s.
- In addition, energy consumptions per kg paddy using STD plate decrease by 10% by the effect of scale up at drying air temperature of 65˚C, air velocity of 1.1 m/s, an inclination angle of 15˚ and an inventory of 2.5 kg.
- Uncertainty in thermal energy consumption for the inventory of 2.5 kg, air temperature of 65˚C air velocity of 1.1m/s for without the use of spirals is found to be ±2.6%, ±2.9%, and ±2.9% and with the use of spirals is ±3%, ±3.9% and ±3.7%, respectively for θ = 0˚, 15˚ and 30˚. Uncertainty in thermal energy consumption for the same condition of air velocity of 2.1m/s for without the use of spirals is found to be ±2.7%, ±3.2% and ±3.1% and with the use of spirals are ±3.4%, ±5.2% and ±4.8%, respectively for θ = 0˚, 15˚ and 30˚.

TH-1488_126103037

7.2 SCOPE FOR FUTURE WORK

The present experimental set-up was developed to investigate performance of a bubbling fluidized bed dryer in terms of effect of inclination of bed, inventory, superficial air velocity and heat input on drying of paddy grains. Improvement of the performance with spiral inserts and a new distributor plate were also investigated. Results obtained are satisfactory. However, following may be investigated in future:

1. Scale-up effect on drying rate is required to be studied for commercialization of the dryer.
2. Drying kinetics and modeling of the same may be studied for improving the dryer.
3. Effect of different types of spirals and incorporation of other types of distributor plates may be attempted to reduce the overall energy consumption rate.

TH-1488_126103037

REFERENCES

Aghbashlo, M., Mobli, H., Rafiee, S., Madadlou, A., 2012. The use of artificial neural network to predict exergetic performance of spray drying process: A preliminary study, Computers and Electronics in Agriculture, 88, pp: 32–43

Ajadi, D. A., and Sanusi, Y. K., (2013). Effect of Relative Humidity on Oven Temperature of Locally Design Solar Carbinet Dryer, Global Journal of Science Frontier Research Physics and Space Science, 13(1).

Akbulut, A., and Durmus, A., 2010, Energy and exergy analyses of thin layer drying of mulberry in a forced solar dryer, Energy, 35 (4), pp: 1754–1763

Akpinar, E. K., 2005. Evaluation of convective heat transfer coefficient of various crops in cyclone type dryer, Energy Conversion and Management, 46, pp: 2439-2454

Aktaş, M., Şevik, S., Doğan, H., Koçak, S., 2013. Mushroom drying with solar assisted heat pump *system*, Energy Conversion and Management, 72, pp: 171–178

Ali, M., and Saeid, M., 2012. Effects of microwave pre-treatment on the energy and exergy utilization in thin-layer drying of sour pomegranate arils, Chemical Industry and Chemical Engineering Quarterly, 18 (1) pp: 63-72

Alkilani, M. M., Sopian, K., Alghoul, M.A., Sohif, M., 2011. Review of solar air collectors with thermal storage units, Renewable and Sustainable Energy Reviews, 15 (3), pp: 1476–1490

Allaf, K., Macías, M. A., Martínez, A. C., Mounir, S., Gaitán, G. M.,2013. Comparative Study of the Effects of Drying Methods on Antioxidant Activity of Dried Strawberry (Fragariavarcamarosa), Procedia Engineering, 42, pp: 267 – 282

Allaf, K., Pérez, C. T., Sabah, M. M., Gaitán, J. G. M., Sobolik, V., Martínez, C. A., 2012. Impact of Instant Controlled Pressure Drop Treatment on Dehydration and Rehydration Kinetics of Green Moroccan Pepper (Capsicum annuum), Procedia Engineering, 42, pp: 978 – 1003

Assari, M. R., Tabrizi H. B., and Najafpour, E., 2013. Energy and exergy analysis of fluidized bed dryer based on two-fluid modeling, International Journal of Thermal Sciences, 64, pp: 213 – 219

Atthajariyakul, S., and Leephakpreeda, T., 2006. Fluidized bed paddy drying in optimal conditions via adaptive fuzzy logic control, Journal of Food Engineering, 75(1), pp:104-114

Aworinde, S. M., Holland, D. J., Davidson, J. F., 2015. Investigation of a swirling flow nozzle for a fluidised bed gas distributor, Chemical Engineering Science, 132, pp. 22–31

TH-1488_126103037

Aziz, M., Oda, T., and Kashiwagi, T., 2013. Enhanced high energy efficient steam drying of algae, Applied Energy, 109, pp: 163–170

Babagana, G., Silas, K., and Mustafa, B. G., 2012. Design and construction of forced/natural convection solar vegetable dryer with heat storage, Journal of Engineering and Applied Sciences, 7(10), pp: 1213-1217

Bal, L.M., Satya, S., and Naik, S.N.,2010. Solar dryer with thermal energy storage systems for drying agricultural food products: A review, Renewable and Sustainable Energy Reviews 14 (80), pp: 2298–2314.

Banh, L. V., and Quoc, H. B., 2003. Studying and fabricating simple small dryers applied in small farms, Omonrice, 11, pp: 126-137.

Bennamouna, L., Khamab, R., and Léonard, A., 2015. Convective drying of a single cherry tomato: Modelling and experimental study Food and Bioproducts Processing, 94, pp: 114-123.

Bennamoun, L., 2011. Reviewing the experience of solar drying in Algeria with presentation of the different design aspects of solar dryers, Renewable and Sustainable Energy Reviews, 15(70), pp: 3371– 3379

Bizhaem, H. K., and Tabrizi, H. B., 2013. Experimental study on hydrodynamic characteristics of gas–solid pulsed fluidized bed, Powder Technology, 237, pp. 14–23.

Bizmark, N., 2010. Sequential modelling of fluidized bed paddy dryer, Journal of Food Engineering, 101, pp. 303–308.

Blácido, D.R.T., P.J. Sobral, P.J.A., and Menegalli, F.C., 2013. Effect of drying conditions and plasticizer type on some physical and mechanical properties of amaranth flour films, LWT - Food Science and Technology 50 (2013) 392-400, 50 (2), pp: 392 – 400.

Brink, H.G.,Saayman, J., and Nicol, W., 2011. Two dimensional fluidised bed reactor: Performance of a novel multi-vortex distributor, Chemical Engineering Journal, 175, pp. 484– 493

Brooker, D B. Arkema, F.W., and Hall, C.W. 1974. Drying Cereal Grains. AVI Publishing Co., West port, CT. U.S.A.

Bukola O. B. and Ayoola P. O. 2008. Performance Evaluation of a Mixed-Mode Solar Dryer. AU.J.T. 11(4), pp: 225-231.

Celma A.R. and Cuadros F., 2009. Energy and exergy analyses of OMW solar drying process, Renewable Energy 34 (3), pp: 660–666

Celma, A. R., Cuadros, F., and Rodríguez, F. L., 2012. Convective drying characteristics of sludge from treatment plants in tomato processing industries, Food and Bio-products Processing, 90, pp.: 224–234

TH-1488_126103037

Chandrakumar B. P., and Jiwanlal, L. B., 2013. Development and performance evaluation of mixed-mode solar dryer with forced convection, International Journal of Energy and Environmental Engineering, 4, pp: 15-23

Chung L. l., Chien H. C and Figel A. 2010. Intermittent Hot Air, Dehumidified Air, Heat Pump and Convective Cum Vacuum Microwave Drying Characteristics and Models, Asean Journal of Chemical Engineering, 10(2), pp: 10-15.

Chyang, C. S., Lieu, K., and Hong, S.S., 2008. The effect of distributor design on gas dispersion in a bubbling fluidized bed, Journal of the Chinese Institute of Chemical Engineers, 39, pp. 685–692.

Ciesielczyk, W., and Iwanowski, J., 2006. Analysis of Fluidized Bed Drying Kinetics on the Basis of Interphase Mass Transfer Coefficient, Drying Technology, 24 (9), pp: 1153-1157

Davidson, J.F., and Harrison, D., 1963. Fluidized Particles, Cambridge University Press, New York.

Davies, R.M., and Taylor, G.I., 1950. The mechanics of large bubbles rising through extended liquids and through liquids in tubes.

Djomeh, Z. E., Askari, G.R.,., and Mousavi, S. M., 2013. Heat and mass transfer in apple cubes in a microwave-assisted fluidized bed drier, Food and Bioproducts Processing, 91(3), pp: 207–215

Duc, L. A., Han, J. W., and Keum, D. H., 2011, Thin layer drying characteristics of rapeseed (Brassica napus L.), Journal of Stored Products Research, 47(1), pp: 32-38

Elkhadraoui, A., Kooli, S., Hamdi, I., and Farhat, A., 2015. Experimental ivestigation and economic evaluation of a new mixed mode solar greenhouse dryer for drying of red pepper and grape,Renewable Energy, 77, pp:1-8.

Ekechukwu, O.V. and Norton, B., 1999. Review of solar-energy drying systems II: an overview of solar drying technology. Energy Conversion & Management, Vol.40 (6), pp. 615-655.

Friesen O.H., and Huminicki D.N. 1987. Grain Aeration and Unheated Air Drying, The mechanics and physics of modern grain aeration management, CRC Press, ISBN 0-8493-1355-4.

Fudholi, A., Othman, M. Y., Ruslan, M. H., Yahya, M., Zaharim, A., and Sopian, K., 2011. The Effects of Drying Air Temperature and Humidity on the Drying Kinetics of Seaweed, Recent Researches in Geography, Geology, Energy, Environment and Biomedicine, ISBN: 978-1-61804-022-0

TH-1488_126103037

Gálvez, A. V., Miranda, M., López, J., Parada, G., 2010. Impact of air-drying temperature on nutritional properties, total phenolic content and antioxidant capacity of quinoa seeds (Chenopodiumquinoa Willd.), Industrial Crops and Products, 32, pp: 258–263

Geldart, D., 1973. Types of Gas Fluidization, Powder Technology, 7, pp.285─292.

Geng, F., Xu, D., Yuan, Z., Yan, Y., 2009. Numerical simulation on fluidization characteristics of tobacco particles in fluidized bed dryers, Chemical Engineering Journal, 150 (2-3), pp: 581–592

Golmohammadi, M., Assar, M., Hamaneh, M. R., Hashemi, S.J., 2015. Energy efficiency investigation of intermittent paddy rice dryer: modeling and experimental study, Food and bio-products processing, 94, pp. 275–283

Górnicki, K., Kaleta, A., Winiczenko, R., Chojnacka, A., 2013. Evaluation of drying models of apple dried in a fluidized bed dryer, Energy Conversion and Management, 67, pp: 179-185

Gummert, M., Aldas, R., Barredo, I.R., Muehlbauer, W., and Quick G.R., 1993. Low-temperature in-store drying system. Project report, IRRI-GTZ Project Postharvest Technologies in the Humid Tropics

Hall, C.W., 1957. Drying farm crops, Department of Agricultural Engineering, Michigan State University, East Lansing.

Hegsted, D. M. 1969. Nutritional value of cereal proteins in relation to human needs. In Protein-enriched cereal foods for world needs, ed., 38—48.

Heijden, H., and Ptasinski, K. J., 2012.Exergy analysis of thermo-chemical ethanol production *via* biomass gasification and catalytic synthesis, Energy, 46 (1), pp: 200-210

Hematian, S., and Hormozi, F., 2015. Drying kinetics of coated sodium per-carbonate particles in a conical fluidized bed dryer, Powder Technology, 269, pp. 30–37

Hemis, O., Choudhary, R., and Dennis, G., 2012. The effect of microwave drying parameters on the germination of wheat seeds, Bio-systems Engineering, 112(3), pp: 202-209

Hepbasli, A., Gungor, A.,Erbay, Z., Gunerhan, H., 2013. Splitting the exergy destruction into avoidable and unavoidable parts of a gas engine heat pump (GEHP) for food drying processes based on experimental values, Energy Conversion and Management, 73, pp: 309–316

Hien, P.H., 2009. Comparative Prefeasibility Study of Paddy Dryer Systems for Farmers or Rice Millers in Tra Vinh, Center for Agricultural Energy and Machinery Nong-Lam University, Ho Chi Minh City, Viet Nam

TH-1488_126103037

Hien, P.H., 1998. Mechanical Dryer and Grain Quality in the Mekong Delta of Vietnam: History and Perspective of Development. Conference on Science, Technology, and Environment for the Mekong Delta, Ca-Mau Province, Vietnam, 24-25 September.

Hossain, M.A., Gottschalk, K., and Hassan, M.S., 2013. Mathematical Model for a Heat Pump Dryer for Aromatic Plant, Procedia Engineering, 56, pp: 510-520

Hosseinpour, S., Rafiee, S., Mohtasebi, S. S., Aghbashlo, M.,2013. Application of computer vision technique for on-line monitoring of shrimp color changes during drying, Journal of Food Engineering, 115 (1), pp: 99–114

Hung, Y. C.,Yemmireddy, V. K., and Chinnan, M. S., 2013. Effect of drying method on drying time physio-chemical properties of dried rabbiteye blueberries,Food Science and Technology,50 (2), pp: 739-745

Ibrahim, M. N., Sarker, M.S.H., and Azizn,AB., 2014. Drying performance and overall energy requisite of industrial inclined bed paddy drying in Malaysia, Engineering Science and Technology, pp. 398 – 409

Isvilanonda, S., and Wattanutchariya, S., 1999. Improved drying of high moisture grains, ACIAR Projects, Kasetsart University, Bangkok.

Inaba, H., 2007. Heat and Mass Transfer Analysis of Fluidized Bed Grain Drying, Memoirs of the Faculty of Engineering, 41, pp: 52-62

Jaiboon, P., Prachayawarakorn, S., Devahastin, S., Soponronnarit, S., 2009. Effects of fluidized bed drying temperature and tempering time on quality of waxy rice, Journal of Food Engineering, 95, pp. 517–524, 2009.

Janas, S., Boutry, S., Malumba, P., Elst, L.V., Béra, F., 2010. Modelling dehydration and quality degradation of maize during fluidized-bed drying, Journal of Food Engineering, 100, pp: 527–534

Jayas. D. S. and Ghosh, P. K. 2006. Preserving quality during grain drying and techniques for measuring grain quality, 9th International Working Conference on Stored Product Protectio,The Royal Palm Plaza Hotel Resort, Campinas, São Paulo, Brazil 15-18 October

Jittanit, W., Saeteaw, N., and Charoenchaisri, A., 2010. Industrial paddy drying and energy saving options, Journal of Stored Products Research, 46 (4), pp: 209 – 213

Jittanit, W., Srzednicki, G., and Driscoll, R., 2010. Modelling of seed drying in fluidised and spouted bed dryers, 10th International Working Conference on Stored Product Protection, Technical University of Lisbon, Spain, pp: 275-280.

Juliano, B. O. 1985. Polysaccharides, proteins and lipids of rice. In Rice: Chemistry and technology, ed., 59—174.

TH-1488_126103037

Kahyaoglu, L. N., Sahin, S., and Gulum Sumnu, G., 2012. Spouted bed and microwave-assisted spouted bed drying of parboiled wheat, Food and Bioproducts Processing, 90, pp.: 301–308

Kalita, P., Mahanta, P., and Saha, U.K., 2014. Study of bed-to-wall heat transfer with twisted tape at the upper splash region of a pressurized circulating fluidized bed unit, International Journal of Heat and Mass Transfer, 78, pp: 260-266

Kalita, P., Saha, U.K., and Mahanta, P., 2013.Effect of biomass blending on hydrodynamics and heat transfer behavior in a pressurized circulating fluidized bed unit, International Journal of Heat and Mass Transfer, 60, pp: 531-541

Karbassi, A., and Mehdizadeh, Z., 2008. Drying Rough Rice in a Fluidized Bed Dryer, Agric. Sci. Technol., 10, pp: 233-241

Kato, K., and Wen, C. Y., 1969. Bubble assemblage model for fluidized bed catalytic reactors, Chemical Engineering Science, 24, pp.1351─69.

Keppler, I., Kocsis, L., Oldal, I., Farkas, I., Csatar, A., 2012. Grain velocity distribution in a mixed flow dryer, Advanced Powder Technology, 23(6), pp: 824–832

Khanali, M., Rafiee, S., Jafari, A., Hashemabadi, S.H., Banisharif, A., 2012. Mathematical modeling of fluidized bed drying of rough rice (Oryza sativa L.) grain, Journal of Agricultural Technology, 8 (3), pp: 795-810

Khatchatourian, O. A., 2012. Experimental study and mathematical model for soya bean drying in thin layer, bio-system engineering, 113, pp-54-61

Kiple, K.F., and Ornelas, K.C., 2003. The Cambridge World History of Food, Cambridge University Press, UK.

Kouchakzadeh, A., and Ghobadi, F., 2012. Modelling of ultrasonic-convective drying of pistachios, Agric Eng Int: CIGR Journal, 14(4) pp: 144－149

Kumar, M., Khatak, P., Sahdev, R. K., Prakash, O., 2011. The effect of open sun and indoor forced convection on heat transfer coefficients for the drying of papad, Journal of Energy in Southern Africa, 22(2), pp: 40-46.

Kunii, D., and Levenspiel, O., 1991. Fluidization Engineering, second edition, Butterworth-Heinemann, Stoneham.

Lamnatou, C., Papanicolaou, E., Belessiotis, V., Kyriakis, N., 2012. Experimental investigation and thermodynamic performance analysis of a solar dryer using an evacuated-tube air collector, Applied Energy 94, 232–243

Law, C. L., Tasirin, S.M., and Daud, W. R. W., 2004. The effect of vertical internal baffles on fluidization hydrodynamics and grain drying characteristics, Chinese. J. Chem. Eng. 12, pp. 801–808

TH-1488_126103037

Lee, K. T., and Boateng, C. O., 2013. Utilisation of Palm Oil Wastes for Biofuel and Other Value-Added Bio-Products: A Holistic Approach to Sustainable Waste Management for the Palm Oil Industry, Advances in Biofuels, pp: 53-87

Lerman, P., and Wennberg, O., 2011. Experimental method for designing a biomass bed dryer, biomass and bio-energy, 35, pp: S31 - S39

Li, H., Chen, Q., Zhang, X., Finney, K. N., 2012. Evaluation of a biomass drying process using waste heat from process industries: A case study, Applied Thermal Engineering, 35, pp: 71-80

Lim, J. H., Lee, Y., Shin, J.H., Bae, K., 2014. Hydrodynamic characteristics of gas–solid fluidized beds with shroud nozzle distributors for hydro-chlorination of metallurgical-grade silicon, Powder Technology, 266, pp. 312–320

Lu, J. J., and Chang. T. T. 1980. Rice in its temporal and spatial perspectives. In Rice: Production and utilization, ed., 1—74. Westport, Conn.

Mabrouk, S. S., Benali E., and Oueslati, H., 2012. Experimental study and numerical modelling of drying, Food and Bio-products Processing, 90, pp: 719–728

Malumba, P., Odjo, S., Dossou, J., Janas, S., François Béra, F., 2012. Influence of drying and hydrothermal treatment of corn on the denaturation of salt-soluble proteins and color parameters, Journal of Food Engineering, 109, pp: 561–570

Malumba, P., Vanderghem, C., Deroanne, C., Béra, F., 2008. Influence of drying temperature on the solubility, the purity of isolates and the electrophoretic patterns of corn proteins, Food Chemistry, 111, pp: 564–572

Marcos, B., Mercier, S., Moresoli, C., Villeneuve, S., Mondor, M., 2013. Sensitivity analysis of parameters affecting the drying behaviour of durum wheat pasta, Journal of Food Engineering, 118(1), pp: 108–116

Martinello, M. A., Munoz, D. J., and Giner, S. A., 2013. Low temperature/natural drying of grain depends strongly on the climate, Bio-system engineering, 114 (2), pp: 187-194

Mcneal, X., 1957. Rice aeration, drying, and storage. Bulletin 593. University of Arkansas, Arkansas, USA.

Meeso, N., Ponkham, K., Soponronnarit, S., Siriamornpun, S., 2012. Modeling of combined far-infrared radiation and air drying of a ring shaped-pineapple with/without shrinkage, Food and Bio-products Processing, 90(2), pp:155–164

Meeso, N., Dondee, S., Soponronnarit, S., Siriamornpun, S., 2011. Reducing cracking and breakage of soybean grains under combined near-infrared radiation and fluidized-bed drying, Journal of Food Engineering, 104 (1), pp: 6–13

Mellmann, J., and Teodorov, T., 2011. Solids transport in mixed-flow dryers, Powder Technology, 205 (1–3), pp: 117–125

TH-1488_126103037

Momenzadeh, L., and Zomorodian, A., 2011. Study of shelled corn shrinkage in microwave-assisted fluidized bed dryer using artificial neural network, International Journal of Agriculture Sciences, 3 (3), pp: 150-155

Mohapatra, S.S., Lakshmi, D.V.N., and Mahanta, P., 2013. Performance Evaluation of Natural Convection Grain Dryer using Phase Change Material for Quality Drying of Paddy, International Journal of Agriculture and Food Science Technology, 4(6), pp: 523-530

Mujumdar, A. S., 2006. Handbook of Industrial Drying, Third Edition, Taylor & Francis Group, LLC.

Munson, B.R., Young, D.F., and Okiishi, T.H., Fundamentals of Fluid Mechanics, John Wiley and Sons, Inc. 4thEdition, Iowa State University, Ames, Iowa, USA.

Muyanja, C., Atukwase, A., and Kaaya, A.N., 2012. Dynamics of Fusarium and fumonisins in maize grains stored in traditional structures (Granary, Mudsilo and *Tua*) commonly used in Uganda, Food Control, 26 (1), pp: 200-205

Nakamura, H., Kondo, T., and Watano, S., 2013. Improvement of particle mixing and fluidization quality in rotating fluidized bed by inclined injection of fluidizing air, Chemical Engineering Science, 91, pp. 70–78

Nilnont, W., Thepa, S., Janjai, S., Kasayapanand, N., Thamrongmas, C., Bala, B.K., 2012. Finite element simulation for coffee drying, Food and Bio-products Processing, 90 (2), pp: 341–350

Ogheneruona, D. E., and Yusuf, M.O.L., 2011. Design and Fabrication of a Direct Natural Convection Solar Dryer for Tapioc, Leonardo Electronic Journal of Practices and Technologies, 18, pp: 95-104

Okoronkwo C.A., Wufo, O.C., Waigwe K.N., Oogueke N.V., Anyanwu, E.E.,2013. Experimental Evaluation of a Fluidized Bed Dryer Performance, The International Journal Of Engineering And Science, 2 (6), pp. 45-53

Oluwaleye, I. O., and Adeyemi, M.B., 2013. Experimental Evaluation of a Batch Hot Air Fluidized Bed Dryer, International Journal of Modern Engineering Research, 3(1), pp. 497-503

Othomer, D.F. 1956. Background, History and Future of Fluid Bed System Fluidization. Reinhold Publishing Corporation, New York.

Ozahi, E., and Demir, H., 2013. A model for the thermodynamic analysis in a batch type fluidized bed dryer, Energy, 59, pp. 617-624

Ozahi, E., and Demir, H., 2015. Drying performance analysis of a batch type fluidized bed drying process for corn and unshelled pistachio nut regarding to energetic and exergetic efficiencies, Measurement, 60, pp. 85–96

TH-1488_126103037

Ozahi, E., and Demir, H., 2014. Presentation of a test rig with its experimental procedure and uncertainty analysis of measurements for batch type fluidized bed drying of corn and unshelled pistachio nut, Measurement, 53, pp. 117–127

Ozbey M. and Soylemez M.S., 2005. Effect of swirling flow on fluidized bed drying of wheat grains, Energy Conversion and Management, 46, pp. 1495–1512.

Panwar, N.L., Kaushik, S. C., and Kothari, S., 2012. A review on energy and exergy analysis of solar dying systems, Renewable and Sustainable Energy Reviews, 16 (5), pp: 2812– 2819.

Pati, J. R., Hotta, S.K., and Mahanta, P., 2015. Effect of heat waste recovery on Drying Characteristics of Sliced Ginger in a Natural Convection Dryer, Procedia Engineering, 105, pp: 145-152.

Peña, J. A. P., 2011. Bubbling Fluidized Bed, When to use this technology?, Foster Wheeler Global Power Group Madrid, Spain presented at IFSA 2011, Industrial Fluidization South Africa Johannesburg, South Africa 15-17 November

Pérez, J. J. C., Flores, M. J. P., Febles, V. G., Domínguez, G. C., 2012. Mathematical modelling of castor oil seeds (Ricinuscommunis) drying kinetics in fluidized bed at high temperatures, Industrial Crops and Products, 38, pp: 64– 71

Pillai, M. G., 2013. Thin layer drying kinetics, characteristics and modeling of plaster of paris, Chemical Engineering Research and Design, 91(6), pp: 1018–1027

Prieto, S., Verdugo, A.S., Briongos, J.V., Santana, D., 2014. The effect of temperature on the distributor design in bubbling fluidized beds, Powder Technology, 261, pp. 176–184

Prommas, R., Rattanadecho, P., and Jindarat, W., 2012. Energy and exergy analyses in drying process of non-hygroscopic porous packed bed using a combined multi-feed microwave-convective air and continuous belt system, International Communications in Heat and Mass Transfer, 39 (2), pp: 242–250

Promvonge, P., 2011. Drying characteristics of peppercorns in a rectangular fluidized-bed with triangular wavy walls, International Communications in Heat and Mass Transfer, 38, pp. 1239–1246

Román, F., and Hensel, O., 2010. Effect of air temperature and relative humidity on the thin-layer drying of celery leaves, Agricultural Engineering International: the CIGR Journal,13(2).

Rordprapat, W., 2005. Comparative study of fluidized bed paddy drying using hot air and superheated steam, Journal of Food Engineering, 71, pp. 28–36

Rowe, P.N., and Partridge, B.A., 1962. Particle movement caused by bubbles in a fluidised bed, in: Interaction Between Fluids & Particles London: Instn Chem. Engrs, pp 135-142.

TH-1488_126103037

Sahin, S., Sumnu, G., and Tunaboyu, F., 2013. Usage of solar-assisted spouted bed drier in drying of pea, Food and Bioproducts Processing, 91 (3), pp: 271–278

Saidur, R., BoroumandJazi, G., Mekhlif, S., Jameel, M., 2012. Exergy analysis of solar energy applications, Renewable and Sustainable Energy Reviews, 16 (1), pp: 350– 356

Sami, S., Etesami, N., and Rahimi, A., 2011. Energy and exergy analysis of an indirect solar cabinet dryer based on mathematical modeling results, Energy, 36 (5), pp: 2847- 2855

Sarker, M.S.H., Ibrahim, M.N., Aziz, N.A., Punan, M.S., 2015. Application of simulation in determining suitable operating parameters for industrial scale fluidized bed dryer during drying of high impurity moist paddy, Journal of Stored Products Research, 61, pp. 76-84

Sarker, S. H., 2015. Energy and exergy analysis of industrial fluidized bed drying of paddy, Energy 84, pp. 131-138

Saxena, D. C., Singh, G. D., Sharma, R., Bawa, A.S., 2008. Drying and re-hydration characteristics of water chestnut (Trapanatans) as a function of drying air temperature, Journal of Food Engineering,87 (2), pp: 213-221.

Sebaiia A.A. and Shalaby S.M., 2013. Experimental investigation of an indirect-mode forced convection solar dryer for drying thymus and mint, Energy Conversion and Management, 74, pp: 109–116

Sevik, S., 2013. Design, experimental investigation and analysis of a solar drying system, Energy Conversion and Management, 68, pp: 227–234

Sharma, G.P., Prasad, S., and Chahar, V.K., *2009*. Moisture transport in garlic cloves undergoing microwave-convective drying, Food and Bio-products Processing, 87, (1), pp: 11-16

Shi, Q., Zheng, Y., and Ya Zhao, Y., 2013. Mathematical modelling on thin-layer heat pump drying of yacon slices, Energy Conversion and Management, 71, pp.: 208-216

Sharma,G.P., Prasad,S., and Chahar, V.K., 2009. Moisture transport in garlic cloves undergoing microwave-convective drying, Food and Bio-products Processing, 87, pp:11-16

Singh, S., and Kumar, S., 2014. Performance evaluation of solar dryer system for optimal operation: mathematical modeling and experimental validation, International Journal of Sustainable Energy. 33(1), pp:141-158.

Singh, S., and Kumar, S., 2013. Solar drying for different test conditions: Proposed framework for estimation of specific energy consumption and CO_2 emissions mitigation, Energy, 51, pp: 27 – 36

TH-1488_126103037

Singh, N. J., and Pandey,R. K., 2012. Convective air drying characteristics of sweet potato cube, Food and Bio-products Processing, 90 (2), pp: 317–322

Singh, P. L., 2011. Silk cocoon drying in forced convection type solar dryer, Applied Energy 88 (5), pp: 1720–1726

Siriamornpun, S., and Kaisoon, O., and Meeso N., 2012. Changes in colour, antioxidant activities and carotenoids of marigold flower resulting from different drying processes, Journal of Functional Foods, 4 (4), pp: 757-766

Sledz, M., 2013. Selected chemical and physico-chemical properties of microwave-convective dried herbs, Food and Bio-products Processing, 91, pp: 421-428

Sobrino, C., Ellis, N., and Vega, M., 2009. Distributor effects near the bottom region of turbulent fluidized beds, Powder Technology, 189, pp. 25–33.

Sobrino, C., Ibañez, J.A.A., Santana, D.,Vega, M., 2008. Fluidization of Group B particles with a rotating distributor, Powder Technology, 181, pp. 273–280.

Sologubik, C.A., Campañone, L.A., Pagano, A.M., Gely, M.C., 2013. Effect of moisture content on some physical properties of barley, Industrial Crops and Products, 43, pp: 762– 767

Somchart, S., 1996. Fluidised-bed paddy drying. In: Grain Drying in Asia. Proceedings of an international Conference, FAO Regional Office for Asia and the Pacific, Bangkok, Thailand, ACIAR Proceedings No. 71, p 201-209

Somchart, S., Prachayawarakorn, S., and Wangji, M.,1996. Progress in commercialisation of fluidized bed paddy dryer

Srinivasakannan, C., and Balasubramanian, N., 2009. An investigation on drying of millet in fluidized beds, Advanced Powder Technology, 20, pp. 298–302

Srinivasakannan, C., Shoaibi, A. A., and Balasubramanian, N., 2012. Continuous Fluidized Bed Drying With and Without Internals: Kinetic Model, Chem. Biochem. Eng, 26 (2), pp: 97–104

Syahrul, S., Hamdullahpur, F., and Dincer, I., *2002*. Thermal analysis in fluidized bed drying of moist particles, Applied Thermal Engineering, 22(15), , pp: 1763-1775

Tang, J., Caparino, O.A., Nindo , C.I., Sablani, S.S., Powers, J.R., Fellman, J.K., 2012. Effect of drying methods on the physical properties and microstructures of mango (Philippine 'Carabao' var.) powder, Journal of Food Engineering, 111, pp: 135–148

Teter, N., 1987. Paddy drying manual, Food and Agricultural Organization of the United Nations, Rome.

Thao, H. M., and Noomhorm, A., 2011. Modeling and Effects of Various Drying Methods on Sweet Potato Starch Properties, Walailak Journal of Science and

TH-1488_126103037

Technology, 8 (2), pp: 139

Tsutsumi, A., Kawabata, M., Kurata, O., Iki, N., 2012. Advanced integrated gasification combined cycle (A-IGCC) by exergy recuperation—technical challenges for future generations, Journal of Power Technologies, 92 (2), pp: 90-100

Tyagi, V.V., Panwar, N.L., Rahim, N.A., Kothari, R., 2012, Review on solar air heating system with and without thermal energy storage system, Renewable and Sustainable Energy Reviews, 16 (4), pp: 2289– 2303

Velazquez, C., Obregon, L., and Quiriones, L., 2013. Model predictive control of fluid bed drying with an inline near infrared (NIR) as moisture sensor, ControlEngineering Practice, 21 (4), pp: 509-517.

Vidan, E. C. L., Lilia, L. L. M., and Ramırez, J. R., 2013. Efficiency of a hybrid solar–gas dryer, Solar Energy, 93, pp: 23–31

Villegas, J. A., Duncan, S. R., Wang, H. G., Yang, W. Q., 2009. Distributed parameter control of a batch fluidised bed dryer, Control Engineering Practice, 17, pp: 1096–1106

Wilde, J. D., 2014. Gas–solid fluidized beds in vortex chambers, Chemical Engineering and Processing, 85, pp. 256–290

Yakubov, B., Tanny, J., and Maron, D. M., 2007. The dynamics and structure of a liquid–solid fluidized bed in inclined pipes, Chemical Engineering; 128, pp. 105–114

Yang, Z., Zhu, E., Zhu, Z., Wang, J., Li, S., 2013. A comparative study on intermittent heat pump drying process of Chinese cabbage seeds, Food and Bioproducts Processing, 91(4), pp: 381-388.

Zarein, M., Samadi, S. H., and Ghobadian, B., 2015. Investigation of microwave dryer effect on energy efficiency during drying of apple slices, Journal of the Saudi Society of Agricultural Sciences, 14(1), pp: 41-47.

Zeng, J. L., Zhu, F. R., Yu, S. B., Xiao, Z. L., 2013. Myristic acid polyaniline as form stable phase change materials for thermal energy storage, Solar Energy Materials & Solar Cells, 114, pp:136–140

Zielinska, M., Zapotoczny, P., Alves-Filho, O. A., Eikevik T. M., Blaszczak, W., 2013. Microwave Vacuum–Assisted Drying of Green Peas Using Heat Pump and Fluidized Bed: A Comparative study between atmospheric Freeze drying and hot air convective drying, Drying Technology, 31, pp: 633–642

Zlatanovic, I., Komatina, M., and Antonijcvic, D., 2013. Low-temperature convective drying of apple cubes, Applied Thermal Engineering, 53(1), pp: 114–123

TH-1488_126103037

LIST OF PUBLICATIONS

LIST OF JOURNAL PUBLICATIONS AND PUBLICATION IN CONFERENCE PROCEEDINGS

1. Phyu Phyu Thant, P.S. Robi and P. Mahanta, 2015, Effect of Incline in an Inclined Bubbling Fluidized Bed Paddy Dryer, International Journal of Scientific Engineering and Technology Research, 4(6), pp. 1190-1196.
2. Phyu Phyu Thant, P. Mahanta and P.S. Robi, 2015, Effect of Spirals in an Inclined Bubbling Fluidized Bed Paddy Dryer, International Journal of Engineering Research and Technology, 4(6), pp. 270-277.
3. Phyu Phyu Thant, P. Mahanta and P.S. Robi, 2015, Performance Enhancement of Inclined Fluidized Bed Paddy Dryer by Design Modification, International Journal of Engineering and Applied Sciences, 2(8), pp. 61-65.
4. Phyu Phyu Thant, P. Mahanta and P.S. Robi, 2015, Effect of Modification of Distributor Plate in anInclined Bubbling Fluidized Bed Paddy Dryer, International Energy Journal, August, 2015 (under peer review).
5. Phyu Phyu Thant, P. Mahanta and P.S. Robi, 2016, IBFB dryer performance in Energy saving option, Energy, 2016 (under peer review)
6. Phyu Phyu Thant, P.S. Robi and P. Mahanta. "Experimental Investigation of Cereal Crop Drying in an Inclined Bubbling Fluidized Bed, 5th International and 26th all India Manufacturing Technology, Design and Research Conference, AIMTDR, Department of Mechanical Engineering, IIT Guwahati, December 12-13, 2014.

TH-1488_126103037

APPENDICES

APPENDIX - A

DESIGN OF DISTRIBUTOR PLATE

Diameter of paddy, $\bar{d}_p$ = 2.7 mm

Bed inventory, I = 10 kg (input paddy)

Operating velocity, U_{0p} = 2.5 m/s

Voidage at minimum fluidization, ε_{mf} = 0.5

Bed cross-section = 0.1 m x 0.1 m

Cross-sectional area of the bed, A_b = 0.1 m x 0.1 m = 0.01 m^2

Density of paddy, $\rho_s = 600\ kg/m^3$

Density of air, $\rho_a = 1.165\ kg/m^3$

Acceleration due to gravity, $g = 9.81 m/s^2$

Height of the bed at minimum fluidization, H_{mf};

$$H_{mf} = \frac{\Delta P}{(1-\varepsilon_{mf}).\rho_s.g} = \frac{\frac{I.g}{A_b}}{(1-\varepsilon_{mf}).\rho_s.g}$$

$$= \frac{I}{(1-\varepsilon_{mf}).A_b.\rho_s}$$

$$= \frac{10\ kg}{(1-0.5)\times 0.01 m^2 \times 600 kg/m^3}$$

= 3.33 m

Bed pressure drop: (ΔP_b)

$$\Delta P_b = (1-\varepsilon_{mf}).\rho_s.g.H_{mf}$$

$$= (1-\varepsilon_{mf}).\rho_s.g.\frac{I}{(1-\varepsilon_{mf}).\rho_s.A_b}$$

$$= \frac{I.g}{A_b}$$

TH-1488_126103037

$$= \frac{10\ kg \times 9.81\ \frac{m}{s^2}}{0.01m^2} = 9810N/m^2$$

Orifice Diameter: (d_{or})

$$d_{or} = d_p = 2.7 \cong 3mm$$

According to the standard available drill bit, d_{or} is chosen to be 3mm.

Minimum distributor pressure drop for uniform distribution: (ΔP_D)

$$\Delta P_D = \Delta P_b \left[0.01 + 0.2\left\{1 - exp\left(\frac{-D}{2H_{mf}}\right)\right\}\right]$$

Equivalent diameter of bed: D

$$D = 4\left(\frac{A_b}{p}\right) = 4 \times \frac{0.01}{4 \times 0.1} = 0.1m$$

$$\Delta P_D = \Delta P_b \left[0.01 + 0.2\left\{1 - exp\left(\frac{-D}{2H_{mf}}\right)\right\}\right]$$

$$= 9810N/m^2 \times \left[0.01 + 0.2\left\{1 - exp\left(\frac{-0.1m}{2 \times 3.33m}\right)\right\}\right]$$

$$= 127.34N/m^2$$

Rearrangement resistance (ΔP_R):

$$\Delta P_R = \rho_g \frac{\left(U_{0P}\frac{A_b}{A}\right)^2}{2g} = 1.165 \times \frac{(2.5 \times 1)^2}{2 \times 9.81} = 0.3711N/m^2 < (P_D/100)$$

For stable and uniform fluidization, the condition of $\Delta P_R < (P_D/100)$ is satisfied.

Thickness of distributor plate: $t = 0.006mm$

Orifice discharge coefficient(C_D):

$$C_D = 0.82\left(\frac{t}{d_{or}}\right)^{0.13} = 0.82\left(\frac{6}{3}\right)^{0.13} = 0.897$$

Gas velocity through orifice: (U_{or})

$$U_{or} = C_D\left(\frac{2\Delta P_D}{\rho_g}\right)^{1/2} = 0.897\left(\frac{2 * 127.34}{1.165}\right)^{1/2} = 13.2\ m/s$$

TH-1488_126103037

Number of orifices per square meter of the distributor:

$$N_{or} = \frac{U_{op}}{U_{or}} \times \frac{1}{\frac{\pi}{4} {d_{or}}^2} = \frac{2.5}{13.26} \times \frac{4}{\pi \times (0.003)^2} = 26672/m^2$$

Total number of holes on the perforated distributor

$$= N_{or} \times A_b = 26672 \times 0.01 = 267 \; numbers$$

Pitch of the orifices on the perforated plate:$= \frac{1}{(N_{or})^{\frac{1}{2}}} = \frac{1}{26672^{\frac{1}{2}}}$

$$= 0.006123 \; m \cong 6.1 \; mm$$

Open area in the distributor$= \frac{\pi}{4} {d_{or}}^2 \times (N_{or})$

$$= \frac{\pi}{4} \times (.003)^2 \times 26672 \times 100 = 18.85\%$$

Final Data:

Standard distributor plate

Diameter of orifice d_{or} = 3 mm

Pitch (square) = 6.1 mm

Thickness of distributor plate = 6 mm

Total numbers of holes = 267 numbers

Percentage opening = 18.85 %

TH-1488_126103037

Modified Distributor Plate

Open area in the distributor= $\frac{\pi}{4} {d_{or}}^2 \times (N_{or})$

$$18.85\% = \frac{\pi}{4} 0.0035^2 \times N_{or}$$

$$N_{or} = 19592.2/m^2$$

Total number of holes on the perforated distributor

$= N_{or} \times A_b = 196\ numbers$

Pitch of the orifices on the perforated plate:= $\frac{1}{(N_{or})^{\frac{1}{2}}} = 0.0071\ m = 7.1\ mm$

Final data:

Diameter of orifice d_{or} = 3.5 mm

Pitch (square) = 7.1 mm

Thickness of distributor plate = 6 mm

Total numbers of holes = 196 numbers

Percentage opening = 18.85 %

TH-1488_126103037

Drawing of standard distributor plate and modified distributor plate are shown below.

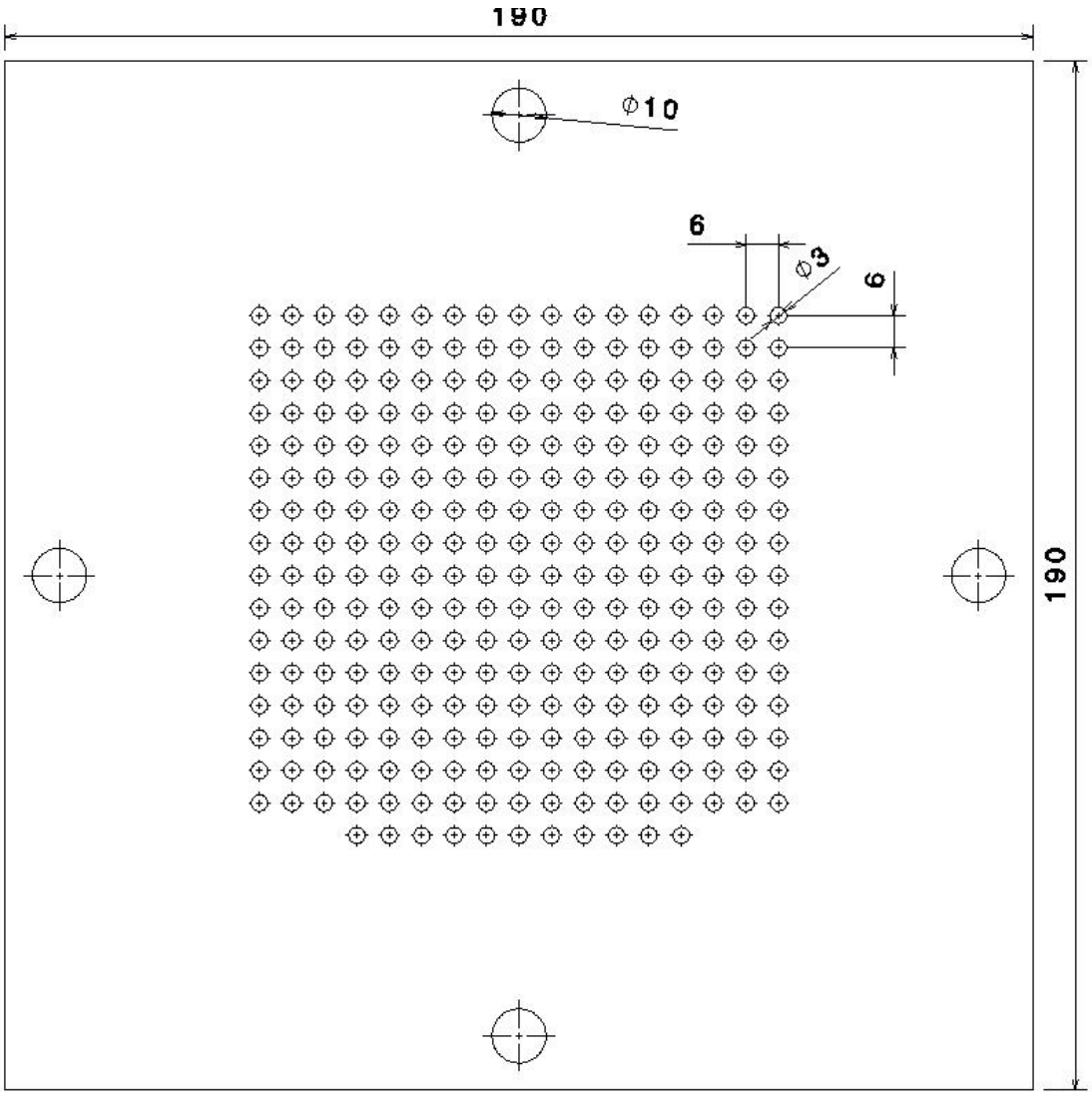

All dimensions are in mm

Fig.A-1 Standard distributor plate

TH-1488_126103037

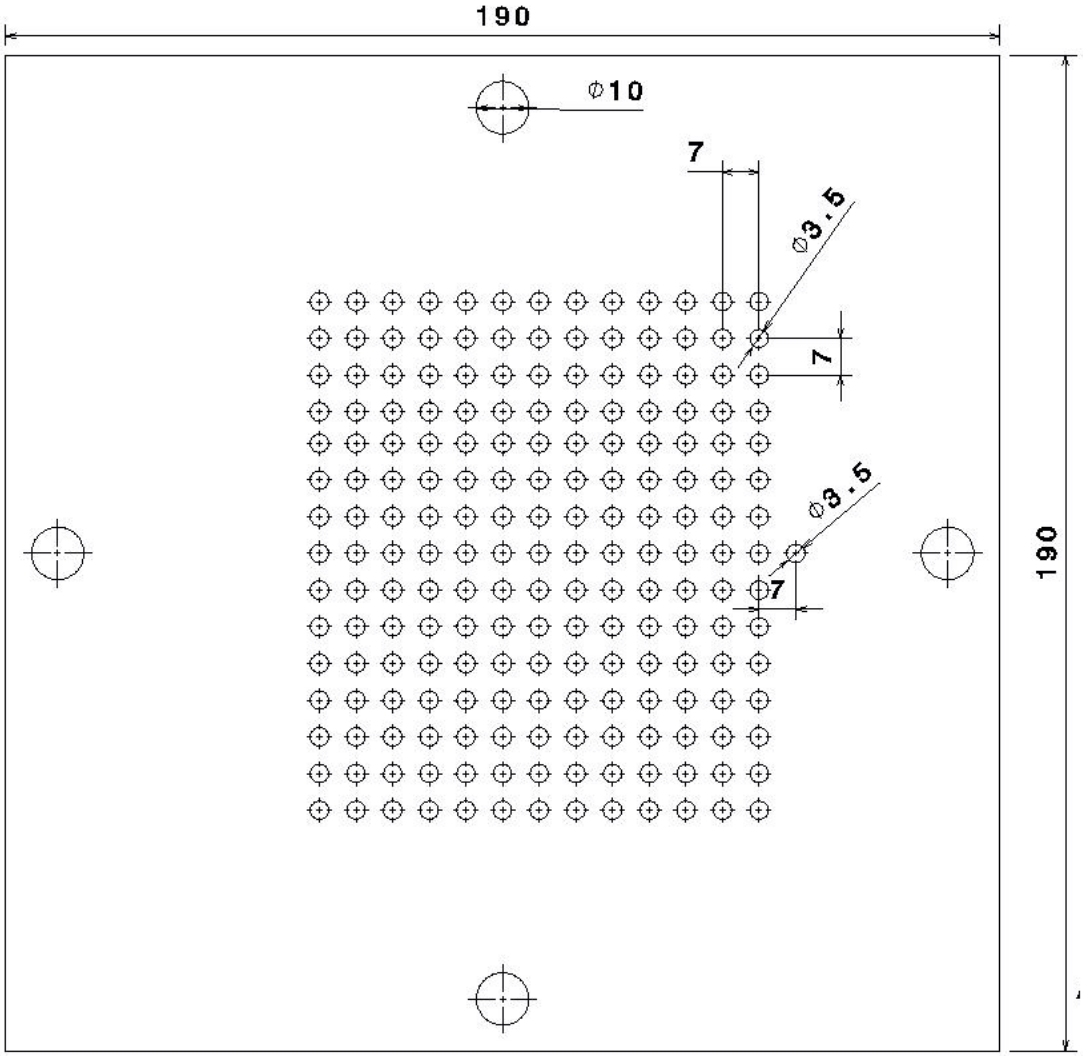

All dimensions are in mm

Fig. A-2 Modified distributor plate

TH-1488_126103037

APPENDIX- B

DESIGN OF ORIFICE PLATE

Applying Bernoulli's theorem to the upstream tapping (1) and to the orifice (2), of the Fig. (B.1) we can write,

$$\frac{V_1^2}{2g} + H_1 = \frac{V_2^2}{2g} + H_2 \tag{B.1}$$

Assuming that the pipe is running full and for the movement that no expansion of the fluid takes place, then

$$A_1 V_1 = A_2 V_2 \tag{B.2}$$

$$\text{Or, } V_1 = \frac{A_2}{A_1} V_2 = m_1 V_2$$

$$\text{where } m_1 = \frac{A_2}{A_1}$$

Now substituting the expression of V_1 to equation (B.1),

$$V_2^2 = \frac{2g(H_1 - H_2)}{1 - m_1^2} \tag{B.3}$$

where, $(H_1 - H_2)$ is the difference of pressure heads between points (1) and (2) of Fig. (B.1) and expressed in meter of air. Now if we substitute $(H_1 - H_2)$ in terms of $(\Delta p)$and express in cm of water, then we can write,

$$p_1 = \rho_a \times g \times H_1 \text{ and } p_2 = \rho_a \times g \times H_2 \tag{B.4}$$

$$\text{Hence, } p_1 - p_2 = \rho_a \times g \times (H_1 - H_2)$$

$$H_1 - H_2 = \frac{p_1 - p_2}{\rho_a \times g} = \frac{\Delta p}{\rho_a \times g} \text{m of water column}$$

$$\text{or, } H_1 - H_2 = \frac{\Delta p \times 100}{\rho_a \times g} \text{ cm of water column}$$

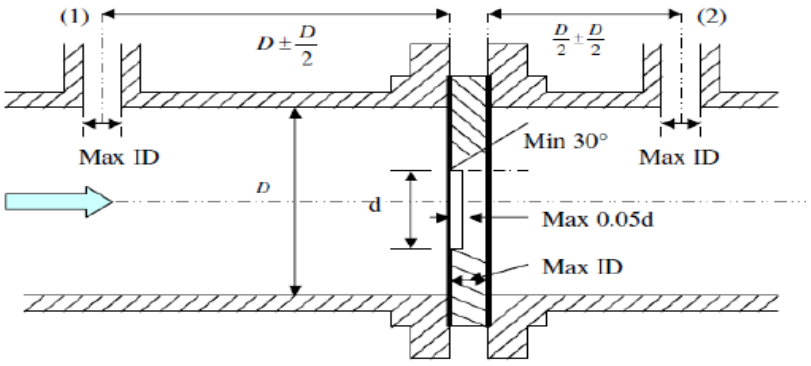

Fig. (B.1) Orifice meter with D and D/2 tapings

TH-1488_126103037

where Δp is the difference in height of manometric fluid (water) in cm of water

Now substituting the expression of $(H_1 - H_2)$ in equation (B.3) we can write

$$V_2^2 = \frac{2\left(\frac{100 \times \Delta p}{\rho_a}\right)}{1-m_1^2} \text{ or } V_2 = \left[\frac{2\left(\frac{100 \times \Delta p}{\rho_a}\right)}{1-m_1^2}\right]^{1/2} \text{ m/s} \quad \text{(B.5)}$$

Theoretical mass flow rate (m_t) of air can be expressed as

$$m_t = \rho_a A_2 V_2 \text{ kg/s}$$

$$\text{Or, } m_t = \rho_a \times \left[\frac{\pi}{4} \times \left(\frac{d_o}{100}\right)^2\right] \times \left[\frac{2\left(\frac{100 \times \Delta p}{\rho_a}\right)}{1-m_1^2}\right]^{1/2} \times 3600 \text{ kg/h}$$

$$\text{Or, } m_t = 3.99 \times d_o^2 \times \frac{(\Delta p \times \rho_a)^{1/2}}{(1-m_1^2)^{1/2}}$$

$$m_t = 3.99 \times d_o^2 \times E \times (\Delta p \times \rho_a)^{1/2} \text{kg/h} \quad \text{(B.6)}$$

$$\text{where, } E = \frac{1}{(1-m_1^2)^{\frac{1}{2}}} = 1.013$$

d_o = diameter of orifice in cm = 4.2 cm

D = inside diameter of pipe = 10.5 cm

Δp = difference in manometric fluid height in cm of water

ρ_a = density of air

$$m_1 = \frac{d^2}{D^2} = \frac{4.2^2}{10.5^2} = 0.16$$

$$R_e = \frac{\rho V D}{\mu} = \frac{V D}{\nu} = \frac{2.5 \times 0.105}{16.04 \times 10^{-6}} = 16365.33$$

For the above Reynolds number and at $\beta = 0.4$, Value of discharge coefficient, C is found to be 0.6095 from IS code 14615 (Part 1):1999, page no.71

Now equation (B.6) implies,

$$m_t = 3.99 \times d_o^2 \times E \times (\Delta p \times \rho_a)^{1/2}$$

$$m_t = 3.99 \times 4.2^2 \times 1.013 \times (\Delta p \times 1.166)^{1/2} = 76.98 \times \sqrt{\Delta p} \text{ kg/h} \quad \text{(B.7)}$$

TH-1488_126103037

The actual mass flow rate (m_a) can be expressed as

$$m_a = C \times z \times m_t \text{kg/h} \quad \text{(B.8)}$$

Or, $m_a = C \times z \times \left[3.99 \times d_o^2 \times E \times (\Delta p \times \rho_a)^{1/2}\right]$

Or, $m_a = C \times z \times 76.98 \times \sqrt{\Delta p}$ kg/h

where,

C = coefficient of discharge = 0.6095

z = velocity of approach factor = 1

or, $m_a = 46.91 \times \sqrt{\Delta p}$ kg/h

or, $m_a = 0.01303 \times \sqrt{\Delta p}$ kg/s (B-9)

In the present case,

$$A_b = 0.01\text{m}^2$$

Superficial velocity,

$$U = \frac{m_a}{\rho \times A_b} = \frac{0.01303\sqrt{\Delta p}}{1.166 \times 0.01} = 1.117\sqrt{\Delta p} \ \text{ms}^{-1} \quad \text{(B-10)}$$

TH-1488_126103037

APPENDIX-C

CALCULATION FOR COST EFFECTIVENESS OF PADDY UNDER SUN DRYING AND DRYING WITH BFB DRYER

Under sun drying

1. Cost for paddy 100kg = 1200 Rs
2. Labor cost= 4 days × 180 Rs/day =720 Rs
3. Total cost = 1200 + 720 = 1920 Rs
4. Milled rice kg for 100kg paddy = 40.5 kg
5. Rice selling price = 50 Rs/kg
6. Total income = 50Rs/kg × 40.5 kg =2025 Rs
7. $Profit_1$ = Total income – Total cost = 2025 – 1920 = 105 Rs

Drying with BFB dryer

1. Cost for paddy 100kg = 1200 Rs
2. Overall electricity cost = 0.954 kWhr/kg ×100kg × 1.25 Rs/kWhr = 119 Rs
3. Total cost = 1200 + 119 = 1319 Rs
4. Milled rice kg for 100kg paddy = 55 kg
5. Rice selling price = 50 Rs/kg
6. Total income = 50Rs/kg × 55 kg =2750 Rs
7. $Profit_2$ = Total income – Total cost = 2750 – 1319 = 1431 Rs

   $Profit_2$ - $Profit_1$ = 1431 – 105 = 1326 Rs or 92.1%

   $Profit_2$ is 92.1% more than $profit_1$.

   It is observed that paddy drying with bubbling fluidized bed dryer is more economy than that of under sun drying.

Limitations of sun drying:

- Not possible during rain or at night. Delays in drying lead to excessive respiration and fungal growth causing grain losses and yellowing.
- Labour intensive and has limited capacity.
- Temperature control is difficult. Overheating of grains can result in low milling quality caused by cracked grains.
- It can waste due to birds and strong wind.
- Large space requirement, dried paddy will have dust and stone and long drying time.

TH-1488_126103037

APPENDIX-D

THERMOCOUPLE CALIBRATION

The calibration of thermocouple is done by keeping one junction of the two dissimilar metals(Copper-Constantan) at constant temperature (at 0 °C) and other junction is maintained at variable temperatures. In order to maintain variable temperature, a water circulating bath is used. A high precision multi-meter is connected in the circuit to see the emf generation. In every 5 °C, the increase of water temperature the emf (milivolt) generation is recorded. The calibration curve so obtained is presented in Fig.D.1.

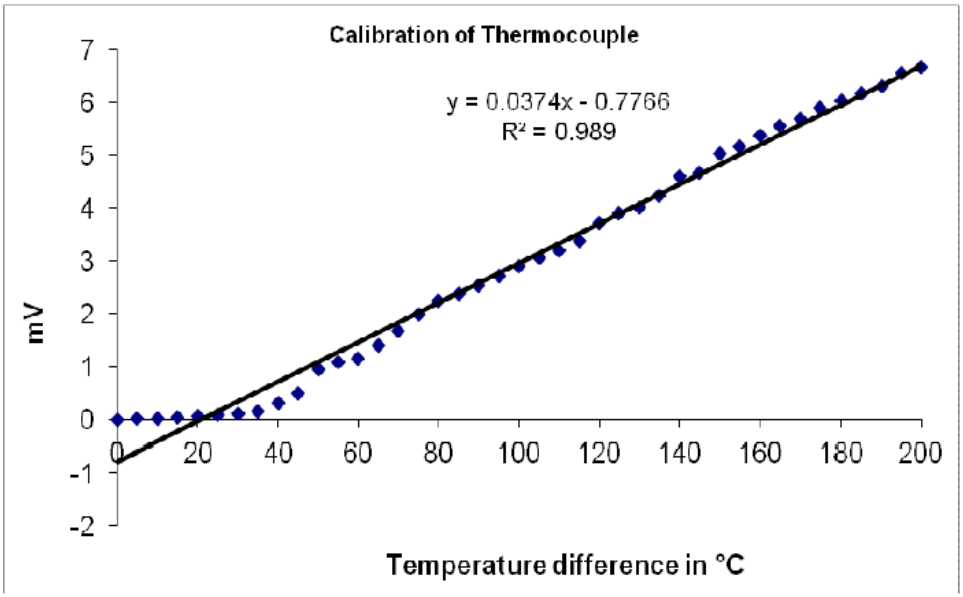

Fig. D.1 Calibration curve for copper-constantan thermocouple

TH-1488_126103037

APPENDIX-E

Table E.1 Instruments used in laboratory and their specifications

Components	Equipments	Specifications
Temperature	Thermocouple	K-type (Chromel and Alumel), Temperature range: 0~1350°C, Sensitivity-40.6μV/ °C, 1.5mm dia×200 mm L with port seal 40mmL,SS 316 Sheath, Grounded with 0.5mm.
Heating system	Electric heaters	3 units of electric heaters having 1kW for each, 45.72 cm L, 5.08 cm width, 1cm thickness
Moisture content	Moisture meter Muffle furnace	Model: PM-410 Moisture accuracy: ±0.5% Model: BST/MF1450 Temperature range: 800-1450˚C Temperature accuracy: ±1˚C Heating element: Silicon carbide (SIC)
Relative humidity	Hygrometer	Model: THM-B2 Humidity range: 10%~99%RH Accuracy: ± 5%RH
Temperature recorder	Data acquisition system	Model: 34970A Make: Agilent Technology
Air supply	Centrifugal Blower	11 kW, HP 15, 2880 rpm,volts 415, Amp 21, 3PH induction motor
Blower energy consumption	Energy meter	AC, 3 Phase, 4 Wire, Static Energy Meter Type: BBLSM-T44, Freq. 50 Hz, Class 1.0, 10-40A, 3×240V, Temp 27˚C Bentex Control & Switchgear Co.

TH-1488_126103037

APPENDIX-F

Uncertainty in moisture measurement (MC in %)

Moisture content (%) of paddy is

$$MC_{wb} = \frac{W_i - W_f}{W_i} \times 100\% = 1 - \frac{W_f}{W_i} \times 100\%$$

MC_{wb}= moisture content (%)wet basis

W_i = initial weight of paddy, g

W_f= final weight of paddy, g

Now,

$$MC_{wb} = f(W_f, W_i)$$

Therefore, uncertainty in moisture measurement in percentage [Bekwith et. al. 2003] is

$$= \frac{Error}{MC_{wb}} \times 100\%$$

$$= \pm 100 \times \sqrt{\left(\frac{a_1}{W_f}\right)^2 + \left(\frac{a_2}{W_i}\right)^2}$$

Here, a_1 and a_2 are uncertainties associated with independent variables W_f and W_i, respectively.

For paddy bed inventory of 500g

W_i =500±5g, a_2 = ±5g

W_f= 290±5g, a_1= ±5g

Thus uncertainty in moisture measurement in percentage is

$$= \pm 100 \times \sqrt{\left(\frac{5}{290}\right)^2 + \left(\frac{5}{500}\right)^2}$$

=±2%

For paddy bed inventory of 1000g

W_i = 1000 ±5g, a_2 = ±5g

W_f= 580 ±5g, a_1= ±5g

Thus uncertainty of moisture content percentage is

$$= \pm 100 \times \sqrt{\left(\frac{5}{580}\right)^2 + \left(\frac{5}{1000}\right)^2} = \pm 1\%$$

TH-1488_126103037

For paddy bed inventory of 1500g

W_i = 1500±5g, a_2 = ±5g

W_f = 870±5g, a_1= ±5g

Thus uncertainty of moisture content percentage is

$$= \pm 100 \times \sqrt{\left(\frac{5}{870}\right)^2 + \left(\frac{5}{1500}\right)^2}$$

$$= \pm 0.7\%$$

For paddy bed inventory of 2000g

W_i = 2000±5g, a_2 = ±5g

W_f = 1160±5g, a_1= ±5g

Thus uncertainty of moisture content percentage is

$$= \pm 100 \times \sqrt{\left(\frac{5}{1160}\right)^2 + \left(\frac{5}{2000}\right)^2}$$

$$= \pm 0.5\%$$

For paddy bed inventory of 2500g

W_i = 2500±5g, a_2 = ±5g

W_f = 1450±5g, a_1= ±5g

Thus uncertainty of moisture content percentage is

$$= \pm 100 \times \sqrt{\left(\frac{5}{1450}\right)^2 + \left(\frac{5}{2500}\right)^2}$$

$$= \pm 0.4\%$$

Maximum uncertainty of percentage moisture content is ±2% and minimum uncertainty of percentage moisture content is ±0.4%.

TH-1488_126103037

Uncertainty in energy consumption [Roy D. Matangoni et. al. 2003]

Thermal energy consumption of paddy drying in fluidized bed is

$$Q = V \times i \times t \times P.F \times 60 \times 10^{-6}, MJ$$

where,

Q = Thermal energy consumption of paddy drying, MJ

V = input voltage, volts

i = current supplied, Ampere

t = drying time, minute

$P.F$ = power factor

Now,

$$Q = f(V, i, t)$$

Therefore, uncertainty of thermal energy consumption = $\frac{Error}{Q} \times 100\%$

$$= \pm 100 \times \sqrt{\left(\frac{a_1}{V}\right)^2 + \left(\frac{a_2}{i}\right)^2 + \left(\frac{a_3}{t}\right)^2}$$

Here, a_1, a_2 and $a_3$are uncertainties associated with independent variables of V, i and t, respectively.

At the input condition of air velocity of 1.1 m/s, air temperature of 65˚C, paddy bed inventory of 2.5kg and inclination angle of 0˚ using modified distributor plate and without the use of spirals for θ= 0˚,

Q = 1.75MJ

V =105.± 1V, a_1 = ±1V

i = 5.2 ± 0.1A, a_2 = ± 0.1A

t = 67 ±1minutes, a_3 = ±1 minute

Uncertainty of thermal energy consumption is

$$= \pm 100 \times \sqrt{\left(\frac{1}{105}\right)^2 + \left(\frac{0.1}{5.2}\right)^2 + \left(\frac{1}{67}\right)^2}$$

= ± 2.6%

TH-1488_126103037

At the input conditions of air velocity of 1.1m/s, air temperature of 65˚C and an inventory of 2.5 kg using modified distributor plate and without the use of spirals for θ= 15˚,

Q =1.32 MJ

V =105.± 1V, a_1 = ±1V

i = 5.2 ± 0.1A, a_2 = ± 0.1A

t = 51 ±1minutes, a_3 = ±1 minute

Uncertainty of thermal energy consumption is

$$= \pm 100 \times \sqrt{\left(\frac{1}{105}\right)^2 + \left(\frac{0.1}{5.2}\right)^2 + \left(\frac{1}{51}\right)^2}$$

$$= \pm 2.9\ \%$$

At the input conditions of air velocity of 1.1m/s, air temperature of 65˚C and an inventory of 2.5 kg using modified distributor plate and without the use of spirals for θ= 30˚,

Q =1.37 MJ

V =105.± 1V, a_1 = ±1V

i = 5.2 ± 0.1A, a_2 = ± 0.1A

t = 53 ±1minutes, a_3 = ±1 minute

Uncertainty of thermal energy consumption is

$$= \pm 100 \times \sqrt{\left(\frac{1}{105}\right)^2 + \left(\frac{0.1}{5.2}\right)^2 + \left(\frac{1}{53}\right)^2}$$

$$= \pm\ 2.9\%$$

At the input conditions of air velocity of 2.1m/s, air temperature of 65˚C and an inventory of 2.5 kg using modified distributor plate and without the use of spirals for θ= 0˚,

Q =1.71 MJ

V =113.6.± 1V, a_1 = ±1V

i = 5.5 ± 0.1A, a_2 = ± 0.1A

t = 57 ±1minutes, a_3 = ±1 minute

TH-1488_126103037

Uncertainty of thermal energy consumption is

$$= \pm 100 \times \sqrt{\left(\frac{1}{113.6}\right)^2 + \left(\frac{0.1}{5.5}\right)^2 + \left(\frac{1}{57}\right)^2}$$

$= \pm 2.7$ %

At the input conditions of air velocity of 2.1m/s, air temperature of 65˚C and an inventory of 2.5 kg using modified distributor plate and without the use of spirals for θ= 15˚,

Q =1.23 MJ

V =113.6.± 1V, $a_1 = \pm 1$V

i = 5.5 ± 0.1A, $a_2 = \pm$ 0.1A

t = 41 ±1minutes, $a_3 = \pm 1$ minute

Uncertainty of thermal energy consumption is

$$= \pm 100 \times \sqrt{\left(\frac{1}{113.6}\right)^2 + \left(\frac{0.1}{5.5}\right)^2 + \left(\frac{1}{41}\right)^2}$$

$= \pm 3.2$ %

At the input conditions of air velocity of 1.1m/s, air temperature of 65˚C and an inventory of 2.5 kg using modified distributor plate and without the use of spirals for θ= 30˚,

Q =1.32 MJ

V =113.6.± 1V, $a_1 = \pm 1$V

i = 5.5 ± 0.1A, $a_2 = \pm$ 0.1A

t = 43 ±1minutes, $a_3 = \pm 1$ minute

Uncertainty of thermal energy consumption is

$$= \pm 100 \times \sqrt{\left(\frac{1}{113.6}\right)^2 + \left(\frac{0.1}{5.5}\right)^2 + \left(\frac{1}{43}\right)^2}$$

$= \pm 3.1$ %

At the input conditions of air velocity of 1.1m/s, air temperature of 65˚C and an inventory of 2.5 kg using modified distributor plate and with the use of spirals for θ= 0˚,

Q =1.22 MJ

TH-1488_126103037

V =105.± 1V, a_1 = ±1V

i = 5.2 ± 0.1A, a_2 = ± 0.1A

t = 47 ±1minutes, a_3 = ±1 minute

Uncertainty of thermal energy consumption is

$$= \pm 100 \times \sqrt{\left(\frac{1}{105}\right)^2 + \left(\frac{0.1}{5.2}\right)^2 + \left(\frac{1}{47}\right)^2}$$

$$= \pm 3\ \%$$

At the input conditions of air velocity of 1.1m/s, air temperature of 65˚C and an inventory of 2.5 kg using modified distributor plate and with the use of spirals for θ= 15˚,

Q =0.806MJ

V =105.± 1V, a_1 = ±1V

i = 5.2 ± 0.1A, a_2 = ± 0.1A

t = 31 ±1minutes, a_3 = ±1 minute

Uncertainty of thermal energy consumption is

$$= \pm 100 \times \sqrt{\left(\frac{1}{105}\right)^2 + \left(\frac{0.1}{5.2}\right)^2 + \left(\frac{1}{31}\right)^2}$$

$$= \pm\ 3.9\%$$

At the input conditions of air velocity of 1.1m/s, air temperature of 65˚C and an inventory of 2.5 kg using modified distributor plate and with the use of spirals for θ= 30˚,

Q =0.858 MJ

V =105.± 1V, a_1 = ±1V

i = 5.2 ± 0.1A, a_2 = ± 0.1A

t = 33 ±1minutes, a_3 = ±1 minute

Uncertainty of thermal energy consumption is

$$= \pm 100 \times \sqrt{\left(\frac{1}{105}\right)^2 + \left(\frac{0.1}{5.2}\right)^2 + \left(\frac{1}{33}\right)^2}$$

$$= \pm 3.7\ \%$$

TH-1488_126103037

At the input conditions of air velocity of 2.1m/s, air temperature of 65˚C and an inventory of 2.5 kg using modified distributor plate and with the use of spirals for θ= 0˚,

Q =1.11 MJ

V =113.6.± 1V, a_1 = ±1V

i = 5.5 ± 0.1A, a_2 = ± 0.1A

t = 37 ±1minutes, a_3 = ±1 minute

Uncertainty of thermal energy consumption is

$$= \pm 100 \times \sqrt{\left(\frac{1}{113.6}\right)^2 + \left(\frac{0.1}{5.5}\right)^2 + \left(\frac{1}{37}\right)^2}$$

$$= \pm 3.4\%$$

At the input conditions of air velocity of 2.1m/s, air temperature of 65˚C and an inventory of 2.5 kg using modified distributor plate and with the use of spirals for θ= 15˚,

Q =0.63 MJ

V =113.6.± 1V, a_1 = ±1V

i = 5.5 ± 0.1A, a_2 = ± 0.1A

t = 21 ±1minutes, a_3 = ±1 minute

Uncertainty of thermal energy consumption is

$$= \pm 100 \times \sqrt{\left(\frac{1}{113.6}\right)^2 + \left(\frac{0.1}{5.5}\right)^2 + \left(\frac{1}{21}\right)^2}$$

$$= \pm 5.2\%$$

At the input conditions of air velocity of 2.1m/s, air temperature of 65˚C and an inventory of 2.5 kg using modified distributor plate and with the use of spirals for θ= 30˚,

Q =0.69 MJ

V =113.6.± 1V, a_1 = ±1V

i = 5.5 ± 0.1A, a_2 = ± 0.1A

t = 23 ±1minutes, a_3 = ±1 minute

TH-1488_126103037

Uncertainty of thermal energy consumption is

$$= \pm 100 \times \sqrt{\left(\frac{1}{113.6}\right)^2 + \left(\frac{0.1}{5.5}\right)^2 + \left(\frac{1}{23}\right)^2}$$

$$= \pm 4.8\%$$

Maximum uncertainty of thermal energy consumption is ±5.2% and minimum uncertainty of thermal energy consumption is ±2.6% for the above mentioned cases.

TH-1488_126103037